Distribution Function. Boltzmann Transport Equation

The central quantity of the semiclassical transport is the distribution function

$$f(\vec{r},\vec{p},t)$$

that measures the probability to find a particle between $\vec{r}$ and $\vec{r}+d\vec{r}$, with momentum between $\vec{p}$ and $\vec{p}+d\vec{p}$, at time t. (Some define $f \cdot d^3\vec{r}\, d^3\vec{p}$ as the probability, which is how it is defined in classical mechanics, and we also did it in ECE 745; the difference is in the units, as $[d^3\vec{r}\, d^3\vec{p}] = (Js)^3$. The definition here is in agreement with Lundstrom's book, and it has proper equilibrium quantum behavior

Homogeneous system, equilibrium

$$f(\vec{r},\vec{p},t) = f_0(p) = \boxed{\frac{1}{e^{\frac{\varepsilon(p)-\varepsilon_F}{k_BT}}+1}}$$

Fermi-Dirac distribution fn

When $\varepsilon(p)-\varepsilon_F > 3.5\, k_BT$, the Fermi-Dirac distribution function can be approximated with a Maxwellian, i.e.,

$$\boxed{f_0^{MB}(p) \approx e^{\frac{\varepsilon_F}{k_BT}} \cdot e^{-\frac{\varepsilon(p)}{k_BT}}}$$ Maxwell-Boltzmann distrib. fn.

Equilibrium form in the presence of built-in fields (no spatial homogeneity)

$$f_0(\vec{r},\vec{p}) = \frac{1}{e^{\frac{E_c(\vec{r})+\frac{p^2}{2m}-\varepsilon_F(\vec{r})}{k_BT(\vec{r})}}+1}$$

One can prove that $\nabla T = 0$, and $\nabla \varepsilon_F = 0$ (constant temperature, Fermi level flat).

<u>How does the distribution function change with external applied fields?</u>

Why would $f(\vec{r},\vec{p},t)$ change in time, i.e., what makes a particle leave the little phase-space volume $d^3\vec{r}\,d^3\vec{p}$?

DIFFUSION
- ~~DRIFT~~ (flight)
- EXTERNAL FORCES => DRIFT
- SCATTERING

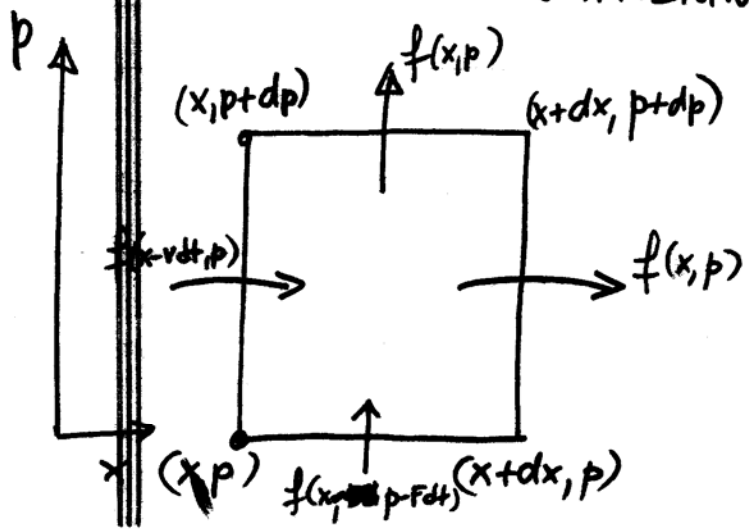

$$f(x,p,t+dt) - f(x,p,t)$$
$$\parallel$$

$$df(x,p,t) = \overbrace{-f(x,p,t) + f(x - v\,dt, p, t)}^{\text{diffusing}}$$

$$\overbrace{-f(x,p,t) + f(x, p - F\,dt, t)}^{\text{external forces} \Rightarrow \text{drift}}$$

$$+ df(x,p,t)_{scatt} + \boxed{\text{generation/recomb. term, if any}}$$

$$-f(x,p,t) + f(x - v\,dt, p, t) \approx -v\,dt \cdot \frac{\partial f}{\partial x} \qquad \text{drift}$$

$$-f(x,p,t) + f(x, p - F\,dt, t) \approx -F\,dt \cdot \frac{\partial f}{\partial p} \qquad \text{external forces}$$

$$\cancel{dt}\left(\frac{\partial f}{\partial t} + v\frac{\partial f}{\partial x} + F\frac{\partial f}{\partial p}\right) = \cancel{dt}\,\frac{\partial f}{\partial t}\Big|_{scatt}$$

1D BTE

Boltzmann transport equation (no gen/recomb.)

$$\boxed{\frac{\partial f}{\partial t} + \frac{\vec{p}}{m^*} \cdot \frac{\partial f}{\partial \vec{r}} + \vec{F}\frac{\partial f}{\partial \vec{p}} = \frac{\partial f}{\partial t}\Big|_{scatt}} \quad \underline{\underline{\text{BTE}}}$$

$\frac{\partial f}{\partial t}\Big|_{scatt}$ — the collision integral

Collisions ~~with~~ of electrons with other particles or scattering centers — transition rate

$$S(\vec{p}, \vec{p}\,') \quad \left[\frac{1}{s}\right]$$

initial final

Depends on the type of scattering process.

Collision integral

$$\left.\frac{\partial f}{\partial t}\right|_{scatt} = \sum_{\vec{p}'} \overbrace{S(\vec{p}',\vec{p}) f(\vec{p}')(1-f(\vec{p}))}^{\text{in-scattering}} - \underbrace{S(\vec{p},\vec{p}') f(\vec{p})(1-f(\vec{p}'))}_{\text{out-scattering}}$$

[$f(\vec{p}) \equiv f(\vec{r},\vec{p},t)$ for short, it is assumed that collisions are instantaneous, and occur locally in space.]

For nondegenerate semiconductors (distribution ~~closed~~ Maxwell Boltzmann in equilibrium; otherwise, more generally $f(\vec{p}) \ll 1$

$$1-f \approx 1$$

non-degenerate

$$\left.\frac{\partial f(\vec{p})}{\partial t}\right|_{scatt} = \sum_{\vec{p}'} S(\vec{p}',\vec{p}) f(\vec{p}') - S(\vec{p},\vec{p}') f(\vec{p})$$

<u>Equilibrium</u> Principle of detailed balance:
$\Rightarrow$ in & out-scattering exactly balanced

$$\boxed{\left.\frac{\partial f_{eq}}{\partial t}\right|_{scatt} = 0}$$

We know of the Fermi-Dirac distrib. fn, and the Maxwell-Boltzmann one, as its nondegenerate limit.

How does one reach these distribution functions after a perturbation?

Thanks to <u>electron-electron interaction</u>, which becomes a very efficient scattering mechanism at doping density above $10^{17}\ cm^{-3}$. (Homework!)
For density $10^{17} - 10^{18}\ cm^{-3}$ we can safely assume that the distribution in equilibrium is Maxwellian.
Above $10^{18}\ cm^{-3}$, it equilibrates into the Fermi-Dirac function.

<u>What do we do away from equilibrium?</u>

Evaluating f is quite difficult. Often people use models & approximations. Common approximations:

- Quasi-Fermi level

$$f(\vec{r},\vec{p},t) = \frac{1}{\exp\left(\frac{\frac{p^2}{2m} + E_{c0}(\vec{r},t) - F_n(\vec{r},t)}{k_B T_L}\right) + 1}$$

will give zero current!

- Displaced Maxwellian

$$f(\vec{r},\vec{p},t) = \exp\left(\frac{F_n(\vec{r},t) - E_{c0}(\vec{r},t)}{k_B T_L}\right) \times \exp\left(-\frac{|\vec{p} - \vec{p}_d|^2}{2m k_B T_L}\right)$$

Relaxation Time Approximation

In case of low external fields, the distribution function can be written as a sum of a large symmetric & a small ~~a~~ anti-symmetric part

$$f = f_S + f_A \,, \qquad f_S \gg f_A$$

where symmetry is with respect to inversion of momentum. When the fields are turned off

$$f_S \to f_0 \text{ (equilibrium)}$$
$$f_A \to 0$$

Collision integral

$$\left.\frac{\partial f}{\partial t}\right|_{scatt} = \left.\frac{\partial f_S}{\partial t}\right|_{scatt} + \left.\frac{\partial f_A}{\partial t}\right|_{scatt}$$

Low fields: $\left.\frac{\partial f_S}{\partial t}\right|_{scatt} \approx \left.\frac{\partial f_0}{\partial t}\right|_{scatt} = 0$ (principle of detailed balance)

$$\left.\frac{\partial f}{\partial t}\right|_{scatt} = \boxed{\left.\frac{\partial f_A}{\partial t}\right|_{scatt} = -\frac{f_A}{\tau_f}}$$

<u>Relaxation time approximation</u>

The collision integral is approximated by introducing a characteristic RELAXATION TIME $\tau_f(\vec{p})$, that describes the evolution of the anti-symmetric part of the distribution function due to scattering. It ~~also~~ is assumed to depend only on the details of the scattering process.

Relaxation time approximation is valid only for either isotropic or elastic scattering events; these are the cases that satisfy

$$\left.\frac{\partial f_A}{\partial t}\right|_{scat} = \sum_{\vec{p}'} S(\vec{p}',\vec{p}) f_A(\vec{p}') - S(\vec{p},\vec{p}') f_A(\vec{p}) =$$

$$= - f_A(\vec{p}) \sum_{\vec{p}'} S(\vec{p},\vec{p}') - S(\vec{p}',\vec{p}) \frac{f_A(\vec{p}')}{f_A(\vec{p})}$$

(Principle of detailed balance: $S(\vec{p},\vec{p}') f_0(\vec{p}) = S(\vec{p}',\vec{p}) f_0(\vec{p}')$)

$$\left.\frac{\partial f_A}{\partial t}\right|_{scat} = - f_A(\vec{p}) \underbrace{\sum_{\vec{p}'} S(\vec{p},\vec{p}') \left[1 - \frac{f_0(\vec{p}) f_A(\vec{p}')}{f_0(\vec{p}') f_A(\vec{p})} \right]}_{\text{these should not depend on } f_0, f_A \text{ !!!}}$$

(Homework: Show that for elastic & isotropic processes the sum does not depend on f_0, f_A !!! See 745 notes & Lundstrom's book.)

<u>Example **1**</u>: Spatially homogeneous sample, perturbed with external fields, then fields turned off, and the sample left to relax:

$$\frac{\partial f}{\partial t} + \frac{\vec{p}}{m} \underbrace{\cancel{\frac{\partial f}{\partial \vec{r}}}}_{\to 0 \text{ homog.}} + \underbrace{\cancel{\vec{F}}}_{\text{no fields}} \cdot \frac{\partial f}{\partial \vec{p}} = \left.\frac{\partial f}{\partial t}\right|_{coll}$$

$$\downarrow \quad \frac{\partial f}{\partial t} = - \frac{f_A}{\tau_f} \approx - \frac{(f - f_0)}{\tau_f} \qquad \frac{\partial f}{\partial t} + \frac{f}{\tau_f} = \frac{f_0}{\tau_f}$$

$$\boxed{f(t) = f_0 + [f(0) - f_0] e^{-t/\tau_f}}$$

Example 2: Uniform electric field, uniform sample; We seek a steady-state solution. Const τ_f.

$$\underbrace{\cancel{\frac{\partial f}{\partial t}}}_{\substack{0 \\ \text{steady state}}} + \underbrace{\cancel{\frac{\vec{p}}{m^*}\cdot\frac{\partial f}{\partial \vec{r}}}}_{\text{homog}} + \vec{F}\cdot\frac{\partial f}{\partial \vec{p}} = \left.\frac{\partial f}{\partial t}\right|_{scatt}$$

$$-e\vec{E}\cdot\frac{\partial f}{\partial \vec{p}} = -\frac{f_A}{\tau_f}$$

$$f_A = +e\vec{E}\cdot\frac{\partial f}{\partial \vec{p}}\cdot\tau_f \qquad \text{(let's assume } \tau_f \approx \text{const.)}$$

$$f \approx f_0 + f_A \approx f_0 + e\tau_f\,\vec{E}\cdot\frac{\partial f_0}{\partial \vec{p}} \approx f_0(\vec{p} + e\tau_f\vec{E})$$

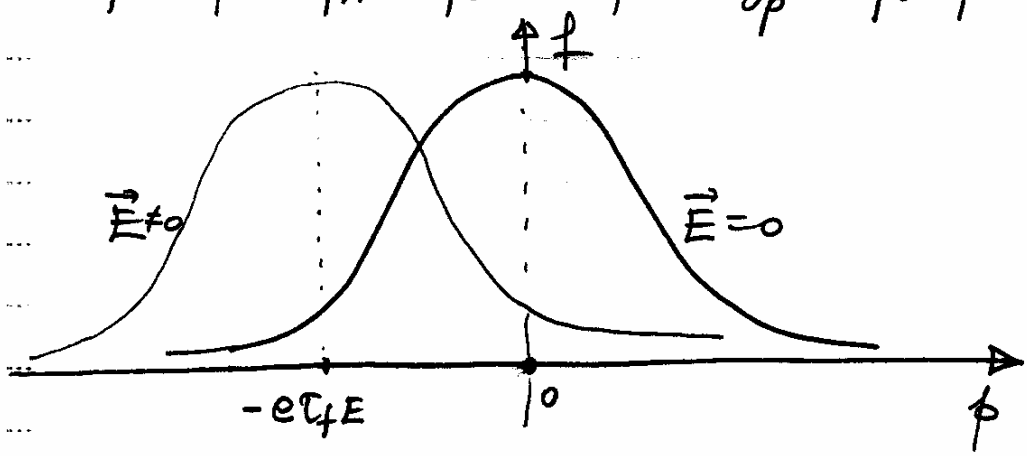

Current? $\vec{J} = -ne\langle\vec{v}\rangle = -\frac{ne}{m^*}\langle\vec{p}\rangle = +\frac{ne}{m^*}\cdot e\tau_f\vec{E}$

Conductivity $\boxed{\sigma = \frac{ne^2\tau_f}{m^*}}$ Drude result

Mobility $\boxed{\mu = \frac{\langle\vec{v}_{\parallel}\rangle}{E} = \frac{e\tau_f}{m^*}}$

Example 3 Homogeneous sample, low homogeneous electric field, steady state, momentum (energy) dependent relaxation time.

$$-e\vec{E}\cdot\frac{\partial f}{\partial \vec{p}} = -\frac{f_A}{\tau_f} \Rightarrow f_A \approx e\tau_f \vec{E}\cdot\frac{\partial f_0}{\partial \vec{p}}$$

$$f_A \approx e\tau_f \vec{E}\cdot\frac{\partial f_0}{\partial \vec{p}} \underset{\text{Max. Boltz.}}{=} -e\tau_f \cdot \frac{(\vec{E}\cdot\vec{p})}{k_B T_L m^*} f_0$$

$$f(\vec{p}) \approx f_0(\vec{p}) + f_0(\vec{p})\left(-\frac{e\tau_f}{k_B T_L m^*}(\vec{E}\cdot\vec{p})\right)$$

$f_0(\vec{p})$: won't contribute to current

$f_0(\vec{p})\left(-\frac{e\tau_f}{k_B T_L m^*}(\vec{E}\cdot\vec{p})\right)$: will contrib. to current, only along the $\vec{E}$ direction

$$\langle \vec{v} \rangle = \frac{\sum_{\vec{p}} \vec{v} f_A(\vec{p})}{\sum_{\vec{p}} f_0(\vec{p})} \qquad \vec{E} = E\vec{e}_z$$

$$\langle v_z \rangle = \frac{1}{\sum_{\vec{p}} f_0(\vec{p})} \cdot \left(\frac{-e\tau_f E}{k_B T_L m^{*2}}\right) \sum_{\vec{p}} p_z^2 f_0(\vec{p})$$

$$= -\frac{eE}{m^*} \frac{\sum_{\vec{p}} \frac{p_z^2}{2m^*} f_0(\vec{p})\tau_f(\vec{p})}{\frac{k_B T_L}{2} \sum_{\vec{p}} f_0(\vec{p})}$$

If τ_f depends on energy only, & not on the direction of the momentum, as is usually the case

$$\langle v_z \rangle = -\frac{eE}{m^*} \frac{\frac{1}{3}\sum_{\vec{p}} \overbrace{\frac{p^2}{2m^*}}^{\varepsilon} f_0(\varepsilon(\vec{p}))\, \tau_f(\varepsilon(\vec{p}))}{\underbrace{\frac{k_B T_L}{2} \cdot n}_{\frac{1}{3}\langle \varepsilon \rangle} V}$$

$$= -\frac{eE}{m^*} \cdot \frac{\langle \varepsilon \tau_f(\varepsilon) \rangle}{\langle \varepsilon \rangle}$$

$$\boxed{\mu = \frac{e}{m^*} \langle\langle \tau_f \rangle\rangle} \qquad \langle\langle \tau_f \rangle\rangle \equiv \frac{\langle \varepsilon \tau_f \rangle}{\langle \varepsilon \rangle}$$

- $\langle \varepsilon \rangle = \frac{3}{2} n k_B T_L = \frac{1}{V} \sum_{\vec{p}} \frac{p^2}{2m^*} f_0(\vec{p})$
- $\langle \varepsilon \tau_f \rangle = \frac{1}{V} \sum_{\vec{p}} \frac{p^2}{2m} \tau_f(\varepsilon(\vec{p})) f_0(\varepsilon(\vec{p}))$

Common scattering mechanisms:

$$\tau_f(\varepsilon) = \tau_0 \left(\frac{\varepsilon(p)}{k_B T_L} \right)^s$$

$$\langle\langle \tau_f \rangle\rangle = \frac{\sum_{\vec{p}} \varepsilon \tau_0 \left(\frac{\varepsilon}{k_B T_L}\right)^s \text{Const.}\; e^{-p^2/2m^* k_B T}}{\sum_{\vec{p}} \text{Const.}\; \varepsilon \cdot e^{-p^2/2m^* k_B T}}$$

$$\sum_{\vec{p}} \rightarrow \frac{V}{(2\pi)^3} \cdot 2 \cdot \frac{1}{\hbar^3} \int d^3\vec{p}$$

$$\langle\langle \tau_f \rangle\rangle = \frac{\tau_0}{(k_B T_L)^s} \frac{\int d^3\vec{p} \cdot \varepsilon^{s+1} e^{-\varepsilon/k_B T}}{\int d^3\vec{p}\; \varepsilon\, e^{-\varepsilon/k_B T}}$$

$$\langle\langle \tau_f \rangle\rangle = \frac{\tau_0}{(k_B T_L)^s} \frac{\int_0^\infty p^2 dp \; \varepsilon^{s+1} e^{-\varepsilon/k_B T}}{\int_0^\infty p^2 dp \; \varepsilon \, e^{-\varepsilon/k_B T}}$$

$$p^2 dp = p\,(p\,dp) = \sqrt{2m^*\varepsilon} \cdot 2m^* d\varepsilon = (2m^*)^{3/2} \varepsilon^{1/2} d\varepsilon$$

$$\langle\langle \tau_f \rangle\rangle = \frac{\tau_0}{\cancel{(k_B T_L)^s}} \cdot \cancel{(k_B T_L)^s} \frac{\int_0^\infty x^{s+3/2} e^{-x} dx}{\int_0^\infty x^{3/2} e^{-x} dx}$$

$$= \tau_0 \boxed{\frac{\Gamma(s+5/2)}{\Gamma(5/2)}}$$

$$\Gamma(z+1) = \int_0^\infty x^z e^{-x} dx$$

$$\Gamma(z+1) = z\Gamma(z) \; ; \quad \Gamma\left(\tfrac{1}{2}\right) = \sqrt{\pi} \; ; \quad \Gamma\left(\tfrac{3}{2}\right) = \frac{\sqrt{\pi}}{2} \; ; \quad \Gamma\left(\tfrac{5}{2}\right) = \frac{3\sqrt{\pi}}{4}$$

$$\boxed{\langle\langle \tau_f \rangle\rangle = \tau_0 \cdot \frac{4}{3\sqrt{\pi}} \cdot \Gamma(s+5/2)}$$

Common scattering mechanisms for which RTA holds

- Acoustic phonon scattering (elastic & isotropic)

$$\frac{1}{\tau(\vec{k})} = \Gamma_{tot}(\vec{k}) = \frac{\Xi_1^2 k_B T}{2\pi \hbar \rho v_s^2} \cdot \left(\frac{2m^*}{\hbar^2}\right)^{3/2} \varepsilon(\vec{k})^{1/2} \Rightarrow \boxed{s_{ac} = -1/2}$$

(isotropic $\tau_m = \tau$)

- Optical phonon scattering : isotropic, not elastic
  (non-polar)

$$\frac{1}{\tau(\vec{k})_{em}^{ab}} = \Gamma_{em}^{ab}(\vec{k}) = \frac{\pi D_0^2}{2\rho\omega_0}\left(N_0 + \frac{1}{2} \mp \frac{1}{2}\right) \cdot \frac{1}{2\pi^2}\left(\frac{2m^*}{\hbar^2}\right)^{3/2} \sqrt{\varepsilon \pm \hbar\omega_0}$$

(Similar thing for inter-valley !!!)

factor is $s = -1/2$ again, but take care of the shift in energy!

- Non-polar optical phonons

  Neither elastic, nor isotropic RTA does not hold

- Ionized impurity scattering

  Not isotropic, but elastic (scattering from a potential center)

  Time to use is the momentum relaxation time:

$$\frac{1}{\tau_m(\vec{k})} = \Gamma_m(\vec{k}) = \frac{N_I Z^2 e^4 m^*}{8\pi\hbar^3 \varepsilon_0^2 \varepsilon_s^2 k^3}\left[\ln\left(1 + 4k^2 L_D^2\right) - \frac{4k^2 L_D^2}{1 + 4k^2 L_D^2}\right]$$

- Weak screening (L_D large), the encircled term behaves as $\sim \frac{1}{k^3}$, so $\tau_m(\varepsilon) \sim \varepsilon^{3/2}$ $\boxed{s_{imp}^{weak} = 3/2}$

- Strong screening, L_D small, expand ln, so the encircled term behaves as

$$\frac{1}{k^3}\left(\cancel{4k^2L_D^2} - \frac{(4k^2L_D^2)^2}{2} - \cancel{(4k^2L_D^2)} + (4k^2L_D^2)^2 + \dots\right.$$

$$= \frac{1}{k^3} \cdot \frac{(4k^2L_D^2)^2}{2} = k \cdot 8L_D^4$$

$$\tau_m(k) \sim k^{-1} \sim \varepsilon^{-1/2} \qquad \boxed{s_{imp}^{strong} = -1/2}$$

Low-Field Transport. Transport Coefficients

We want to describe flow of charge and heat under low fields: low electric field, temperature gradient and possibly a low magnetic field.

- <u>No magnetic field</u>

$$f(\vec{r},\vec{p},t) = f_S(\vec{r},\vec{p},t) + f_A(\vec{r},\vec{p},t)$$

$$f_S = \frac{1}{\exp\theta + 1}, \quad \theta = \left[E_{co}(\vec{r},t) + \varepsilon(\vec{p}) - F_u(\vec{r},t)\right]/k_B T_L$$

also fn of $(\vec{r},t)$

Steady state solution + RTA

$$\underbrace{\cancel{\frac{\partial f}{\partial t}}}_{0} + \frac{\vec{p}}{m^*}\frac{\partial f}{\partial \vec{r}} + \vec{F}\cdot\frac{\partial f}{\partial \vec{p}} = -\frac{f_A}{\tau_f}$$

← RTA approx for collision integral

$f_S \gg f_A$ OK

Also, assumptions $\left|\frac{\partial f_S}{\partial \vec{r}}\right| \gg \left|\frac{\partial f_A}{\partial \vec{r}}\right|$; $\left|\frac{\partial f_S}{\partial \vec{p}}\right| \gg \left|\frac{\partial f_A}{\partial \vec{p}}\right|$

Not easy to justify, but under these assumptions the final result is in agreement with the assumptions (self-consistency of the approach).

$$\hookrightarrow \quad \frac{\vec{p}}{m^*}\cdot\frac{\partial f_S}{\partial \vec{r}} + \vec{F}\cdot\frac{\partial f_S}{\partial \vec{p}} = -\frac{f_A}{\tau_f}$$

$$\frac{\partial f_s}{\partial \vec{r}} = \frac{df_s}{d\theta}\cdot\frac{\partial\theta}{\partial\vec{r}} = \frac{df_s}{d\theta}\times\left\{\frac{\nabla E_{co}-\nabla F_n}{k_B T_L} + \right.$$

$$\left. + \left(E_{co}+\mathcal{E}(\vec{p})-F_n\right)\cdot\nabla\left(\frac{1}{k_B T_L}\right)\right\}$$

$$\frac{\partial f}{\partial \vec{p}} = \frac{df_s}{d\theta}\cdot\frac{\partial\theta}{\partial\vec{p}} = \frac{df_s}{d\theta}\cdot\frac{\vec{p}}{m^* k_B T_L}$$

Therefore, we obtain that

$$f_A = -\tau_f\left\{\frac{\vec{p}}{m^*}\cdot\left[\cancel{\frac{\nabla E_{co}}{k_B T}} - \frac{\nabla F_n}{k_B T} + \left(E_{co}+\mathcal{E}(\vec{p})-F_n\right)\nabla\frac{1}{k_B T_L}\right]\right.$$

$$\left. + \underbrace{\vec{F}}_{-\nabla\vec{E}_{co}}\cdot\cancel{\frac{\vec{p}}{m^* k_B T_L}}\right\}\frac{df_s}{d\theta}$$

($\vec{F} = -\nabla\vec{E}_{co}$ when <u>no mag field</u>)

$$\boxed{f_A = \frac{\tau_f}{k_B T}\left(-\frac{df_s}{d\theta}\right)\left(\frac{\vec{p}}{m^*}\cdot\vec{\mathcal{F}}\right)}$$

$\mathcal{F}$ – generalized force

$$\boxed{\vec{\mathcal{F}} = -\vec{\nabla}F_n + T_L\left(E_{co}+\mathcal{E}(\vec{p})-F_n\right)\vec{\nabla}\left(\frac{1}{T_L}\right)}$$

If one assumes that τ_f depends on the magnitude of $\vec{p}$ and not direction, then we see that f_A is of the form

$$f_A = g(p)\cos\theta, \quad \theta = \text{angle between } \vec{p} \text{ and } \vec{\mathcal{F}}$$

- <u>Current</u>

Charge transport & heat transport are inseparable.

Charge current $\boxed{\vec{J} = -\frac{e}{V}\sum_{\vec{p}} \vec{v} f_A(\vec{p})}$

Heat current ?

$$\vec{J}_W = -\frac{e}{V}\sum_{\vec{p}} \mathcal{E}(\vec{p}) f_A(\vec{p})$$

NO! This has a drift component, we want just the random component

A bit of help from thermodynamics

$$dQ = dU - F_n dN$$

$$\vec{J}_Q = \vec{J}_U - F_n \vec{J}_N$$

heat current

"kin. energy" current + "pot. energy current" = total energy

"particle current" — that's our charge current without the $-e$

$$\boxed{\vec{J}_Q = \frac{1}{V}\sum_{\vec{p}} \vec{v} f_A(\vec{p}) \Big[\underbrace{E_{C0} + \mathcal{E}(\vec{p})}_{\substack{\text{total energy} \\ \text{(potential + kinetic)}}} - F_n \Big]}$$

If we put in the form we obtained for f_A, $f_A = \frac{\tau_f}{k_B T}\left(-\frac{df_s}{d\theta}\right) \times \left(\frac{\vec{p}}{m^*}\cdot\vec{F}\right)$

$$\vec{J} = -\frac{e}{V}\sum_{\vec{p}} \frac{\tau_f(p)}{k_B T_L}\left(-\frac{df_s}{d\theta}\right)\vec{v}(\vec{v}\cdot\vec{F})$$

$$\vec{J}_Q = \frac{1}{V k_B T_L}\sum_{\vec{p}} \vec{v}\,\tau_f(p)\left(-\frac{df}{d\theta}\right)(\vec{v}\cdot\vec{F})\Big[E_{C0} + \mathcal{E}(\vec{p}) - F_n\Big]$$

Transport Coefficients

There are 4 transport tensors that can be deduced from the coupled current equations

$$\vec{J} = [\sigma]\nabla\left(\frac{F_n}{e}\right) + [B]\nabla\left(\frac{1}{T_L}\right)$$

$$\vec{J}_Q = [p]\nabla\left(\frac{F_n}{e}\right) + [K]\nabla\left(\frac{1}{T_L}\right)$$

These tensors are diagonal for cubic semiconductors, but in general they needn't be.

Conductivity tensor

$$\sigma_{ij} = \frac{-e^2}{k_B T V} \cdot \sum_{\vec{p}} v_i v_j \tau_f(p) \overset{= -f_s \text{ (nondeg)}}{\frac{df_s}{dE}} =$$

$$= \delta_{ij} \underbrace{\frac{e^2}{k_B T m^*}}_{\frac{2}{3}\langle E\rangle} \cdot \underbrace{\frac{1}{V}}_{} \underbrace{\sum m^* v_i^2 \tau_f(\vec{p}) \frac{df_s}{dE}}_{\frac{2}{3}\frac{1}{V}\underbrace{\sum \frac{m^* v^2}{2} \tau_f(p) \frac{df_s}{dE}}_{n\langle E\tau\rangle}}$$

$$= \delta_{ij} \frac{e^2}{m^*} \cdot n \frac{\langle E\tau_f\rangle}{\langle E\rangle} = \delta_{ij} \frac{e^2 n}{m^*} \langle\langle \tau_f \rangle\rangle$$

what we got before

Anisotropic effective mass

In case of silicon, per valley we have $\frac{n}{6}$ electrons. Say for one of the ellipsoids the electric field coincides with its ~~longer~~ principal axis corresponding to m_e^*. Then

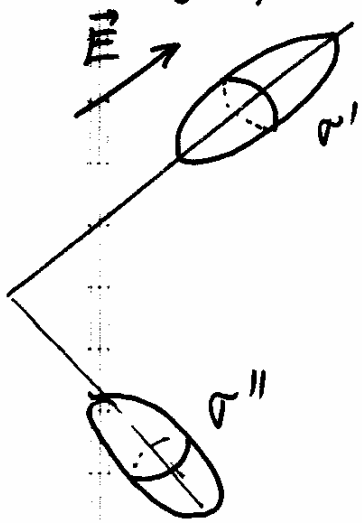

$$\sigma' = \frac{n}{6} \cdot e \cdot \frac{e\langle\langle\tau\rangle\rangle}{m_e^*}$$

There will be two valleys with such σ'. However, there will be another 4 with

$$\sigma'' = \frac{n}{6} \cdot e \cdot \frac{e\langle\langle\tau\rangle\rangle}{m_t^*}$$

Total $\quad \sigma = 2\sigma' + 4\sigma'' = \frac{ne^2\langle\langle\tau\rangle\rangle}{6}\left(\frac{2}{m_e^*} + \frac{4}{m_t^*}\right)$

Conductivity mass m_c^*

$$\boxed{\frac{1}{m_c^*} = \frac{1}{3m_e^*} + \frac{2}{3m_t^*}}$$

High degree of symmetry $\longrightarrow$ mass anisotropy will not be seen in experiment

Transport in a weak magnetic field

$$\boxed{\frac{\vec{p}}{m^*}\cdot\vec{\nabla}f + \left[-e\vec{E} - e(\vec{v}\times\vec{B})\right]\cdot\frac{\partial f}{\partial\vec{p}} = -\frac{f_A}{\tau_f}}$$

The procedure for magnetic field present will require keeping terms of order $\vec{B}\cdot\vec{F}$ and/or $\vec{B}\times\vec{F}$, i.e., it requires starting from the solution for $E\neq 0$ as the beginning, and then perturbing it. Namely, if we were to start with $E=0, B=0$, then

$$(\vec{v}\times\vec{B})\cdot\frac{\partial f_s}{\partial\vec{p}} \approx \underbrace{(\vec{v}\times\vec{B})\cdot\vec{v}}_{0}\cdot\left(-\frac{f_s}{m^* k_B T}\right)$$

and the B-field term would then vanish. Therefore, we have to have some information on the anti-symmetric part of the distribution function. (In a nutshell, to see the effect from magnetic field, you have to have net current first.)

$$f_A' = f_A'(E\neq 0, B=0) = \frac{\tau_f}{k_B T}\left(-\frac{df_s}{d\theta}\right)\left(\frac{\vec{p}}{m^*}\cdot\vec{F}\right)$$

$$-e(\vec{v}\times\vec{B})\cdot\frac{\partial f_A'}{\partial\vec{p}} = -\frac{f_A''}{\tau_f}$$

$$f_A'' = \tau_f\, e(\vec{v}\times\vec{B})\cdot\frac{\partial}{\partial\vec{p}} f_A'$$

Terms from f_A' that produce $\vec{v}$ will die out when they meet $\vec{v}\times\vec{B}$ in the dot product, so

$$f_A'' = \tau_f\, e(\vec{v}\times\vec{B})\cdot\vec{\mathcal{F}} \cdot \frac{\tau_f}{k_B T m^*}\left(-\frac{\partial f_s}{\partial \theta}\right)$$

$$= -\frac{e\tau_f^2}{m^* k_B T}\cdot\left(\frac{\partial f_s}{\partial \theta}\right)\cdot \underbrace{(\vec{v}\times\vec{B})\cdot\vec{\mathcal{F}}}_{(\vec{B}\times\vec{\mathcal{F}})\cdot\vec{v}} \quad \text{(cyclic perms.)}$$

$$\vec{J} = -\frac{e}{V}\sum_{\vec{p}} \vec{v}\,(f_A' + f_A'')$$

The first term will yield just $\vec{J} = [\sigma]\vec{E}$, where

The second term will yield $\vec{\mathcal{F}} = -\vec{\nabla}\vec{F}_n = -e\vec{E}$ (no conc. grad.)

$$\vec{J}'' = +\frac{e}{V}\sum_{\vec{p}} \vec{v}\,\frac{e\tau_f^2}{m^* k_B T}\left(\frac{\partial f_s}{\partial \theta}\right)\left[\vec{B}\times(-e\vec{E})\right]\cdot\vec{v}$$

$$= \frac{1}{V}\sum_{\vec{p}} \frac{e^3\tau_f^2}{m^* k_B T}\left(-\frac{\partial f_s}{\partial \theta}\right)\underbrace{\left\{(\vec{B}\times\vec{E})\cdot\vec{v}\right\}}_{\sum_{ijk}\varepsilon^{ijk} v_i B_j E_k}\vec{v}$$

tensor Levi-Civita

$$J_\ell'' = \frac{1}{V}\sum_{\vec{p},i,j,k} \frac{e^3\tau_f^2}{m^* k_B T}\left(-\frac{\partial f_s}{\partial \theta}\right)\varepsilon^{ijk} v_i v_\ell B_j E_k$$

~~We saw that when $\tau =$~~

$$\boxed{\sigma_{\ell k}'' = \frac{1}{V}\sum_{\vec{p},i,j} \frac{e^3\tau_f^2}{m^* k_B T}\left(-\frac{\partial f_s}{\partial \theta}\right)\varepsilon^{ijk} v_i v_\ell B_j}$$

- Diagonal terms $l=k$. $\sum_{i,j} \varepsilon^{ijl} v_i v_l B_j$. This one needs to be integrated later over θ, φ, and it will give a non-zero result only for $i=l$. However, then we will have $\sum_j \varepsilon^{ljl} v_l^2 = 0$ because of the repeated index in ε.

Diagonal terms all zero $\rightarrow$ no mag. field contrib to the conductivity tensor

- Off-diagonal terms

$l \neq k$. Again, the only non-zero after angular integr.

$$\sigma''_{lk} = \frac{1}{V} \sum_{\vec{p}, j} \frac{e^3 \tau_f^2}{m^* k_B T} \left(-\frac{\partial f_s}{\partial \theta}\right) \varepsilon^{ljk} v_l^2 B_j$$

12 $\quad \sum_j \varepsilon^{1j2} v_1^2 B_j = v_1^2 (-B_3)$

13 $\quad \sum_j \varepsilon^{1j3} v_1^2 B_j = v_1^2 B_2$

$\vdots$

$$\sigma'' = \begin{array}{|c|c|c|} \hline 0 & -\gamma B_3 & +\gamma B_2 \\ \hline \gamma B_3 & 0 & -\gamma B_1 \\ \hline -\gamma B_2 & +\gamma B_1 & 0 \\ \hline \end{array}$$

$$\sigma = \frac{1}{V}\cdot\frac{2}{3}\sum_{\vec{p}}\frac{e^3\tau p^2}{m^{*2}\underbrace{k_B T}_{\frac{2}{3}\langle\varepsilon\rangle}}\cdot\left(-\frac{\partial f_s}{\partial\theta}\right)\cdot\frac{m^* v^2}{2}$$

f_s

$$= \frac{e^3 n}{m^{*2}}\cdot\frac{\langle\tau^2\varepsilon\rangle}{\langle\varepsilon\rangle}$$

$$= \frac{e^3 n}{m^{*2}}\cdot\langle\langle\tau^2\rangle\rangle$$

$$\sigma_0 = \frac{e^2 n}{m^*}\frac{\langle\tau\varepsilon\rangle}{\langle\varepsilon\rangle} = \frac{e^2 n}{m^*}\langle\langle\tau\rangle\rangle$$

$$\sigma = \frac{e}{m^*}\cdot\underbrace{\left(\frac{ne^2}{m^*}\cdot\langle\langle\tau\rangle\rangle\right)}_{\sigma_0}\cdot\frac{\langle\langle\tau^2\rangle\rangle}{\langle\langle\tau\rangle\rangle}$$

$$= \sigma_0\cdot\underbrace{\left(\frac{e}{m^*}\cdot\langle\langle\tau\rangle\rangle\right)}_{=\mu}\underbrace{\left(\frac{\langle\langle\tau^2\rangle\rangle}{\langle\langle\tau\rangle\rangle^2}\right)}_{=r_H}$$

Hall factor

$$\boxed{\sigma = \sigma_0\cdot\mu\cdot r_H}$$

$$r_H\cdot\mu = \mu_H$$

Hall factor — drift mob — Hall mobility

$$\sigma = \sigma_0\begin{pmatrix} 1 & -\mu_H B_3 & \mu_H B_2 \\ \mu_H B_3 & 1 & -\mu_H B_1 \\ -\mu_H B_2 & \mu_H B_1 & 1 \end{pmatrix}$$

4. Monte Carlo simulation of bulk semiconductors

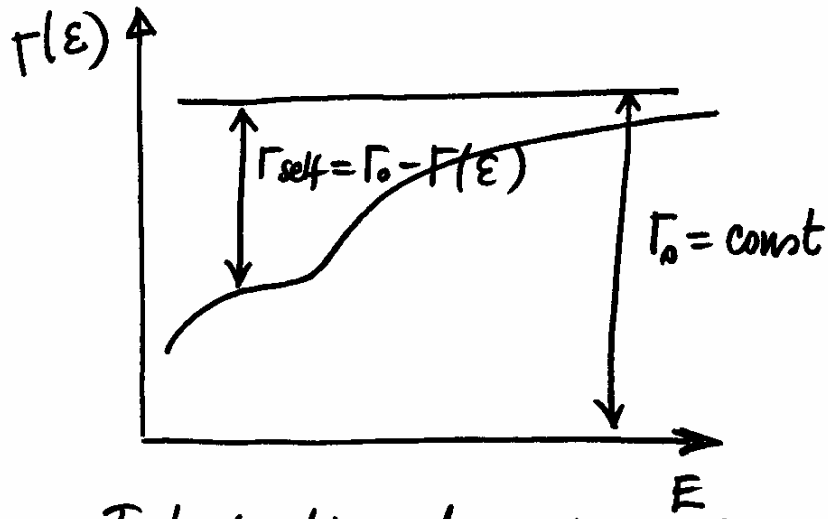

Introduction of self-scattering greatly simplifies the mathematics, as it appears that the total scattering rate is independent of energy

$$\Gamma_0 = \Gamma_{self}(\varepsilon) + \Gamma_{tot}(\varepsilon)$$

$$= \Gamma_{self}(\varepsilon) + \sum_{\substack{i \text{ over all} \\ \text{scatt. mech}}} \Gamma_i(\varepsilon)$$

If you have $n(\varepsilon,t)$ electrons at time t, due to scattering at $t+dt$ you will have lost

$$n(\varepsilon, t+dt) - n(\varepsilon, t) = -\Gamma_0 \, n(\varepsilon, t) \, dt$$

$$\frac{dn(\varepsilon,t)}{dt} = -\Gamma_0 \, n(\varepsilon,t)$$

Since we chose $\Gamma_0 = const.$ this eqn does not depend on ε

$$n(\varepsilon,t) = n(\varepsilon,0)\, e^{-\Gamma_0 t}$$

Probability of one electron scatters for the first time between t and $t+dt$

$$P(t)dt = \Gamma_0 \cdot \underbrace{e^{-\Gamma_0 t}}_{\text{probability that it survived without collision since } t=0} dt$$

Where do random numbers come in?
We need to embody the fact that ~~all~~ scattering times are equally probable

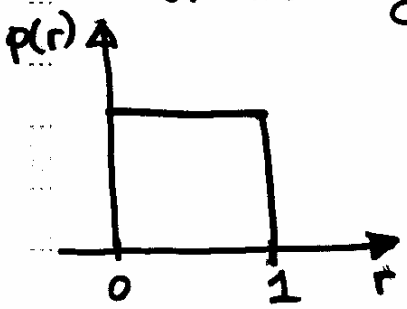

$$P(r)dr = P(t)dt$$

For r's between 0 and 1,
$P(r) = 1$

$$dr = P(t)\,dt$$

$$\int_0^{r_c} dr = \int_0^{t(r_c)} P(t)dt = \Gamma_0 \int_0^{t(r_c)} e^{-\Gamma_0 t} dt$$

$$= \cancel{\Gamma_0} \left. \frac{e^{-\Gamma_0 t}}{-\cancel{\Gamma_0}} \right|_0^{t(r_c)}$$

23

$$\boxed{r_c = 1 - e^{-t(r_c)\Gamma_0}}$$

computer generated # between 0 and 1

$r_1 = 1 - r_c$ ← also a uniformly distributed ~~[illegible]~~ random #

$$\boxed{t = -\frac{\ln(r_1)}{\Gamma_0}}$$

FREE FLIGHT TIME

Selection of a scattering event

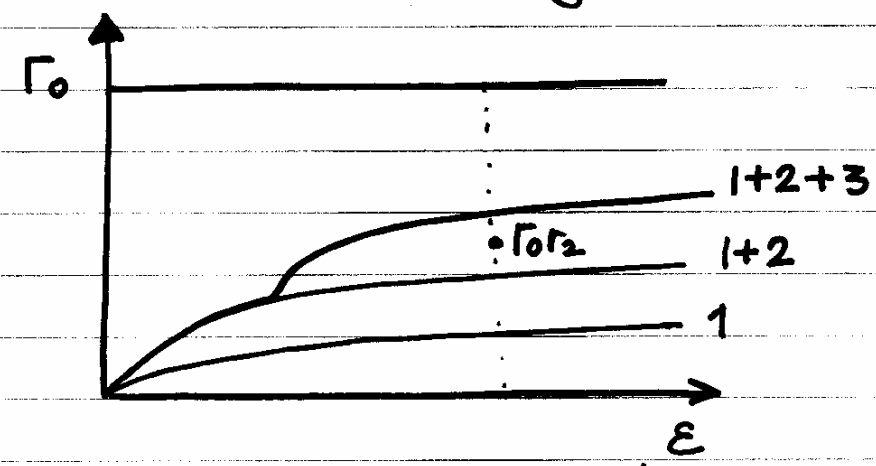

In this case, mechanism 3 is selected

A new random # to select the scattering mechanism

j-th scatt. event is selected if

$$\boxed{\sum_{i=1}^{j-1} \Gamma(i) \leq r_2 \cdot \Gamma_0 < \sum_{i=1}^{j} \Gamma(i)}$$

second random # you need

Updating momentum after scattering

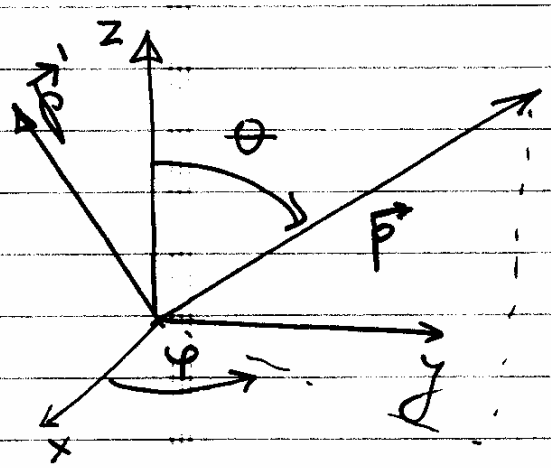

$\vec{p}$ – initial momentum w/ respect to it we measure the distribution of the final angle (from particle's pt of view)

How to select final states? In the rotated coordinate system

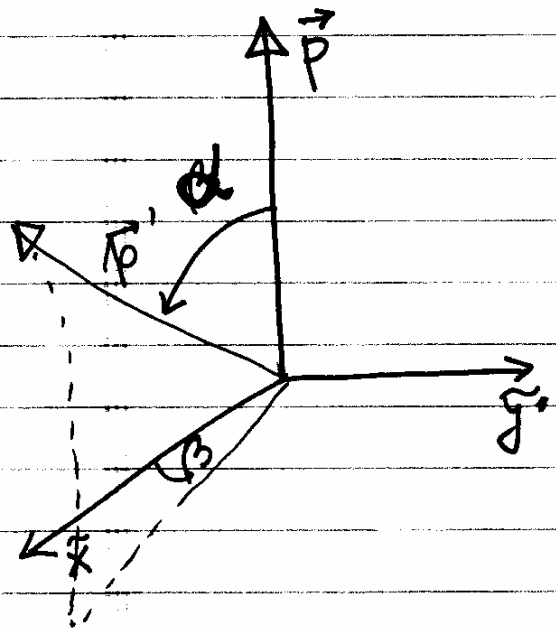

$$P(\beta)\,d\beta = \frac{\int_0^{\pi} S(\vec{p},\vec{p}')\sin\alpha\, d\alpha}{\int_0^{2\pi} d\beta \int_0^{\pi} \sin\alpha\, d\alpha\; S(\vec{p},\vec{p}')} \cdot d\beta$$

~~For isotropic scattering~~

We have not seen any scattering mechanism that would bear a dependence on β, thus

$$P(\beta)\,d\beta = \frac{d\beta}{2\pi} = \underbrace{P(r_3)}_{1}\, dr_3$$

$1 \leftarrow$ uniformly distrib between 0 & 1

~~$\beta = 2\pi r_3$~~

Azimuthal angle distrib. $\boxed{\beta = 2\pi \cdot r_3}$ Our 3rd random number

Distribution of the polar angle

$$P(\alpha)\,d\alpha = \frac{\int_0^{2\pi} d\beta\, S(\vec{p},\vec{p}')\sin\alpha\, d\alpha\, d\beta}{\int_0^{2\pi} d\beta \int_0^{\pi} S(\vec{p},\vec{p}')\sin\alpha\, d\alpha\, d\beta} = \left(\text{since nothing depends on } \beta\right)$$

$$= \frac{S(\vec{p},\vec{p}')\sin\alpha\, d\alpha}{\int_0^{\pi} S(\vec{p},\vec{p}')\sin\alpha\, d\alpha} = P(r_4)\,dr_4$$

For isotropic scattering (S does not depend on α)

$$P(r_4)\,dr_4 = P(\alpha)\,d\alpha = \frac{\sin\alpha\, d\alpha}{\int_0^{\pi}\sin\alpha\, d\alpha} = \frac{\sin\alpha\, d\alpha}{2}$$

$$\int_0^{r_4} dr_4 = \int_0^{\alpha(r_4)} \frac{\sin\alpha\, d\alpha}{2} = -\frac{\cos\alpha}{2}\Big|_0^{\alpha(r_4)} = \frac{1-\cos\alpha(r_4)}{2}$$

$$\boxed{r_4 = \frac{1-\cos\alpha(r_4)}{2}}$$ isotropic

Note: the distribution over the solid angle is uniform $P(\Omega)\,d\Omega = \frac{1}{4\pi}\,d\Omega$

However, that does not mean the distribution over α is uniform

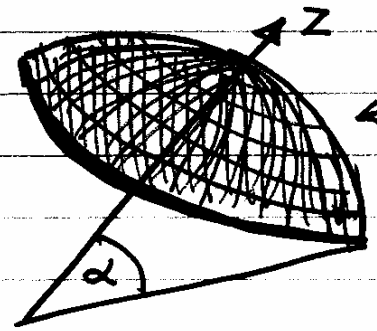

this is $4\pi \cdot r_4$

In the case of anisotropic scattering,

$$\boxed{r_4 = \frac{\int_0^{\alpha(r_4)} S(\vec{p},\vec{p}')\sin\alpha\, d\alpha}{\int_0^{\pi} S(\vec{p},\vec{p}')\sin\alpha\, d\alpha}}$$ anisotropic

Initialization of the carrier distribution

We know that the probability of filling a state with energy $\mathcal{E}$ is given by

$$f(\mathcal{E}) = \frac{1}{e^{\frac{\mathcal{E}-\mathcal{E}_F}{k_BT}}+1} \underset{\text{nondegen.}}{\sim} e^{-\left(\frac{\mathcal{E}-\mathcal{E}_F}{k_BT}\right)}$$

The quantity that is distributed according to the Maxwell Boltzmann is actually momentum

$$\frac{\int_{-\infty}^{p_i} e^{-p_i^2/2mk_BT}\, dp_i}{\int_{-\infty}^{\infty} e^{-p_i^2/2mk_BT}\, dp_i}$$

However, the above integral does not exist in a closed form (it's an error function!), and is thus inconvenient

What is used instead is an exponential dependence of the probability distribution ~~of~~ on the energy, while bearing in mind that the ~~expectation~~ average thermal energy per carrier should be $(3/2)k_BT$.

Initial energy distribution

An approximate way of sampling energy according to a Maxwellian distribution is using

$$r_5 = e^{-\varepsilon/(3/2\, k_B T)}$$

This form captures the exponential decay of the probability, and ensures that $\langle \varepsilon \rangle = 3/2\, k_B T$.

It is not the exact distribution, because energies are actually distributed according to

$$p(\varepsilon)\,d\varepsilon = \frac{g(\varepsilon)\, e^{-\varepsilon/k_B T}\, d\varepsilon}{\int_0^\infty g(\varepsilon)\, e^{-\varepsilon/k_B T}\, d\varepsilon}, \quad \text{in 3D } g(\varepsilon) \sim \sqrt{\varepsilon}$$

and it cannot be integrated analytically for an arbitrary ε, which makes the selection of ε by using random numbers difficult.

Bottom line, initialize energy according to

$$\varepsilon(r_5) = -\frac{3}{2} k_B T \ln r_5$$

To assign momentum direction, use prescription for isotropic scattering.

• Why can't we simply use $\Gamma_{max}(\mathcal{E})$ from the scattering table for an electron of given energy? Why do we need self-scattering at all?

Consider ~~electro~~ $n(0)$ electrons that started with energy $\mathcal{E}(0) = \frac{\hbar^2 \vec{p}^2}{2m}$. Then, those that have remained unscattered till time t, have a chance of being lost to scattering with the probability per unit time given by $\Gamma\left(\frac{(\vec{p} - e\vec{E}t)^2}{2m^*}\right)$

$$\frac{dn}{dt} = -\Gamma\left(\frac{(\vec{p} - e\vec{E}t)^2}{2m^*}\right) \cdot n$$

$$n(t) = n(0) \exp\left(-\int_0^t d\tau\, \Gamma\left[\frac{(\vec{p} - e\vec{E}\tau)^2}{2m^*}\right]\right)$$

Probability of being unscattered after t is

$$\frac{n(t)}{n(0)} = \exp\left(-\int_0^t d\tau\, \Gamma\left[\frac{(\vec{p} - e\vec{E}\tau)^2}{2m^*}\right]\right)$$

Probability of scattering for the first time after time t

$$P(t)\,dt = \Gamma\left(\frac{(\vec{p} - e\vec{E}t)^2}{2m^*}\right) \exp\left(-\int_0^t d\tau\, \Gamma\left[\frac{(\vec{p} - e\vec{E}\tau)^2}{2m}\right]\right) dt$$

$$\parallel \qquad\qquad\qquad \parallel$$

$$P(r_1)\,dr_1 \qquad dt\left(-\frac{d}{dt}\left\{\exp\left(-\int_0^t d\tau\, \Gamma\left[\frac{(\vec{p} - e\vec{E}\tau)^2}{2m}\right]\right)\right\}\right)$$

$$r_1 = -\exp\left(-\int_0^t d\tau\, \Gamma\left(\frac{(\vec{p}-e\vec{E}\tau)^2}{2m^*}\right)\right) + 1$$

$1 - r_1 = r_1'$ (also a uniformly distributed ~~[illegible]~~ random number)

$$r_1' = \exp\left(-\int_0^{t(r_1')} d\tau\, \Gamma\left[\frac{(\vec{p}-e\vec{E}\tau)^2}{2m^*}\right]\right)$$

$$\boxed{\int_0^{t(r_1)} d\tau\, \Gamma\left(\frac{(\vec{p}-e\vec{E}\tau)^2}{2m^*}\right) = -\ln r_1'}$$

So for an electron ~~[illegible]~~ starting with energy $\mathcal{E}(0) = p^2/2m^*$, free flight time ~~[illegible]~~ would have to be generated by matching the above integral with $-\ln r_1'$, and do so for all initial energies and all possible r's $\leftrightarrow$ flight times, if that's something you want to look up in a table.

Just imagine how much more difficult it is in a device, where during the flight the position changes, and w/ the position possibly the electric field changes.

5. High-Field Transport

Velocity saturation

Gain of the energy from the field balanced by emission of phonons.

$$\frac{dW}{dt} = \vec{J}_n \cdot \vec{E} - \left\langle\!\left\langle \frac{1}{\tau_E} \right\rangle\!\right\rangle (W - W^0)$$

energy balance equation

gain from field — loss from scattering

W – total energy, $W = nu$, u – energy per carrier

$\vec{E} = E_z \vec{e}_z$ $\quad J_{nz} = n e \mu_n E + n D_n \frac{dn}{dz}$

(near equilibrium $\frac{D}{\mu} = \frac{kT}{e}$, but in general it is $\frac{2u_{zz}}{e}$, where u_{zz} is 'z-direction energy', obtained by averaging ~~and~~ $p_z v_z$.)

~~Homogeneous case: $J_{nz} = n e \mu_n E$ and $u = u_z$~~

$$J_{nz} = \frac{1}{E} \cdot \left\langle\!\left\langle \frac{1}{\tau_E} \right\rangle\!\right\rangle \cdot n (u - u^0)$$ from energy balance eqn.

$$\left\langle\!\left\langle \frac{1}{\tau_E} \right\rangle\!\right\rangle \sim \frac{1}{\langle \tau_E \rangle}$$ up to a factor of order unity

We know that, if emission of energetic (optical or intervalley) phonons dominates, and they're assumed dispersionless

$$\frac{1}{\tau_E} = \sum S(\vec{p}, \vec{p}') \left(1 - \frac{\varepsilon - \hbar\omega_0}{\varepsilon}\right) = \frac{\hbar\omega_0}{\varepsilon} \cdot \frac{1}{\tau}$$

For non-polar phonons or intervalley phonons

$$\frac{1}{\tau_m} = \frac{1}{\tau}$$

so $\quad \tau_E = \tau_m \cdot \frac{\varepsilon}{\hbar\omega_0} \Rightarrow \langle \tau_E \rangle \underset{\text{approx.}}{\approx} \langle \tau_m \rangle \frac{\varepsilon u}{\hbar\omega_0}$

$$J_{nz} = \cancel{n}e v_d \approx \frac{1}{E} \cdot \frac{1}{\langle \tau_\varepsilon \rangle} \cdot \cancel{n}(u - u_0)$$

$$e \cdot E \cdot \frac{e\langle \tau_m \rangle}{m^*} = \frac{1}{E} \cdot \frac{1}{\langle \tau_\varepsilon \rangle} \cdot (u - u_0)$$

For $u \gg u_0$ (high fields, much energy gained from the field)

$$e^2 \frac{E \langle \tau_m \rangle}{m^*} \approx \frac{1}{E} \cdot \cancel{u} \cdot \frac{1}{\langle \tau_m \rangle} \cdot \frac{\hbar\omega_0}{\cancel{u}}$$

$$\langle \tau_m \rangle^2 = \frac{\hbar\omega_0 \cdot m^*}{(eE)^2}$$

$$\boxed{\langle \tau_m \rangle = \frac{\sqrt{\hbar\omega_0 m^*}}{eE}}$$

Momentum relaxation rate behaves as $1/E$, therefore velocity behaves as

$$v_d = \frac{eE}{m^*} \cdot \langle \tau_m \rangle = \frac{\cancel{eE}}{m^*} \cdot \frac{\sqrt{\hbar\omega_0 m^*}}{\cancel{eE}}$$

$$\boxed{v_d = \sqrt{\frac{\hbar\omega_0}{m^*}}}$$

INDEPENDENT OF E!!!

Distribution function in the presence of a strongly inelastic and anisotropic scattering (e.g. POP)

$$\frac{\partial f}{\partial t} + \frac{\vec{p}}{m^*}\cdot\frac{\partial f}{\partial \vec{r}} + (e\vec{E})\cdot\frac{\partial f}{\partial \vec{p}} = \left.\frac{\partial f}{\partial t}\right|_{scatt}$$

Looking for a steady state solution ($\frac{\partial f}{\partial t}=0$) in bulk (homogeneous, $\frac{\partial f}{\partial \vec{r}}=0$).

We'll split the scattering mechanisms into: elastic or isotropic, and describe these cumulatively by the relaxation time approximation & a relaxation time τ_f (remember that for isotropic $\tau=\tau_m$ is used, and for elastic τ_m.)

The remaining inelastic, anisotropic scatt. mechanism we will describe in simplified terms (see D.K. Ferry, "Semiconductor Transport," p. 171):

imagine the particle can be accelerated by the field until it reaches $\hbar\omega_0$ (your dispersionless optical phonon), and then it gets scattered back to zero energy (we do not allow carriers to have more than $\hbar\omega_0$ energy, or momentum magnitude $p_0 \equiv \sqrt{2m^*\hbar\omega_0}$

$$\left.\frac{\partial f}{\partial t}\right|_{scatt} = \underbrace{-\frac{f_A}{\tau_f}\Big|_{\substack{elastic\\ isotropic}}}_{RTA} + \left.\frac{\partial f}{\partial t}\right|_{\substack{inelastic\\ anisotropic}}, \text{ where}$$

Choose positive p-axis in the direction opposite the field, i.e. the direction of the expected drift velocity!

$$\left.\frac{\partial f}{\partial t}\right|_{\substack{\text{incl.}\\ \text{anisotr}}} = -a f(p_0)\left[\delta(p-p_0)+\delta(p+p_0) - 2\delta(p)\right]$$

If we work in 1D

$$+eE\frac{\partial f}{\partial p} = -\frac{f_A}{\tau_f} - a f(p_0)\left[\delta(p-p_0)+\delta(p+p_0)-2\delta(p)\right]$$

If we change $p \to -p$

$$+eE\left.\frac{\partial f}{\partial p}\right|'_{-p} = +eE\left(\frac{\partial f_S}{\partial p}+\frac{\partial f_A}{\partial p}\right)\Big|_{-p}$$

$$= +eE\left(-\left.\frac{\partial f_S}{\partial p}\right|_p + \left.\frac{\partial f_A}{\partial p}\right|_p\right)$$, so we've got

At p:

$$+eE\frac{\partial f_S}{\partial p} + eE\frac{\partial f_A}{\partial p} = -\frac{f_A}{\tau_f} - a f(p_0)\left[\delta(p-p_0)+\delta(p+p_0) - 2\delta(p)\right]$$

At −p, written in terms of those at p

$$+eE\frac{\partial f_S}{\partial p} + eE\frac{\partial f_A}{\partial p} = \frac{f_A}{\tau_f} - a f(p_0)\left[\ -\ \|\ -\ \right]$$

$$\Downarrow$$

$$\boxed{\begin{aligned} eE\frac{\partial f_S}{\partial p} &= -\frac{f_A}{\tau_f} \\ eE\frac{\partial f_A}{\partial p} &= -a f(p_0)\left[\delta(p-p_0)+\delta(p+p_0) - 2\delta(p)\right] \end{aligned}}$$

Let's find the antisymmetric part of the distribution function, f_A, from the second of the equations

(Choose $a = +eE$, a matter of convenience)

$$\frac{\partial f_A}{\partial p} = -f(p_0)\left[\delta(p-p_0) + \delta(p+p_0) - 2\delta(p)\right]$$

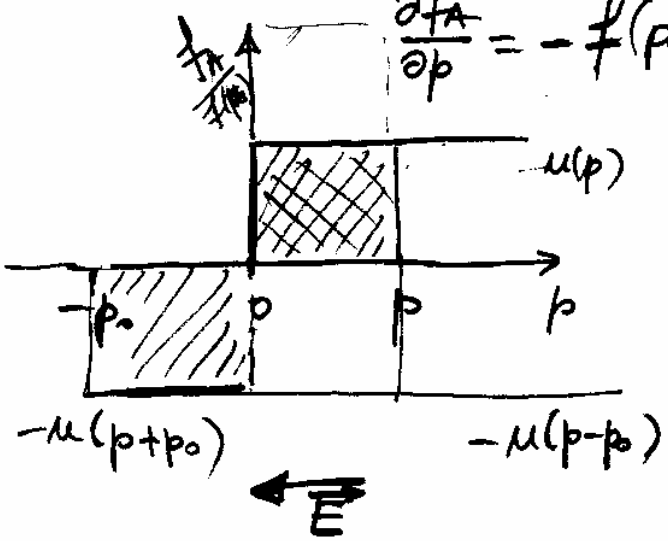

$$f_A = f(p_0)\left[2u(p) - u(p-p_0) - u(p+p_0)\right]$$

(integration const. must be zero, in order for f_A to be antisymmetric)

Note how a had to be chosen so $af(p_0)$ is negative, because we expect that from f_A we'll have more carriers at $p>0$ than at $p<0$ (due to the field.)

Now go back to

$$eE\frac{\partial f_s}{\partial p} = -\frac{1}{\tau_f}\cdot f(p_0)\left[2u(p) - u(p-p_0) - u(p+p_0)\right]$$

$$f_s(p) = +\frac{f(p_0)}{eE\tau_f}\left[C + \begin{cases} -(p-p_0), & 0<p<p_0 \\ +(p+p_0), & -p_0<p<0 \end{cases}\right.$$

f_s has to vanish at $|p| \geq p_0$ (the model for inelastic scattering prevents us from having momenta larger than p_0)

$$f_s(p_0^+) = f_s(-p_0^-) = 0$$

Another reasoning we can use is that at $p \to p_0^+$, the distribution function will vanish, as the electric field accelerates the carriers towards the positive values

$$f_s(-p_0^+) + f_A(-p_0^+) = -f(p_0) + \frac{f(p_0)}{eE\tau_f} \cdot C = 0$$

$$C = eE\tau_f$$

If we take instead of the momentum-dependent τ_f its averaged, say, double-bracketed value, C becomes

$$\boxed{C \approx E \cdot m^* \mu}$$

Altogether,

$$f(p) = f_s(p) + f_A(p) = \begin{cases} 0 < p < p_0 : \dfrac{f(p_0) \cancel{- E\tau_f}\, e\tau_f}{\cancel{eE\tau_f}} - \\ \qquad - (p - p_0)\dfrac{f(p_0)}{eE\tau_f} + f(p_0) \\ -p_0 < p < 0 : \cancel{f(p_0)} + \dfrac{f(p_0)(p+p_0)}{eE\tau_f} \\ \qquad - \cancel{f(p_0)} \\ |p| \geq p_0 : \quad 0 \end{cases}$$

$$\boxed{f(p) = f(p_0) \begin{cases} 0, & |p| \geq p_0 \\ 2 - \dfrac{(p-p_0)}{eE\tau_f}, & 0 < p < p_0 \\ \dfrac{p+p_0}{eE\tau_f}, & -p_0 < p < 0 \end{cases}}$$

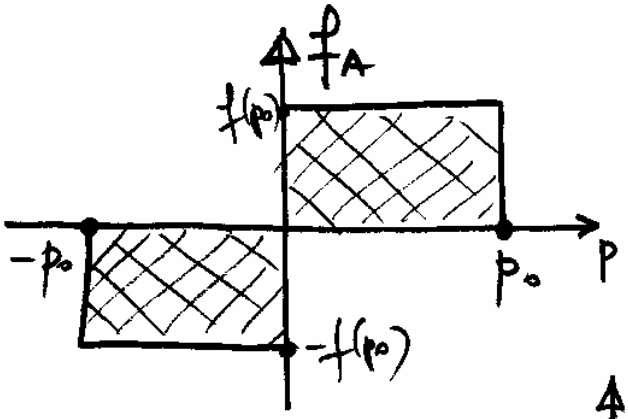

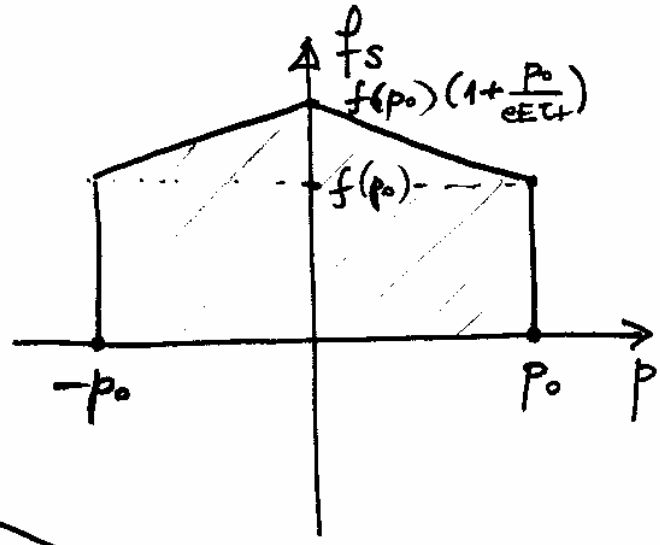

With field

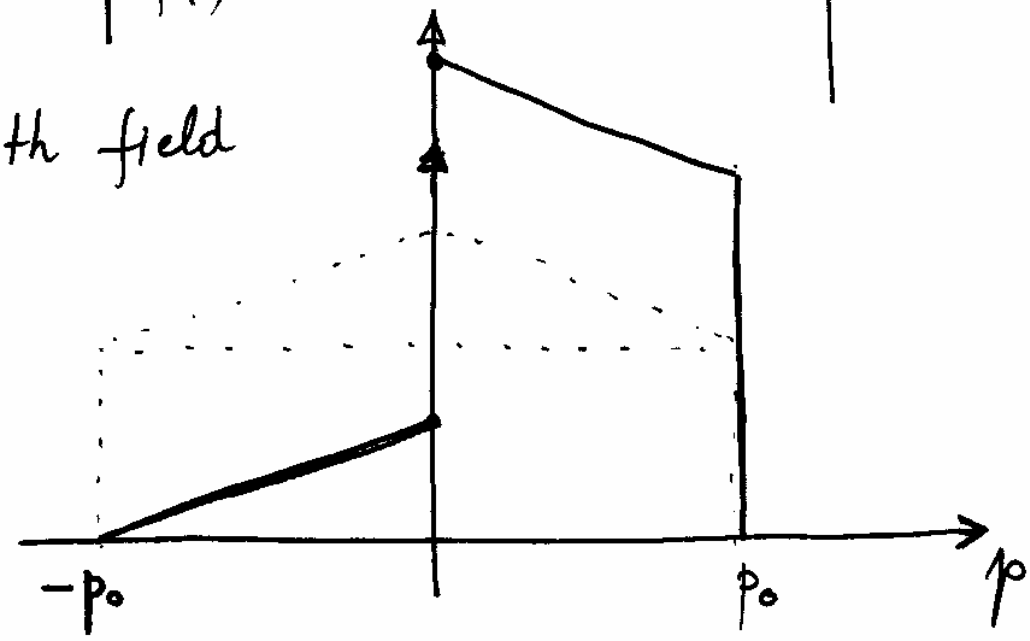

Much more heavily populated are the positive momentum states

How do we get $f(p_0)$? From normalization

$$n = \frac{1}{V}\sum_{\beta} f(p) = \frac{1}{\cancel{V}}\cdot\frac{2\cancel{V}}{2\pi}\cdot\int_{-\infty}^{\infty} f_S(p)\,dp$$

$$= \frac{1}{\pi}\cdot\int_{-p_0}^{p_0} f_S(p)\,dp = \frac{2}{\pi}\cdot\int_0^{p} f_S(p)\,dp =$$

$$= \frac{2f(p_0)}{\pi}\int_0^{p} dp\left(1-\frac{(p-p_0)}{eE\tau_f}\right) = \frac{2f(p_0)}{\pi}\cdot\left(p_0-\frac{p_0^2}{2eE\tau_f}+\frac{p_0^2}{eE\tau_f}\right)$$

$$= \frac{2f(p_0)}{\pi}\cdot p_0\left(1+\frac{p_0}{2eE\tau_f}\right)$$

$$\langle v \rangle = \frac{1}{V} \sum f_*(\vec{p}) \frac{\vec{p}}{m^*} \cdot \frac{1}{n}$$

$$= \frac{1}{V} \cdot \frac{2V}{2\pi} \cdot 2 \cdot \int_0^{p_0} f(p_0) \frac{p\,dp}{m^*} \cdot \frac{1}{n}$$

$$= \frac{2}{\pi} \cdot \frac{1}{n} \cdot \frac{p_0^2}{2m^*} f(p_0) =$$

$$= \frac{p_0^2}{m^* \pi} \cdot \frac{f(p_0)}{2 f(p_0)\, p_0 \left(1 + \frac{p_0}{2eE\tau}\right)}$$

$$\boxed{\langle v \rangle = \frac{v_0}{2\left(1 + \frac{v_0}{2\mu \cdot E}\right)}}$$

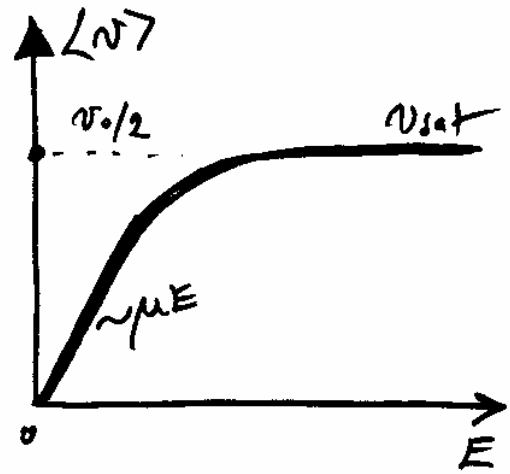

as $E \to 0$

$$\langle v \rangle = \frac{v_0 \cdot 2\mu E}{2(\underbrace{2\mu E + v_0}_{v_0})} \approx \mu E$$

OK!

as $E \to \infty$ $\langle v \rangle \to \frac{v_0}{2}$

Velocity overshoot

Non-stationary effect. Results from the fact that energy relaxation time (which can also be shown to be the time needed by the distribution function to adjust is longer than the momentum relaxation time

$\vec{E} = -E\vec{e_z}$
1D again

$$\frac{\partial f}{\partial t} + \frac{eE}{\cancel{m^*}}\frac{\partial f}{\partial p} = -\frac{1}{\tau_f} f_A - eEf(p_0,t)\left[\delta(p+p_0) + \delta(p-p_0) - 2\delta(p)\right]$$

Laplace transform in time

$$s f(p,s) + eE\frac{\partial f(p,s)}{\partial p} = -\frac{1}{\tau_m} f_A(p,s) - eEf(p_0,s)\left[\ \ldots\ \right]$$

! Note that $f(p_0)$ is now a function of time in the time domain (of s in the Laplace domain), and it is certainly a function of the applied electric field.

Splitting into symmetric & antisymmetric:

$$s f_A(p,s) + eE\frac{\partial f_S(p,s)}{\partial p} = -\frac{1}{\tau_m} f_A(p,s)$$

$$s f_S(p,s) + eE\frac{\partial f_A}{\partial p}(p,s) = -eEf(p_0,s)\left[\delta(p+p_0) + \delta(p-p_0) - 2\delta(p)\right]$$

Boundary conditions used before:

- $f(-p_0,t) = 0 \implies f(-p_0,s) = 0$

Due to the new $sf(p,s)$ terms, we cannot perform as straightforward an integration as before. However, we can note that away from the points $-p_0$, $+p_0$, and 0 (where the δ-functions are active), the equations become:

$$sf_s(p,s) + eE\frac{\partial f_A}{\partial p} = 0$$

$$sf_A(p,s) + eE\frac{\partial f_s}{\partial p} = -\frac{1}{\tau_f} f_A$$

$$\frac{\partial f_A}{\partial p} = -\frac{s}{eE} f_s$$

$$\frac{\partial f_s}{\partial p} = -\frac{(s + 1/\tau_f)}{eE} f_A$$

$$\frac{\partial^2 f_A}{\partial p^2} = -\frac{s}{eE}\frac{\partial f_s}{\partial p} = +\frac{s}{eE}\cdot\frac{(s+1/\tau_f)}{eE} f_A$$

$$\frac{\partial^2 f_s}{\partial p^2} = \frac{s(s+1/\tau_f)}{(eE)^2} f_s$$

$+$

$$\boxed{\frac{\partial^2 f(p,s)}{\partial p^2} - \frac{s(s+\tau_f^{-1})}{(eE)^2} f(p,s) = 0}$$

This equation holds in the Laplace domain for the total distrib. fn., away from $-p_0$, $+p_0$, and 0.

$$f^{\pm}(p,s) = A^{\pm}\exp\left(\frac{\gamma p}{F}\right) + B^{\pm}\exp\left(-\frac{\gamma p}{F}\right)$$

$$F = eE, \quad \gamma = \left[s(s+1/\tau_f)\right]^{1/2}$$

Solve for $-p_0 < p < 0$ & $0 < p < p_0$, and then sew them up (superscript $\pm$ denotes positive or negative values of p.)

- <u>Boundary conditions</u>

1) $f(p \to -p_0^+, t) = 0 \implies f(-p_0, s) = 0$

2) f will have jumps between regions around $\pm p_0, 0$. Integrate the initial equation around $\tilde{p}$, where $\tilde{p} = \pm p_0, 0$ (meaning you integrate from $\tilde{p}-\varepsilon$ to $\tilde{p}+\varepsilon$, and let $\varepsilon \to 0$).

$$eE\int_{\tilde{p}-\varepsilon}^{\tilde{p}+\varepsilon} \frac{\partial f}{\partial p}\,dp = eE\,f(p_0,s) \begin{cases} 2, & \tilde{p} = 0 \\ -1, & \tilde{p} = \pm p_0 \end{cases}$$

3) $$\left.\frac{\partial f}{\partial p}\right|_{p \to p_0^+} = \frac{f(p_0,s)}{eE\tau_f}$$

This comes from $\frac{\partial f_s}{\partial p} = -\frac{f_A}{eE\tau_f} = -\frac{(-f(p_0,s))}{eE\tau_f} = \frac{f(p_0,s)}{eE\tau_f}$

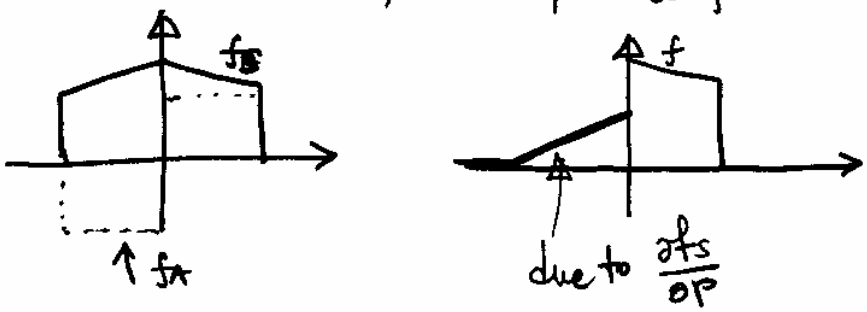

Negative momenta

$$1) \Rightarrow f^-(p_0;s) = A^- \exp\left(\frac{-\gamma p_0}{F}\right) + B^- \exp\left(\frac{\gamma p_0}{F}\right) = 0$$

$$3) \Rightarrow \frac{\partial f^-}{\partial p}(-p_0^+, s) = \frac{\gamma}{F}\left[A^- \exp\left(-\frac{\gamma p_0}{F}\right) - B^- \exp\left(\frac{\gamma p_0}{F}\right)\right] = \frac{f(p_0,s)}{F\tau_m}$$

$+$

$$\frac{\gamma}{F}\cdot 2A^- \exp\left(-\frac{\gamma p_0}{F}\right) = \frac{f(p_0,s)}{F\tau_m}$$

$$A^- = \frac{1}{2\gamma\tau_m} f(p_0,s)\exp(\gamma p_0/F)$$

$$f^-(p,s) = \frac{1}{2\gamma\tau_m} f(p_0,s)\left(e^{\frac{\gamma(p_0+p)}{F}} - \exp\left(-\frac{\gamma p_0}{F}\right) e^{-\frac{\gamma p}{F}}\right)$$

$$\boxed{f^-(p,s) = \frac{f(p_0,s)}{\gamma\tau_m}\sinh\left[\frac{\gamma(p+p_0)}{F}\right]}$$

Positive momenta

$$f^+(p,s) = f(p_0,s)\left(1 + \frac{1}{\gamma\tau_m}\sinh\left[\frac{\gamma(p+p_0)}{F}\right]\right)$$

$\ldots$

$$\langle v(s)\rangle = \frac{v_0/2s}{1 + \frac{F}{p_0\gamma^2\tau_f}\left[\cosh\left(\frac{\gamma p_0}{F}\right) - 1\right]}$$

When $t \to \infty$,

$$v_d^{\text{steady}} = \lim_{t\to\infty} \langle v(t)\rangle = \lim_{s\to 0} s\langle v(s)\rangle = \lim_{s\to 0} \frac{v_0/2}{1+\frac{F}{p_0\gamma^2\tau_f}\left[\cosh\left(\frac{\gamma p_0}{F}\right)-1\right]}$$

$$= \lim_{s\to 0} \frac{v_0/2}{1+\frac{F}{p_0\gamma^2\tau_f}\cdot\frac{1}{2}\frac{\gamma^2 p_0^2}{F^2}}$$

(s is hidden in γ)

$s\to 0$ $\gamma \to 0$

$$= \frac{v_0/2}{1+\frac{p_0}{2\tau_f F}}$$

$$= \frac{v_0/2}{1+\frac{v_0}{2\mu E}}$$

$\nearrow E\to 0,\ v_d \approx \mu E$

$\searrow E\to\infty,\ v_d \to v_0/2$

For intermediate times, when there's overshoot, we need to expand the $\cosh(\ldots)$ to include higher order terms in s.

Values for which $s\langle v(s)\rangle$ diverges, determine whether there is overshoot or not.

Denominator $=0$ is what interests us at present.

$$1+\frac{F}{p_0\gamma^2\tau_f}\left[\cosh\left(\frac{\gamma p_0}{F}\right)-1\right]=0$$

Electron Temperature Approach

When electron-electron scattering is strong ($n > 10^{17}\,cm^{-3}$) the distribution function can be assumed in the drifted Maxwellian form, with an effective electron temperature $T_e > T_L$.

Example: $E = 50\,kV/cm$ (very high)

$v_d \sim 10^7\,cm/s$

$u \sim 200\,meV$ (almost 10 times the thermal energy at 300K!)

$$\frac{m v_d^2}{2} \sim 0.03\,eV \ll u$$

$$u = \frac{3}{2} k_B T_e \gg \frac{3}{2} k_B T_L$$

Relation between D_n & μ_n is still Einstein's relation (comes out of Maxwellian form)

$$\frac{D_n}{\mu_n} = \frac{k_B T_e}{e} \leftarrow \text{now the electron temperature!}$$

From the balance equations (homog. case)

$$\frac{\partial \vec{P}}{\partial t} = -n e \vec{E} - \left\langle\!\left\langle \frac{1}{\tau_m} \right\rangle\!\right\rangle \vec{P} \qquad (b.e.\ 1)$$

$$\frac{\partial W}{\partial t} = \vec{J} \cdot \vec{E} - \left\langle\!\left\langle \frac{1}{\tau_E} \right\rangle\!\right\rangle (W - W^{\circ}) \qquad (b.e.\ 2)$$

steady state conditions

From (b.e. 1) ← momentum balance equation

$$n m^* v_{dx} = -neE \left\langle\!\left\langle \frac{1}{\tau_m} \right\rangle\!\right\rangle^{-1}$$

$$v_d = \frac{eE}{m^*} \left\langle\!\left\langle \frac{1}{\tau_m} \right\rangle\!\right\rangle^{-1}$$

From (b.e. 2) ← energy balance equation

$$\vec{J}\cdot\vec{E} = \left\langle\!\left\langle \frac{1}{\tau_E} \right\rangle\!\right\rangle (W - W^0)$$

$$-\cancel{n}e\vec{v}_d\cdot\vec{E} \approx \left\langle\!\left\langle \frac{1}{\tau_E} \right\rangle\!\right\rangle \cdot \frac{3}{2} k_B (T_e - T_L) \cdot \cancel{n}$$

$$e \cdot \frac{eE^2}{m^*} \cdot \left\langle\!\left\langle \frac{1}{\tau_m} \right\rangle\!\right\rangle^{-1} \approx \frac{3}{2} k_B \left\langle\!\left\langle \frac{1}{\tau_E} \right\rangle\!\right\rangle (T_e - T_L)$$

$$\boxed{\frac{T_e}{T_L} = 1 + \frac{2}{3} \frac{e^2E^2}{m^*} \left\langle\!\left\langle \frac{1}{\tau_m} \right\rangle\!\right\rangle^{-1} \left\langle\!\left\langle \frac{1}{\tau_E} \right\rangle\!\right\rangle^{-1}}$$

Make sure now, when the averages are computed, in the distribution function T_e is present! However, in quantities such as the number of phonons, T_L is still the quantity of interest.

In silicon, dominant mechanism for energy relaxation is intervalley scattering (acoustic & ionized impurity scattering are both elastic mechanisms), while for momentum relaxation we should consider all of them (ionized imp. scattering should not be too important at room T, unless doping is really high; also, it prefers small angles.)

Acoustic phonons & mobility at $T_e > T_L$

$$\frac{1}{\tau(\vec{p})} = \text{Const.}\ k_B T_L \cdot \sqrt{\varepsilon}$$

$$= -\text{h}\ k_B T_L \cdot \left(\frac{\varepsilon}{k_B T_E}\right)^{1/2} \cdot k_B T_E)^{1/2}$$

$$= -\text{h}\ (k_B T_L)^{3/2} \left(\frac{\varepsilon}{k_B T_E}\right)^{1/2} \cdot \left(\frac{T_E}{T_L}\right)^{1/2}$$

$$\left\langle\!\left\langle \frac{1}{\tau_m} \right\rangle\!\right\rangle_{T_e} = \left\langle\!\left\langle \frac{1}{\tau_m} \right\rangle\!\right\rangle_{T_L} \cdot \sqrt{\frac{T_E}{T_L}}$$

$$\tau_0(T_E) = \tau_0(T_L) \cdot \sqrt{\frac{T_L}{T_e}}$$

$$\mu_n(T_E) = \mu_n(T_L) \cdot \sqrt{\frac{T_L}{T_E}}$$

Energy relaxation via intervalley phonons

$$\frac{1}{\tau(\vec{p})} \sim \sqrt{\varepsilon \pm \hbar\omega_{if} - \Delta E_{if}}$$

$$\frac{1}{\tau_E(\vec{p})} \sim \frac{\hbar\omega_{if}}{\varepsilon} \sqrt{\varepsilon \pm \hbar\omega_{if} - E_{if}} \overset{\text{high } E,\ \text{large } \varepsilon\text{'s}}{\sim} \frac{\hbar\omega_{if}}{\sqrt{\varepsilon}} =$$

$$= \text{Const.} \left(\frac{\varepsilon}{k_B T_e}\right)^{-1/2} \left(\frac{T_e}{T_L}\right)^{-1/2}$$

$$= \text{const.} \left(\frac{\varepsilon}{k_B T_e}\right)^{-1/2} \sqrt{\frac{T_L}{T_e}}$$

$$\left\langle\!\left\langle \frac{1}{\tau_E} \right\rangle\!\right\rangle = \text{Const}_E \cdot \sqrt{\frac{T_L}{T_e}}$$

$$\boxed{\frac{T_e}{T_L} = 1 + \frac{e^2 E^2}{m^*} \cdot \text{Const. indep. of } T_e}$$

$$\frac{T_e}{T_L} = 1 + \left(\frac{E}{E_{cr}}\right)^2$$

$$\boxed{\mu(E) = \underset{\substack{\uparrow \\ \text{low-field}}}{\mu^\circ} \cdot \frac{1}{\sqrt{1+(E/E_{cr})^2}}}$$

Field-dependent mobility

$E_{cr} \sim 7 \times 10^3$ V/cm critical field

Extra high fields $\mu = \mu_0 \frac{E_{cr}}{E}$

giving $\boxed{v_d = \mu E = \mu_0 \frac{E_{cr}}{E} \cdot E = \mu_0 \cdot E_{cr}}$

velocity saturation

Introduction to Mesoscopic Transport

Most mesoscopic physics is based on exploiting the 2D electron gas formed at the AlGaAs/GaAs heterointerface

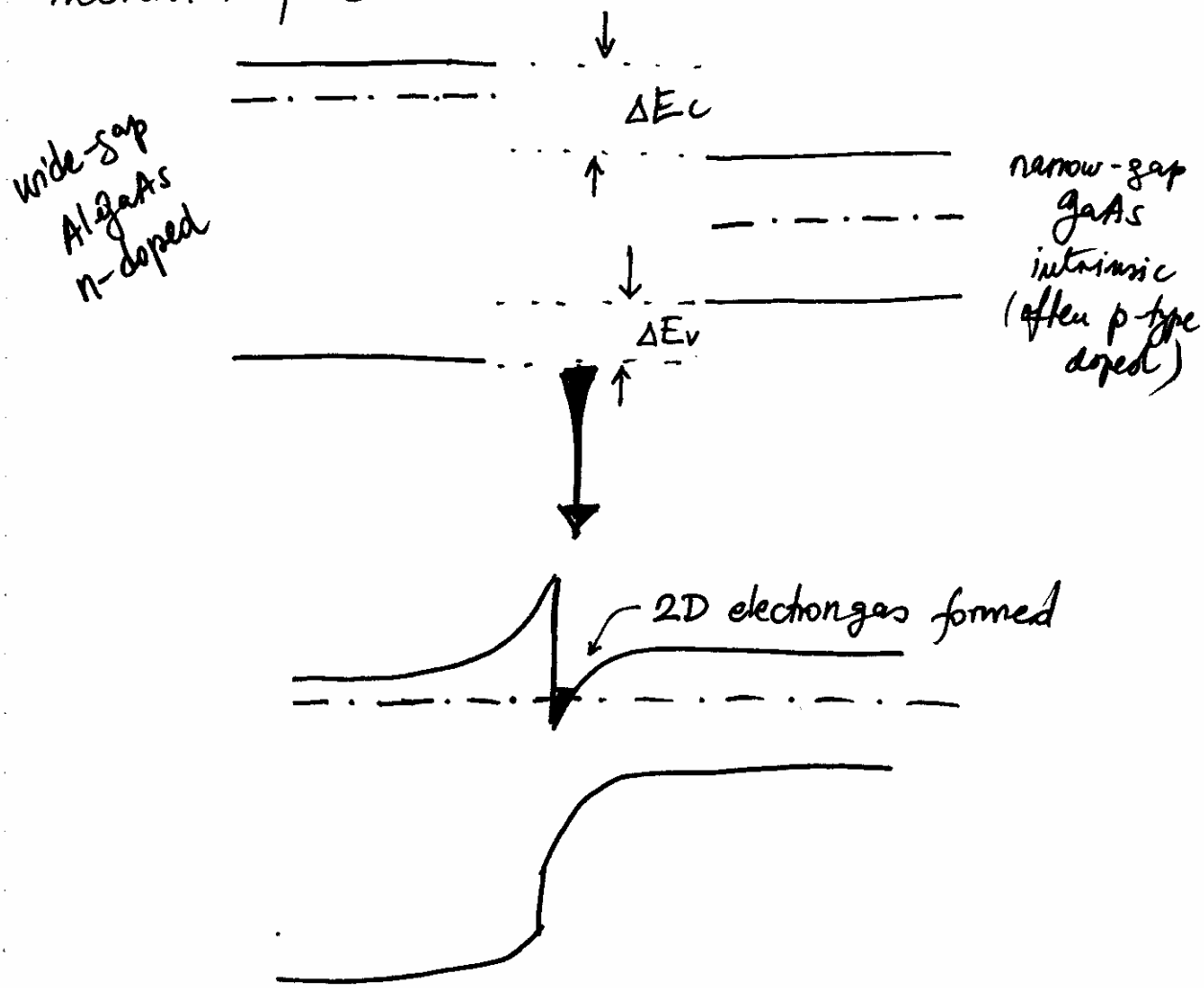

The 2D electron gas is degenerate, i.e., Fermi level will be above the conduction band edge.

AlAs & GaAs are lattice-matched, so you don't have strain effects.

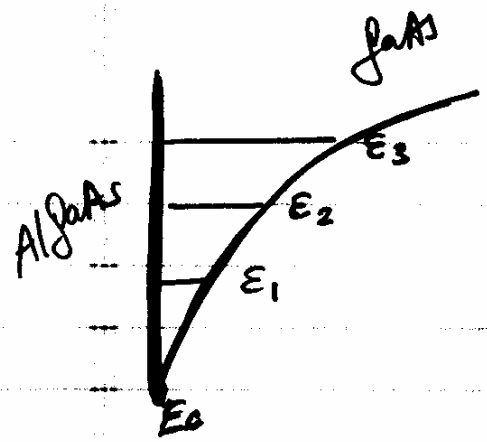

There will be subbands formed in the confinement potential at the interface, found by solving the Schrödinger equation in the growth direction

$$\left[-\frac{\hbar^2}{2m}\frac{d^2}{dz^2}+V(z)\right]\phi_i(z) = \varepsilon_i\cdot\phi_i(z)$$

$i=1,2,3,\ldots$

Instead of having free electrons, described by 3D plane waves, now we have a quasi 2D system, with subbands, and energies given by

$$\mathcal{E}(n,k_x,k_y) = \underset{\substack{\uparrow\\ \text{cond band}\\ \text{bottom}}}{\mathcal{E}_c} + \underset{\substack{\uparrow\\ \text{n-th}\\ \text{bound state}\\ \text{from confinement}\\ \text{along } z}}{\varepsilon_n} + \frac{\hbar^2}{2m^*}(k_x^2+k_y^2)$$

• <u>Density of states & charge density</u>

For a 3D free electron gas, density of states per unit volume is given by

$$g_{3D}(\mathcal{E}) = \frac{2}{(2\pi)^3}\cdot 4\pi\, k^2\frac{dk}{d\mathcal{E}}$$

$$\mathcal{E} = \mathcal{E}_c + \frac{\hbar^2k^2}{2m^*}$$

$$d\mathcal{E} = \frac{\hbar^2 k\,dk}{m^*}$$

$$= \frac{1}{\pi^2}\cdot(\mathcal{E}-\mathcal{E}_c)^{1/2}\left(\frac{2m^*}{\hbar^2}\right)^{1/2}\cdot\frac{m^*}{\hbar^2}$$

$$= \frac{1}{2\pi^2}\left(\frac{2m^*}{\hbar^2}\right)^{3/2}(\mathcal{E}-\mathcal{E}_c)^{1/2}$$

In case of confinement along one direction, so that the subbands with edges $\varepsilon_1, \varepsilon_2, \varepsilon_3$, etc. are formed

$$g_{\substack{\text{Quasi}\\2D}}(\varepsilon) = \frac{2}{(2\pi)^2} \cdot \sum_{\substack{i \\ \varepsilon_c+\varepsilon_i<\varepsilon}} 2\pi \frac{k\,dk}{d\varepsilon} \qquad \varepsilon = \varepsilon_c + \varepsilon_i + \frac{\hbar^2 k^2}{2m^*}$$

$$d\varepsilon = \frac{\hbar^2 k\,dk}{m^*}$$

$$= \frac{1}{\pi} \sum_{\substack{i \\ \varepsilon_c+\varepsilon_i<\varepsilon}} \frac{m^*}{\hbar^2}$$

$$= \frac{m^*}{\pi\hbar^2} \sum_i \Theta(\varepsilon - \varepsilon_i - \varepsilon_c)$$

$\sim 2.9\times10^{10}\ \frac{1}{\text{cm}^2\,\text{meV}}$

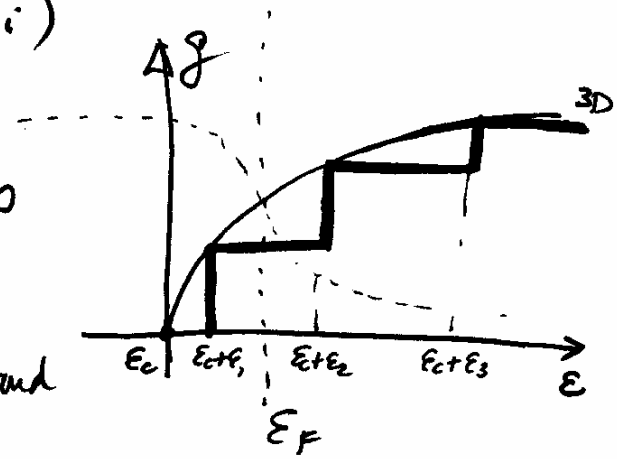

Very typically, for the 2D gas at the heterointerface, the Fermi level will fall between the first & the second subband

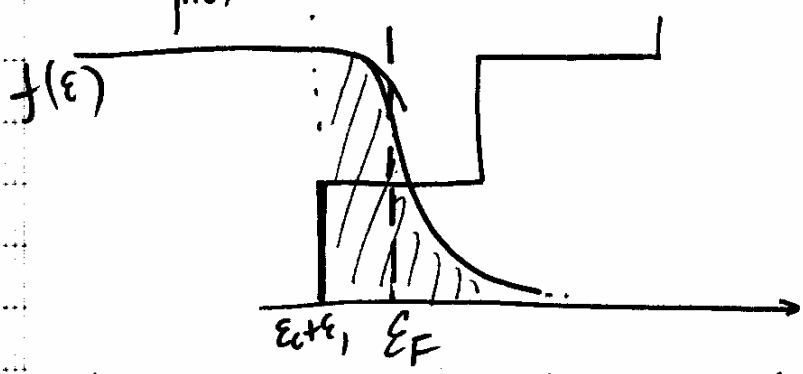

At low temperatures, the distribution function will be step-like, so most of the interesting phenomena are due to electrons at the Fermi surface.

Sheet carrier density

$$n_s = \int g(\varepsilon) f(\varepsilon)\, d\varepsilon \simeq \{\varepsilon_F - \overbrace{[\varepsilon_c+\varepsilon_1]}^{\varepsilon_s\text{ - subband bottom}}\} \cdot \frac{m^*}{\pi\hbar^2}$$

$10^{11} - 10^{12}\ cm^{-2}$

$$n_s = \frac{m^*}{\pi\hbar^2}\cdot(\varepsilon_F - \varepsilon_s) = \frac{\hbar^2 k_F^2}{2\cancel{m^*}}\cdot\frac{\cancel{m^*}}{\pi\hbar^2}$$

1 subband in Quasi 2D structure, Fermi wavevector vs. density

$$\boxed{k_F = \sqrt{2\pi n_s}}$$

Characteristic lengths for mesoscopic physics

- **De Broglie wavelength**

Since most physics will occur around the Fermi level, it is the Fermi wavelength

$$\lambda_F = \frac{2\pi}{k_F} = \sqrt{\frac{2\pi}{n_s}}$$

Mid-range $n_s = 5\times10^{11}\ cm^{-2}$ $\qquad \lambda_F \approx \sqrt{\frac{2\pi}{5\times10^{11}}} = \underline{\underline{35\ nm}}$

- **Mean free path**

Distance travelled before momentum is destroyed

$$L_m = v_F\cdot\tau_m = \frac{\hbar}{m^*}\sqrt{2\pi n_s}\cdot\underbrace{\tau_m}_{\substack{100\,ps\\ \text{OK at}\\ \text{low } T}} \approx \underline{\underline{30\,\mu m}}$$

-

- <u>Phase relaxation length</u>

Different origins at different temperatures: electron-electron interaction at low T, phonons at higher T

If $\tau_\phi < \tau_m$ $\quad l_\phi = v_F \tau_\phi$

$\tau_\phi > \tau_m$ $\quad l_\phi^2 = D\tau_\phi$

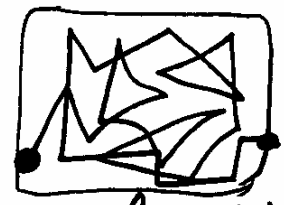

$l_\phi \ll v_F \tau_\phi$

Thermal decoherence starts being important at elevated temperatures

$$l_T = \sqrt{D\tau_T}, \qquad \tau_T = \frac{\hbar}{k_B T} \leftarrow \left\{ \text{depicts thermal speed} \right.$$

Magnetoresistance in 2D electron gas

• Classical Hall effect

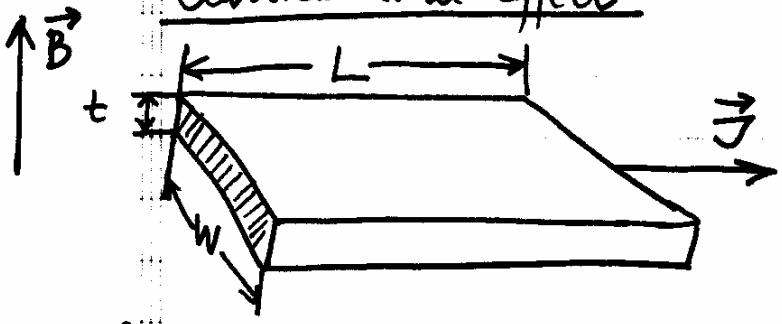

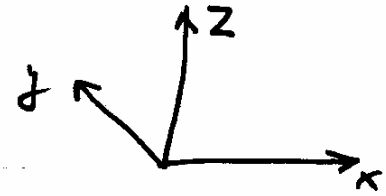

$\vec{J} = J\vec{e}_x$, $\vec{B} = B\vec{e}_z$

Conductivity tensor at low fields & $\vec{B} = B\vec{e}_z$

$$[\sigma] = \sigma_0 \begin{bmatrix} 1 & -\mu_H B & 0 \\ \mu_H B & 1 & 0 \\ 0 & 0 & 1 \end{bmatrix}$$

Resistivity tensor $[\rho] = [\sigma]^{-1}$

$$[\rho] = \frac{1}{\sigma_0} \cdot \underbrace{\frac{1}{1+(\mu_H B)^2}}_{\text{it's second order in } B} \cdot \begin{bmatrix} 1 & -\mu_H B & 0 \\ \mu_H B & 1 & 0 \\ 0 & 0 & 1 \end{bmatrix}^T$$

$$= \underbrace{\frac{1}{\sigma_0}}_{\rho_0} \begin{bmatrix} 1 & \mu_H B & 0 \\ -\mu_H B & 1 & 0 \\ 0 & 0 & 1 \end{bmatrix}$$

$\vec{E} = [\rho]\vec{J}$

$$\boxed{E_x = \rho_0 J_x, \quad E_y = -\mu_H B \rho_0 J_x}$$

$$\frac{V_x}{L} = \rho_0 J_x = \rho_0 \frac{I_x}{Wt}$$

$$V_x = \frac{L}{W} \cdot \frac{1}{\sigma_0 t} I_x$$

longitudinal resistance

$$V_x = \frac{L}{W} \cdot \frac{1}{n e \mu t} \cdot I_x \qquad \boxed{R_{xx} = \frac{L}{W} \cdot \frac{1}{n_s e \mu}}$$

n_s, sheet density

From $E_y = -\mu_H B \rho_0 J_x$

$$\frac{V_y}{W} = \frac{\mu_H B}{n e \mu} \cdot \frac{I_x}{tW}$$

($\mu = \mu_H$ if we assume $r_H = 1$)

$$V_y = \frac{B}{n_s e} \cdot I_x \qquad \boxed{R_{yx} = \frac{B}{n_s e}}$$

transverse resistance

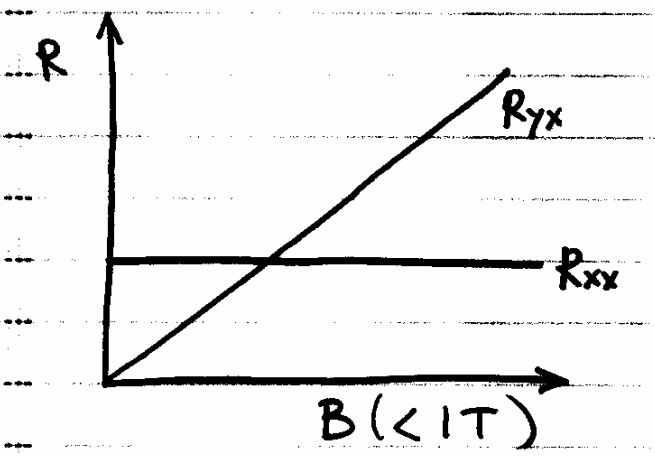

In the classical Hall regime, the longitudinal resistance is independent of B-field, whereas the transverse resistance depends on B linearly.

How would you get n_s & μ?

$$\boxed{n_s = \frac{B}{e} \cdot \frac{1}{R_{yx}} = \frac{B I_x}{e V_y}}$$

$$\mu = \frac{L}{W} \cdot \frac{1}{e n_s} \cdot \frac{1}{R_{xx}} = \frac{L}{W} \cdot \frac{1}{e R_{xx}} \cdot \frac{R_{yx} e}{B}$$

$$\boxed{\mu = \frac{L}{W} \cdot \frac{V_y}{V_x} \cdot \frac{1}{B}}$$

At higher magnetic fields, the behavior of both the longitudinal and the transverse resistance changes.

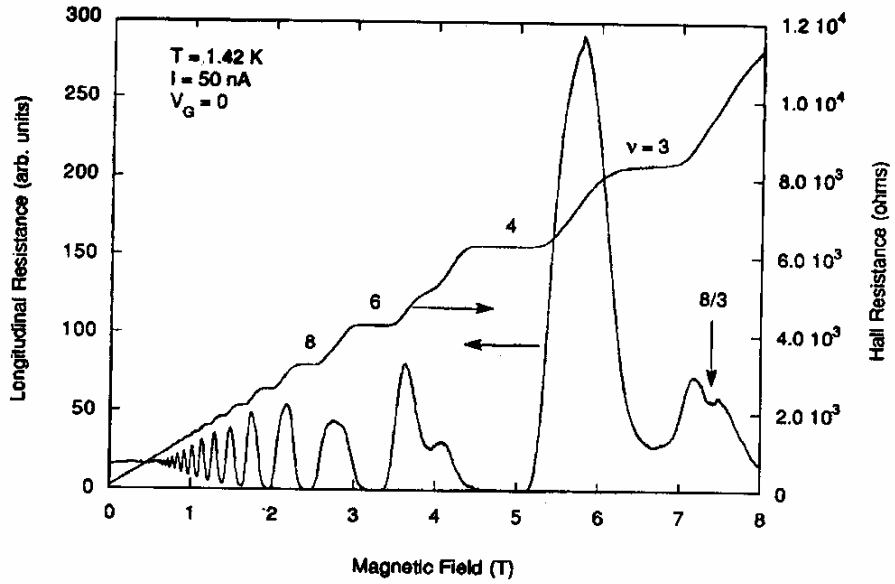

Fig. 2.32. Experimental plot of the longitudinal resistance (left axis) and Hall resistance (right axis) as a function of magnetic field for an AlGaAs/GaAs 2DEG structure.

Oscillations in the longitudinal resistance at high magnetic fields are known as <u>Shubnikov-de Haas oscillations</u>. Minima in the longitudinal resistance are virtually zero.

At those magnetic fields at which longitudinal resistance has a minimum, the transverse (Hall) resistance has <u>plateaus</u>. Plateaus in the Hall resistance of 2DEG are signatures of the (integer) <u>Quantum Hall effect</u>.

SdH Oscillations and Landau levels

In a magnetic field along the z-axis, in the so-called Landau gauge

$$\vec{A} = (-By, 0, 0)$$

the Schrödinger equation reads

$$\frac{(\hat{\vec{p}} - (-e)\vec{A})^2}{2m^*}\psi = (\mathcal{E} - \mathcal{E}_s)\psi$$

$\mathcal{E}_s$ – lowest subband bottom

$$\frac{1}{2m^*}\left[-i\hbar\frac{\partial}{\partial x}\vec{e}_x - i\hbar\frac{\partial}{\partial y}\vec{e}_y - eBy\,\vec{e}_x\right]^2\psi = (\mathcal{E} - \mathcal{E}_s)\psi$$

$$\frac{1}{2m^*}\left[-\hbar^2\frac{\partial^2}{\partial x^2} - \hbar^2\frac{\partial^2}{\partial y^2} + (eBy)^2 + 2i\hbar eBy\frac{\partial}{\partial x}\right]\psi = (\mathcal{E} - \mathcal{E}_s)\psi$$

Assume form $\psi(x,y) = \frac{1}{\sqrt{L}}e^{ik_x x}\cdot\chi(y)$

$$\frac{1}{2m^*}\left[-\hbar^2\frac{d^2}{dy^2} + (eBy - \hbar k_x)^2\right]\chi(y) = (\mathcal{E} - \mathcal{E}_s)\chi(y)$$

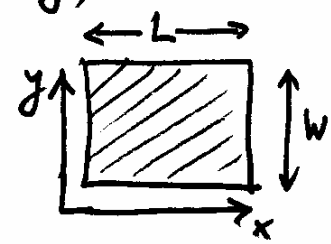

$$\left\{-\frac{\hbar^2}{2m^*}\frac{d^2}{dy^2} + \frac{m^*}{2}\cdot\underbrace{\left(\frac{eB}{m^*}\right)}_{\substack{\omega_c \\ \text{cyclotron} \\ \text{frequency}}}^2\left(y - \frac{\hbar k_x}{eB}\right)^2\right\}\chi(y) = (\mathcal{E} - \mathcal{E}_s)\chi(y)$$

$y_0(k_x)$

The equation obtained is the equation for a linear harmonic oscillator of frequency ω_c, with the equilibrium position at $y_0(k_x) = \frac{\hbar k_x}{eB}$.

The energies are given by

$$\mathcal{E}(n, k_x) = \mathcal{E}_s + \left(n + \frac{1}{2}\right)\hbar\omega_c$$

Equidistant spectrum

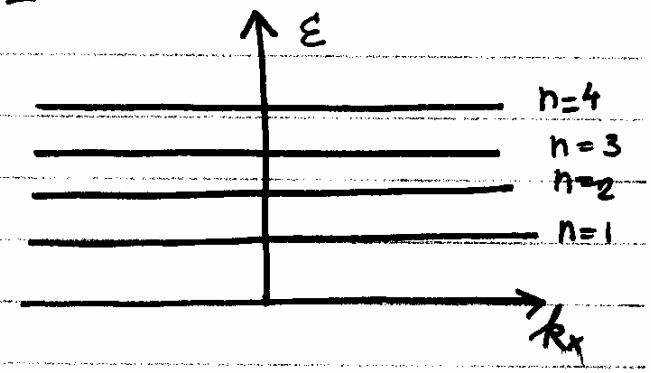

How many electrons can you put in one Landau level?

$$\Delta k_x = \frac{2\pi}{L} \quad \text{leads to} \quad \Delta y_0 = \frac{\hbar}{eB} \cdot \Delta k_x = \frac{\hbar}{eB} \cdot \frac{2\pi}{L}$$

Total # in one Landau level

$$N_{tot} = \underset{\substack{\uparrow \\ \text{spin}}}{2} \cdot \frac{W}{\Delta y_0} = \cancel{2} \cdot \frac{WLeB}{\cancel{2}\pi\hbar} = WL \cdot \frac{2eB}{h}$$

DOS per unit area per Landau level

$$\frac{2eB}{h} = \frac{m}{\pi\hbar^2} \cdot \underbrace{\frac{\hbar eB}{m}}_{\hbar\omega_c}$$

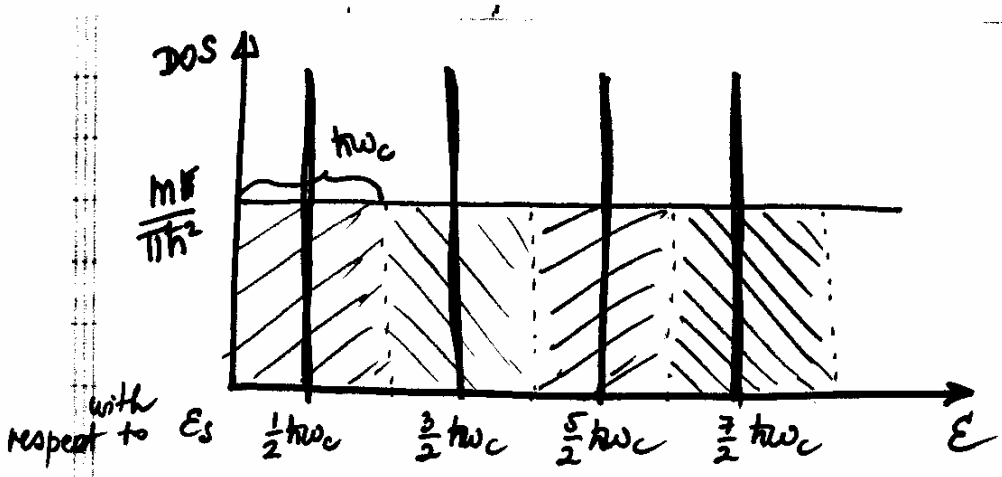

Those $\pm\frac{\hbar\omega_c}{2}$ around a level snap into it!

With increasing magnetic field

- spacing between Landau levels increases
- capacity of a single Landau level increases

When you're dealing with an isolated 2DEG, it will have a fixed number of particles

$$n_s = \frac{2eB}{h} \cdot N_{fill} \qquad B\uparrow \quad N_{fill}\downarrow$$

$$B_1 = \frac{n_s h}{2e} \cdot \frac{1}{1}, \quad B_2 = \frac{n_s h}{2e} \cdot \frac{1}{2}, \quad B_3 = \frac{n_s h}{2e} \cdot \frac{1}{3}$$

$B > B_1$ first level filled $\quad \mathcal{E}_F(B) = \left(1 + \frac{1}{2}\right) \cdot \hbar \frac{eB}{m^*}$

$B_1 > B > B_2$ second level filled $\quad \mathcal{E}_F(B) = \left(2 + \frac{1}{2}\right) \hbar \cdot \frac{eB}{m^*}$

$B_2 > B_1 > B_3$ third — $\quad \mathcal{E}_F(B) = \left(3 + \frac{1}{2}\right) \hbar \frac{eB}{m^*}$

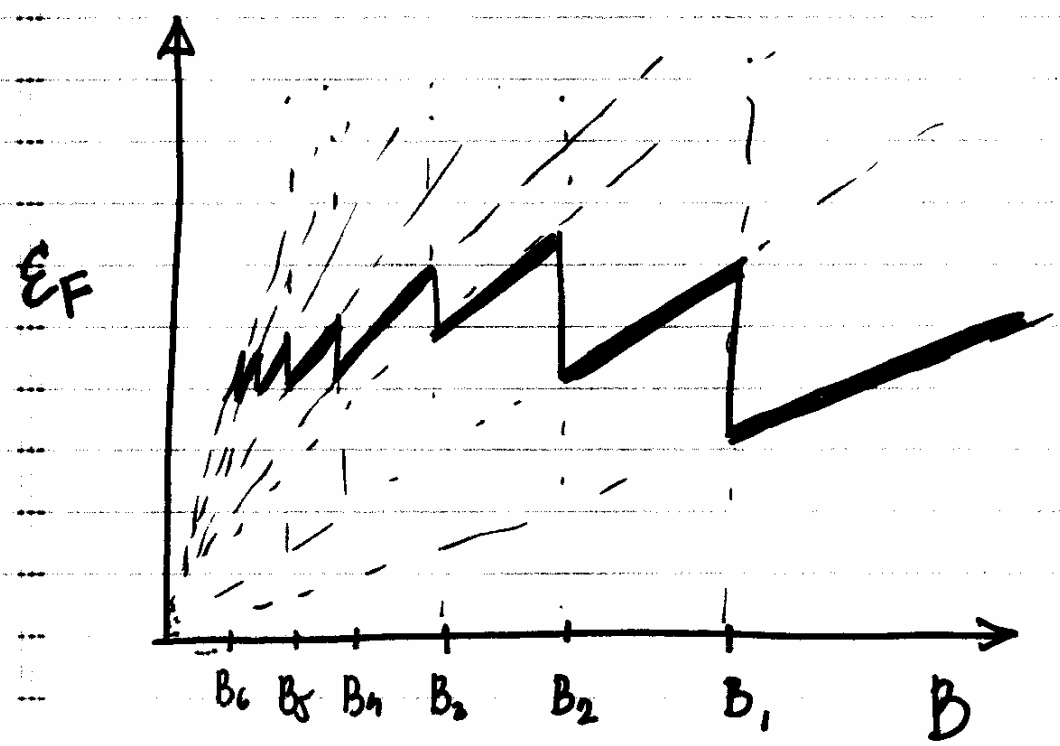

What is the origin of Shubnikov-de Haas oscillations? In case there are external leads that fix the Fermi level, but <u>not the number</u> of particles.

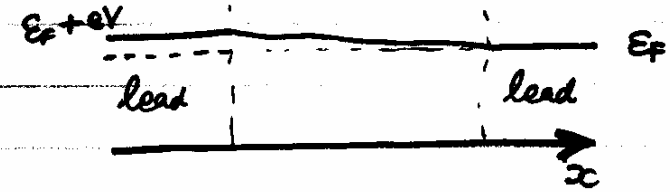

You can consider everything to occur at ε_F when bias is low.

So with fixed ε_F, <u>increasing</u> B, the spacing between Landau levels <u>increases</u>

Why are Landau levels broad?

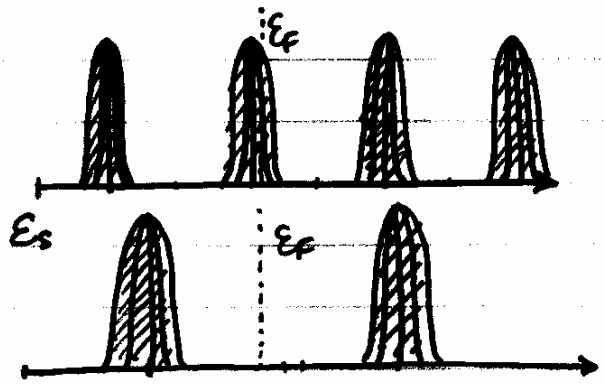

ε_F between Landau levels – <u>minimum</u> in long <u>resistance</u>

Shubnikov-de Haas oscillations are a result of the Fermi level moving through the Landau levels as the magnetic field is swept.

Minima in resistance occur when the Fermi level lies between two Landau levels. Maxima correspond to the Fermi level coinciding with one of the Landau levels.

Determine the 2D density of states from Shubnikov – de Haas oscillations

Peaks in resistance occur at

$$\mathcal{E}_F = \left(n + \tfrac{1}{2}\right)\hbar\omega_c(B_n)$$

And the zero-field $n_s(B=0)$ and $\mathcal{E}_F$ are related by

$$n_s = \frac{m^*}{\pi\hbar^2}\cdot\mathcal{E}_F$$

$\cancel{B_{n+1} = B_n}$

$$\frac{\mathcal{E}_F}{\hbar\frac{eB_{n+1}}{m^*}} - \frac{\mathcal{E}_F}{\hbar\frac{eB_n}{m^*}} = (n+1) - n = 1$$

$$\frac{m^*}{\hbar e}\cdot\mathcal{E}_F\cdot\underbrace{\Delta\left(\frac{1}{B}\right)}_{\substack{\text{oscillation period} \\ \text{(oscillations are in } \underline{\underline{1/B}}\text{)}}} = 1$$

$$\frac{\cancel{m^*}}{\cancel{\hbar} e}\cdot\frac{\pi\hbar^{\cancel{2}}}{\cancel{m^*}}\cdot n_s\cdot\Delta\left(\frac{1}{B}\right) = 1$$

$$\frac{h}{2e}\cdot n_s\cdot\Delta\left(\frac{1}{B}\right) = 1$$

1 # per level per B

$$\boxed{n_s = \frac{2e}{h}\cdot\frac{1}{\Delta\left(\frac{1}{B}\right)}}$$

get the zero-field 2D density

Edge States

- How is the current conducted, since we should classically have closed orbits?
- Why is R_{xx} zero when E_F is between levels and not when it coincides w/ a Landau level?
- Why is the Hall ~~resistivity~~ conductance quantized, i.e., the plateaus in the resistance are given by

$$\frac{1}{R_{xy}^{plat.}} = n \cdot \frac{e^2}{h}$$

The answer lies within the <u>EDGE STATES</u>.

Instead of a conductor boundless in the y direction, we impose a confining potential. ~~Ita~~ This way we get a quantum wire, with more or less thickness.

Confining potential for a split gate quantum wire

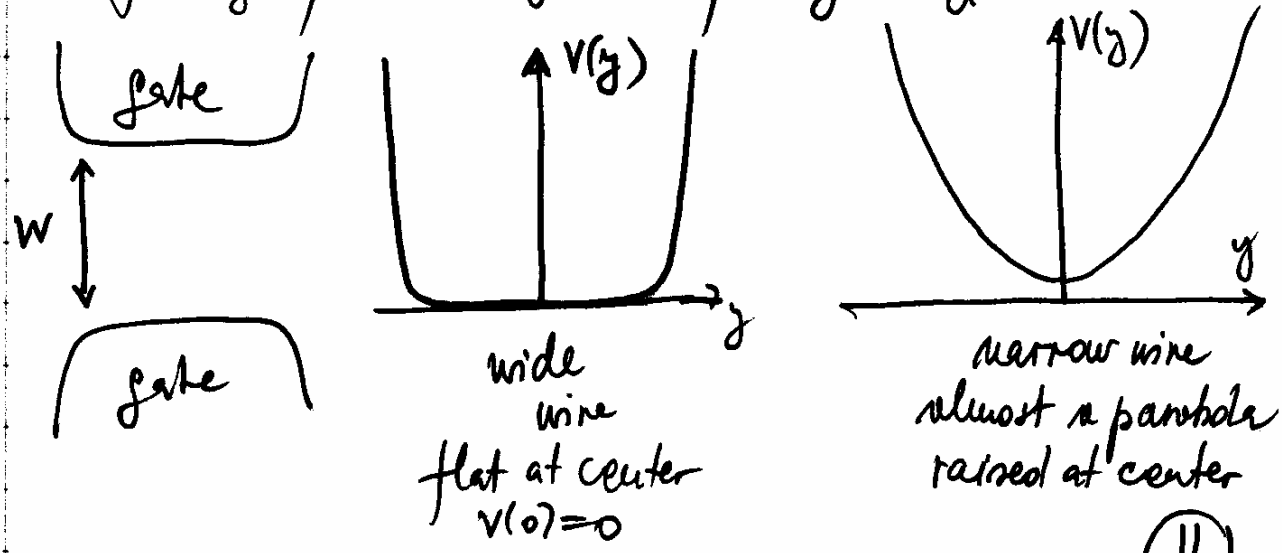

For the parabolic potential assumed, in a magnetic field, the modified Schrödinger equations

$$\left[\frac{-\hbar^2}{2m^*}\frac{d^2}{dy^2} + \frac{m^*\omega_c^2}{2}\left(y - \frac{\hbar k_x}{eB}\right)^2 + \frac{m^*\omega_0^2 y^2}{2}\right]\chi(y) = (\varepsilon - \varepsilon_s)\chi(y)$$

When added together, there's a new parabolic potential and a new center of the parabola

$$(\omega_c^2+\omega_0^2)\, y^2 - \omega_c^2 2 y_0(k_x) + y_0(k_x)^2\,\omega_c^2$$

$$= \underbrace{(\omega_c^2+\omega_0^2)}\left[y - y_0(k_x)\cdot\frac{\omega_c^2}{\omega_c^2+\omega_0^2}\right]^2 +$$

$$+ y_0^2\omega_c^2 - y_0^2\frac{\omega_c^4}{\omega_c^2+\omega_0^2} =$$

$$= \omega_{c0}^2\,(y - y_0') + y_0^2\,\underbrace{\frac{\omega_0^2\omega_c^2}{\omega_c^2+\omega_0^2}}_{\omega_{c0}^2} \quad ; \; y_0' = y_0\frac{\omega_c^2}{\omega_c^2+\omega_0^2}$$

Energy spectrum

$$\boxed{\varepsilon_{n,k_x} = \varepsilon_s + \frac{m^*}{2}\,\frac{\omega_0^2\omega_c^2}{\omega_0^2+\omega_c^2}\cdot y_0^2(k_x) + \left(n+\frac{1}{2}\right)\hbar\omega_{c0}}$$

shift upward

hybrid freq.

Velocity (group) $v = \frac{\partial \varepsilon_n}{\partial k_x} = \frac{m^*}{2} \cdot \frac{\omega_0^2 \omega_c^2}{\omega_0^2 + \omega_c^2} \cdot 2\left(\frac{\hbar}{eB}\right)^2 \cdot k_x$

These indeed move in the x-direction !!!

Spectrum vs. B

- $B=0$

$$\varepsilon_{n,k_x} = \varepsilon_s + \frac{m^*}{2} \cdot \left(\frac{eB}{m^*}\right)^2 \cdot \left(\frac{\hbar k_x}{eB}\right)^2 + \left(n+\frac{1}{2}\right)\hbar\omega_0$$

$$= \varepsilon_s + \frac{\hbar^2 k_x^2}{2m^*} + \left(n+\frac{1}{2}\right)\hbar\omega_0$$

ordinary particle in a parabolic potential

- $B \to \infty$ $(\omega_c \gg \omega_0)$

$$\varepsilon_{n,k_x} = \varepsilon_s + \underbrace{\frac{m^*}{2} \cdot \omega_0^2 \cdot \left(\frac{\hbar k_x}{eB}\right)^2}_{\frac{(\hbar k_x)^2}{2m^*} \cdot \frac{\omega_0^2}{\omega_c^2}} + \left(n+\frac{1}{2}\right)\hbar\omega_c$$

will be very small

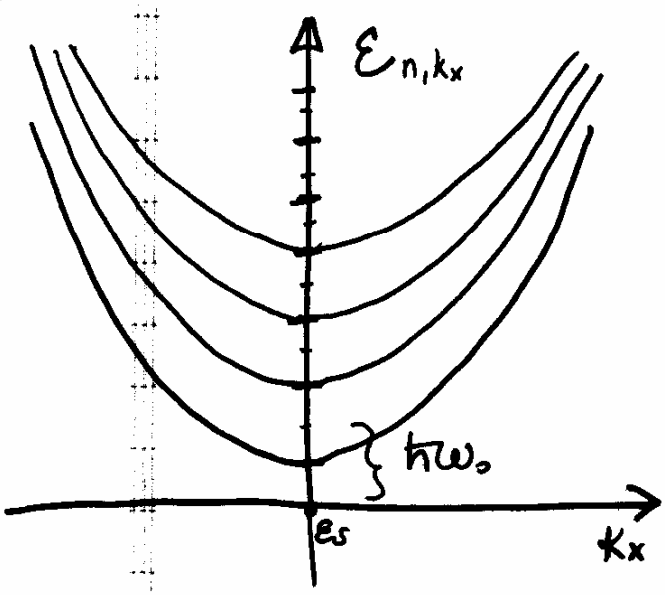

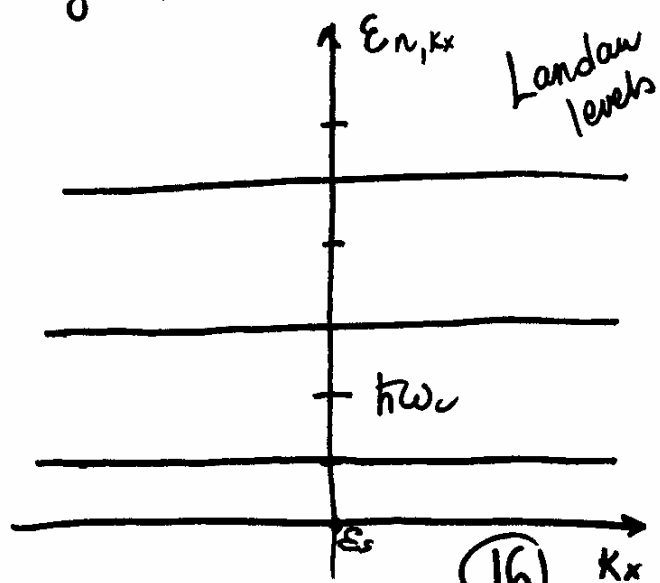

Where are the edge states?

$$v_x = \frac{1}{\hbar}\frac{\partial E_{n,k_x}}{\partial k_x} = \frac{1}{\hbar}\frac{m^*}{\cancel{2}} \cdot \frac{\omega_0^2\omega_c^2}{\omega_0^2+\omega_c^2}\,\cancel{2}\,y_0(k_x)\cdot\frac{\hbar}{eB}\cdot\frac{1}{\hbar}$$

$$\boxed{y_0(k_x) = v_x \cdot \frac{\omega_0^2+\omega_c^2}{\omega_0^2\omega_c}}$$

Velocity is proportional to displacement!!!

States carrying current ~~to the~~ in the positive direction move to one side of the sample, while those carrying current in the opposite direction move to the other side!!!

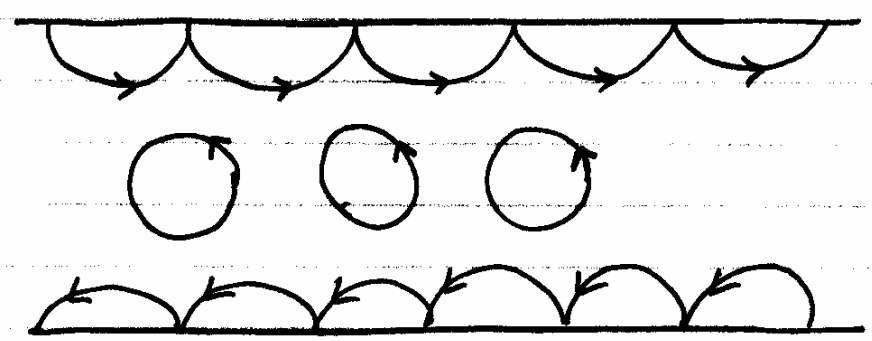

$B\uparrow \quad r_c = \frac{v_F}{\omega_c} \downarrow$ small radius paths, don't feel confinement too much

Magnetic depopulation of subbands

$$\mathcal{E}_{n,k_x} = \mathcal{E}_s + \left(n-\frac{1}{2}\right)\hbar\omega_{c0} + \underbrace{\frac{m^*}{2}\cdot y_0^2(k_x)\cdot\frac{\omega_0^2\omega_c^2}{\omega_{c0}^2}}$$

$$y_0^2(k_x) = \cancel{\left(\frac{eB}{\hbar}k_x\right)^2}\left(\frac{\hbar k_x}{eB}\right)^2$$

$$\frac{m^*}{2}\cdot k_x^2\cdot\frac{\hbar^2 k_x^2}{(eB)^2}\cdot\frac{\omega_0^2\omega_c^2}{\omega_{c0}^2} =$$

$$= \frac{\hbar^2 k_x^2}{2m^*}\cdot\frac{\omega_0^2\cancel{\omega_c^2}}{\omega_{c0}^2\cancel{\omega_c^2}} \equiv \frac{\hbar^2 k_x^2}{2m^*(B)}$$

$$\boxed{m^*(B) = m^*\frac{\omega_{c0}^2}{\omega_0^2} > m^*}$$

Become heavy in a magnetic field.

We rewrite

$$\mathcal{E}_{n,k_x} = \mathcal{E}_s + \left(n-\frac{1}{2}\right)\hbar\omega_{c0} + \frac{\hbar^2 k_x^2}{2m^*(B)}$$

With increasing field, the bands become spread out and flat.

How many subbands are populated at a given Fermi level $\mathcal{E}_F$?

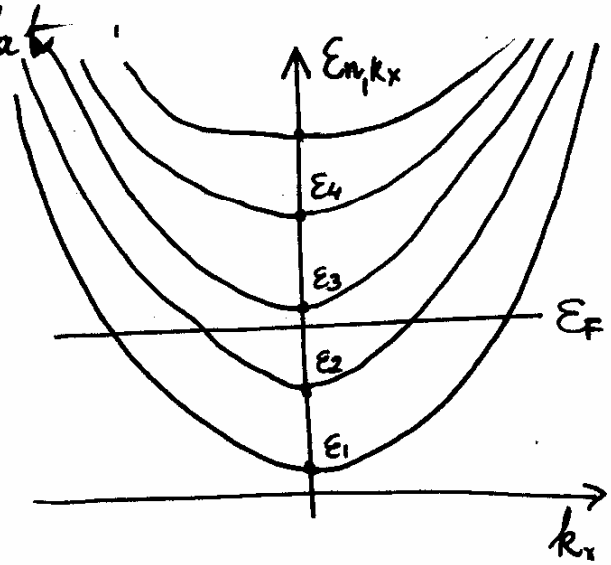

At high fields, we expect behavior as for Landau levels with no confinement.
At low fields, we may expect quite a few levels to be filled.

For a given $\mathcal{E}_F$, the density of states per unit length is:

$$g_{1D} = \underset{\substack{\uparrow \\ \text{spin}}}{\cancel{2}} \cdot \frac{1}{2\pi} \cdot \underset{\substack{\uparrow \\ \pm\text{ momenta}}}{2} \sum_{\mathcal{E}_n < \mathcal{E}} \frac{dk_x}{d\mathcal{E}}$$

$$dk_x = \frac{1}{k_x} \cdot d\mathcal{E} \cdot \frac{m^*(B)}{\hbar^2} \; ; \quad \frac{dk_x}{d\mathcal{E}} = \frac{m^*(B)}{\hbar^2} \cdot \frac{\hbar}{\sqrt{2m^*(B)[\mathcal{E}-\mathcal{E}_n]}}$$

$$g_{1D}(\mathcal{E}) = \frac{1}{\pi}\left(\frac{2m^*(B)}{\hbar^2}\right)^{1/2} \sum_{\mathcal{E}>\mathcal{E}_n} \frac{1}{\sqrt{\mathcal{E}-\mathcal{E}_n}}$$

Number of electrons for a given Fermi level

$$n_{1D} = \frac{1}{\pi}\left(\frac{2m^*(B)}{\hbar^2}\right)^{1/2} \sum_{\mathcal{E}>\mathcal{E}_n} \int_0^{\mathcal{E}_F} \frac{d\mathcal{E}}{\sqrt{\mathcal{E}-\mathcal{E}_n}}$$

$$= \frac{2}{\pi}\left(\frac{2m^*(B)}{\hbar^2}\right)^{1/2} \cdot \sum_{n,\, \mathcal{E}_F>\mathcal{E}_n} \sqrt{\mathcal{E}_F - \mathcal{E}_n}$$

If the number of populated subbands is large and we're pinpointing just the field when a subband is being depopulated

$$\mathcal{E}_F = \left(N - \frac{1}{2}\right)\hbar\omega_{co} \qquad \mathcal{E}_F - \mathcal{E}_n = (N-n)\hbar\omega_{co}$$

$$n_{1D} \cong \frac{2}{\pi} \cdot \left(\frac{2m^*(B)}{\hbar^2}\right)^{1/2} \cdot \sqrt{\hbar\omega_{co}} \cdot \underbrace{\sum_{\nu=0}^{N-1} \sqrt{\nu}}_{\approx \int_0^{N-1} \sqrt{\nu}\, d\nu = \frac{2}{3} \nu^{3/2} \Big|_0^{N-1} \approx \frac{2}{3} N^{3/2}}$$

$$\boxed{n_{1D} \cong \frac{2}{\pi} \cdot \left(\frac{2m^*(B)\omega_{co}}{\hbar}\right)^{1/2} \cdot \frac{2}{3} N^{3/2}}$$

$$m^*(B) = m^* \frac{\omega_{co}^2}{\omega_0^2}$$

$$\boxed{n_{1D} \cong \frac{4}{3\pi} \cdot \left(\frac{2m^*}{\hbar}\right)^{1/2} \cdot \frac{\omega_{co}^{3/2}}{\omega_0} \cdot N^{3/2}}$$

$$\boxed{N = \frac{1}{\omega_{co}} \cdot \left(\frac{3\pi}{4} n_{1D}\omega_0\right)^{2/3} \cdot \left(\frac{\hbar}{2m^*}\right)^{1/3}}$$

At high B, $N \sim \frac{1}{B}$ → from the slope we get $n_{1D}\omega_0$

$$\boxed{N = \frac{1}{\sqrt{\left(\frac{eB}{m^*}\right)^2 + \omega_0^2}} \left(\frac{3\pi}{4} n_{1D}\omega_0\right)^{2/3} \left(\frac{\hbar}{2m^*}\right)^{1/3}}$$

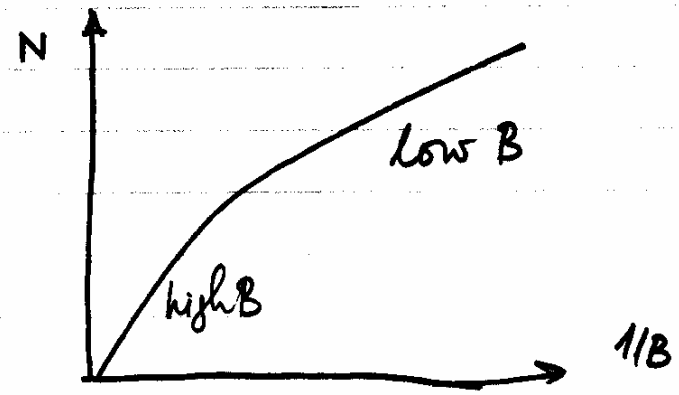

Where the slope changes is low B ⟷ high B

From a fit determine n_{1D} and ω_0.

Effective width is most easily found from

$$n_{2D} = \frac{n_{1D}}{W_{eff}} = \frac{2eB}{h} N(B) \text{ for large } B$$

$$= \frac{2\cancel{eB}}{h} \cdot \left(\frac{3\pi}{4} n_{1D}\,\omega_0\right)^{2/3} \left(\frac{\hbar}{2m^*}\right)^{1/3} \cdot \frac{m^*}{\cancel{eB}}$$

[We have presumably already found n_{1D}, ω_0.]

$$\boxed{W_{eff} = 2\pi\, n_{1D}^{1/3} \left[\frac{2\hbar}{3\pi m^* \omega_0}\right]^{2/3}}$$

Quantum Hall Effect

Wide quantum wire

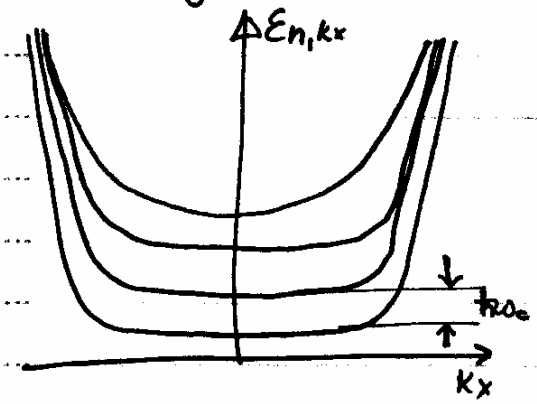

Narrow

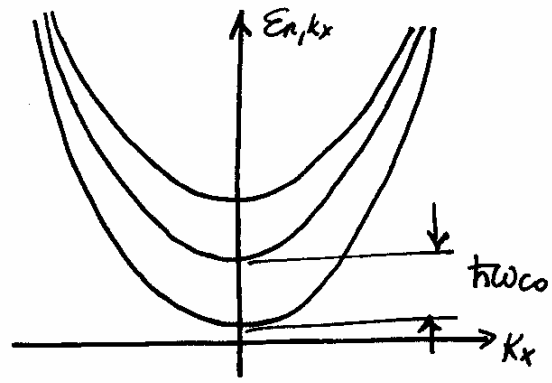

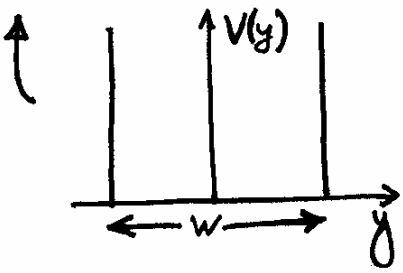

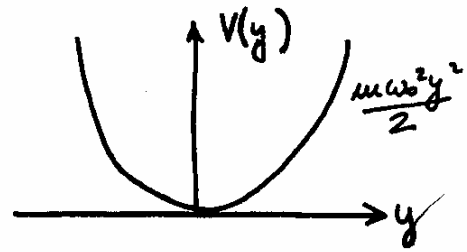

Wide wire: W much greater than the cyclotron radius.

At zero applied bias, the Fermi level is the same everywhere, and equal ε_F (or μ – common notation for the chemical potential; it's the same thing as ε_F).

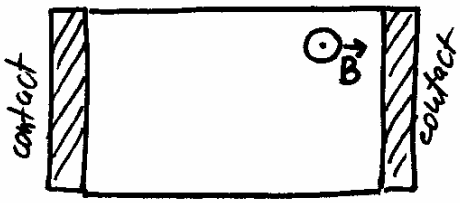

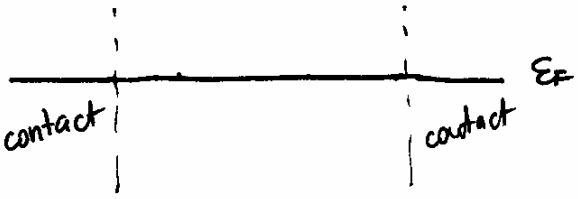

We are using the approximation of REFLECTIONLESS CONTACTS, meaning that all that ~~comes~~ gets transmitted into the contact goes through, i.e., once an electron has reached a contact it does not get reflected back.

When voltage is applied (negative voltage on the LHS), the LHS chemical potential is lifted by eV

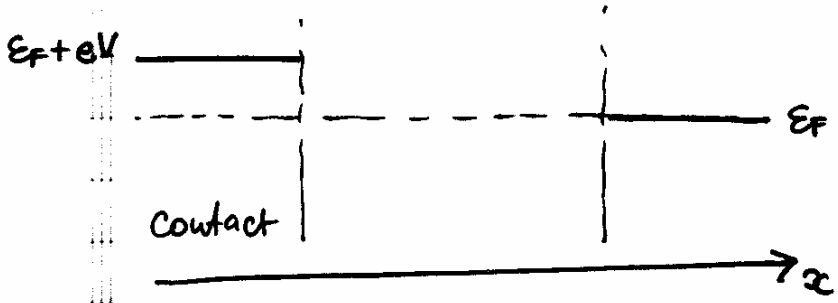

We can say that all the states with $k_x > 0$ have originated in the left contact, and all those with $k_x < 0$ have originated in the right contact (this comes out of the reflectionless leads approximation): states w/ different directions of $\vec{k}$ have different chemical potential

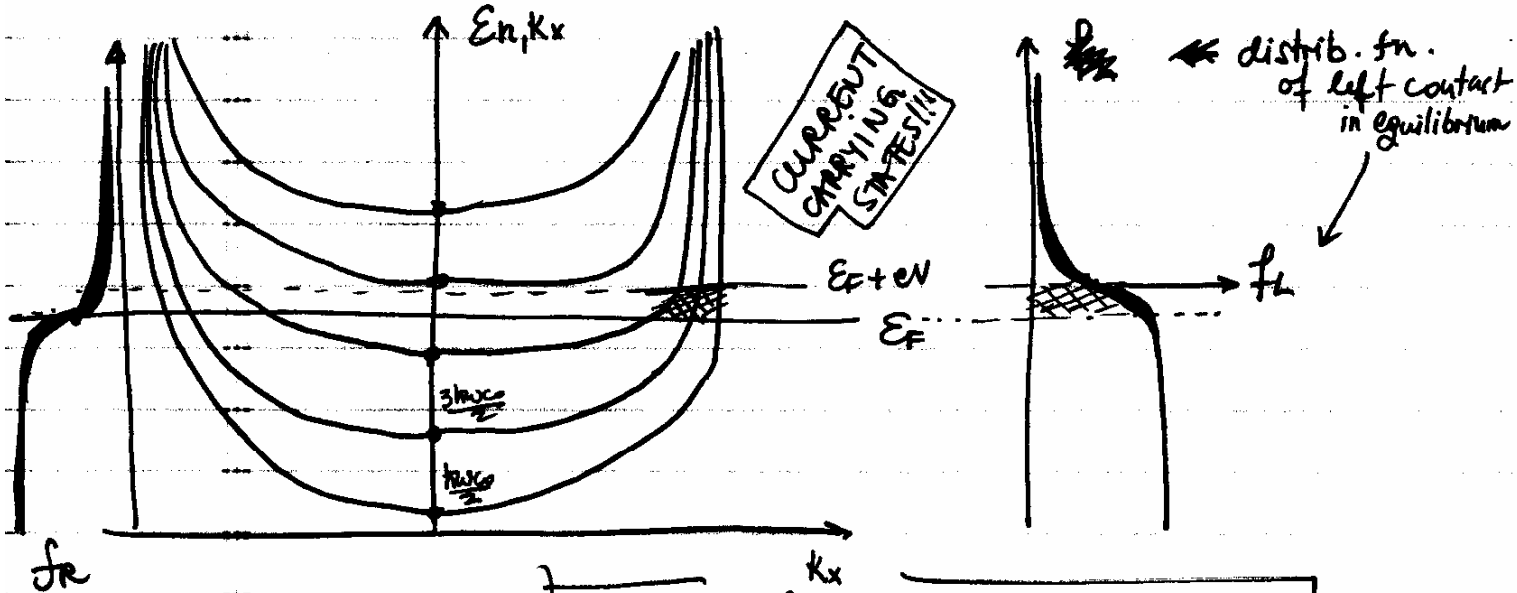

States that give net current are w/ $k_x > 0$ and within $\varepsilon_F < \varepsilon < \varepsilon_F + eV$

When the Fermi level is between two Landau levels (more precisely: between the bottoms of two 1D subbands), the current is carried by positive-k_x edge states. This current flow is BALLISTIC, i.e., there is no ~~dissipation~~ randomization of momentum.

Why? Because in order to have the momentum randomized, there have to be states of significantly different momentum to scatter into, and there have to be mechanisms of scattering to get you there.

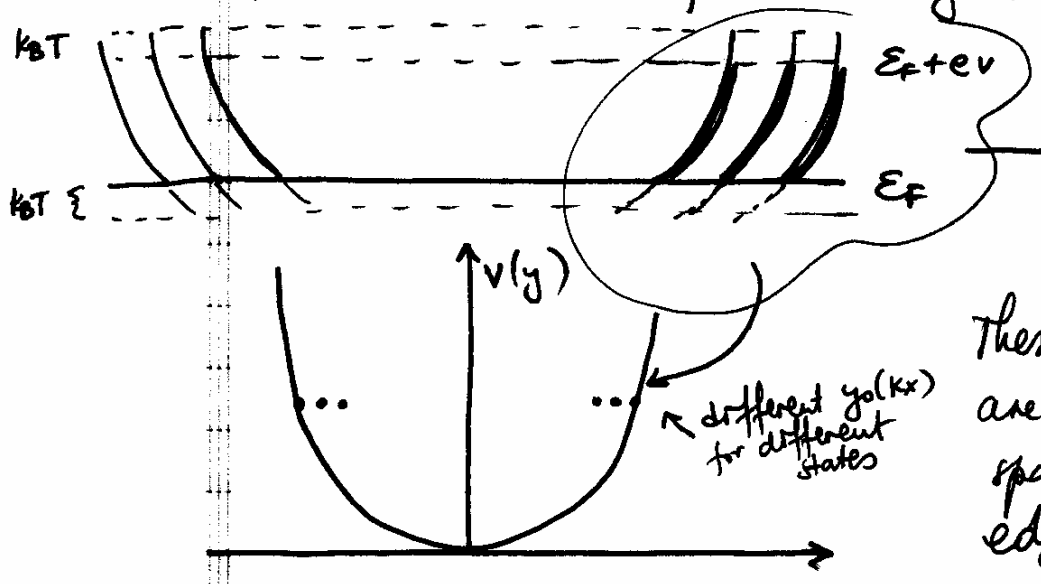

Current-carrying states

These states (edge states) are localized in real space near the opposite edges.

The overlap between two wavefunctions with opposite k's that have the same energy is NEGLIGIBLE WHEN ε_F is between two subband minima.

1) Low T, no phonons — no inelastic scattering (except e-e, but it conserves total momentum)

2) Scattering mostly by impurities (& e-e) → elastic

To lose momentum, you need to scatter with constant energy (only elastic scattering present) all the way to the opposite end! Scattering inefficient due to small overlap

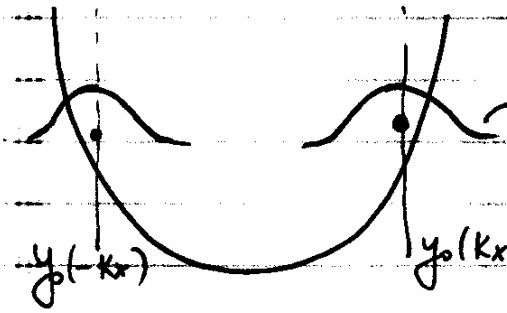

$$\psi_n(x,y) \sim e^{ik_x} H_n(\xi)\, e^{-\xi^2/2}$$

↑ exp decay

$$\xi \sim [y - y_0(k_x)]$$

We know that scattering rates are $\sim \langle \psi_{final} | \hat{H}_{int} | \psi_{init} \rangle$, and when $\langle \psi_{final} | \psi_{initial} \rangle = 0$ the scattering element is negligible too.

- When the Fermi level is ~~below~~ at a Landau level (bottom of subband), then $k_x > 0$ to $k_x < 0$ possible because of much larger wavefunction overlap, and

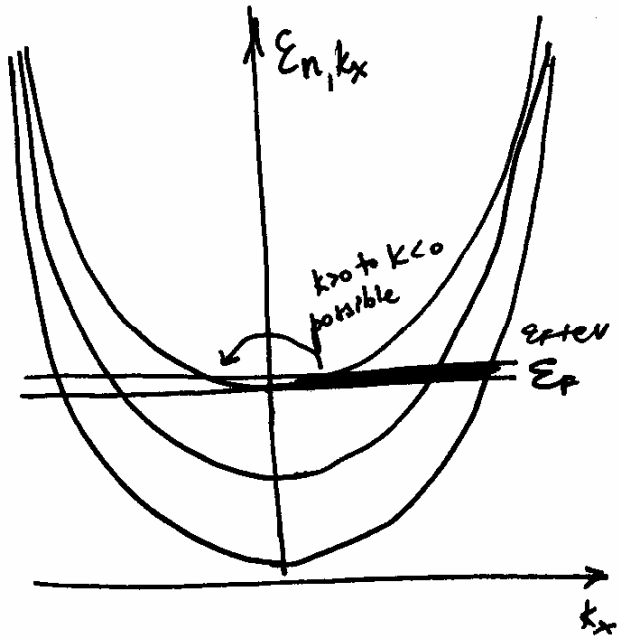

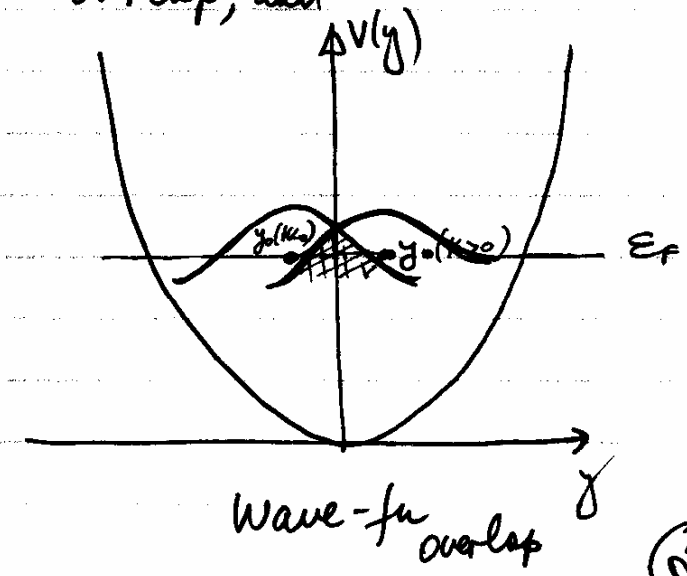

Each subband conducts balistically when $\varepsilon_n < \varepsilon_F < \varepsilon_{n+1}$, and with substantial scattering at $\varepsilon_F \sim \varepsilon_n \pm k_B T$. The wider the wire, the flatter the dispersion between levels, the smaller the overlap between edge states

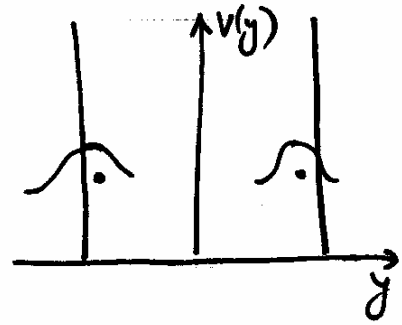

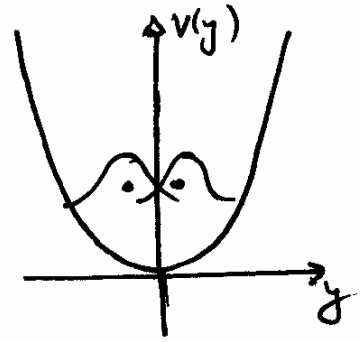

That's why in very narrow wires Shubnikov-de Haas minima don't go to zero, like in wide 2D samples.

So we've seen finally why at $\varepsilon_n < \varepsilon_F < \varepsilon_{n+1}$ $R_{xx} = 0$, and at $\varepsilon_F \sim \varepsilon_n \pm k_B T$ R_{xx} has a peak, i.e., we've explained <u>Shubnikov-de Haas oscillations</u>.

But where do the plateaus in R_{xy} come from?

How much current is transmitted per subband?

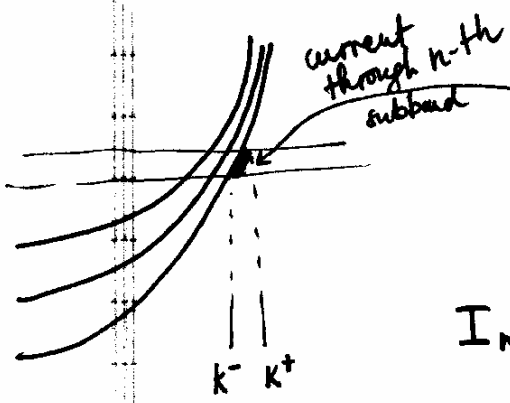

$$I_n = e \cdot \underset{\substack{\uparrow \\ \text{spin}}}{2} \cdot \frac{1}{2\pi} \int_{k_n^-}^{k_n^+} v(k_x)\,dk_x$$

where $\varepsilon_{n,k_n^+} = \varepsilon_F + eV$, $\varepsilon_{n,k_n^-} = \varepsilon_F$

$$I_n = \frac{e}{\pi} \cdot \int_{k_n^-}^{k_n^+} \frac{\hbar k_x}{m^*}\,dk_x = \frac{e\hbar}{\pi m^*} \cdot \frac{k_x^2}{2}\Big|_{k_n^-}^{k_n^+}$$

$$= \frac{e}{\pi\hbar} \cdot \varepsilon \Big|_{\varepsilon_F}^{\varepsilon_F + eV} = \frac{e}{\pi\hbar} \cdot eV$$

$$I_n = \frac{2e^2}{h} \cdot V$$ ← independent of

↖ universal conductance quantum

Current carried per 1D subband is independent of the subband bottom energy, it is simply

$$I_{\substack{\text{per} \\ \text{1D subband}}} = \frac{2e^2}{h} \cdot V$$

$$\boxed{G_{\substack{\text{per} \\ \text{subband}}} = \frac{2e^2}{h}}$$ conductance quantum

Total conductance?

$$G = \frac{2e^2}{h} \cdot N \,, \quad N \text{ number of "propagating modes"}$$

$$\boxed{\text{Modes} \equiv \text{channels} \equiv \text{subbands}}$$ ← people use these interchangeably

$$\boxed{\#\text{ of propagating modes} \equiv \text{number of subbands whose bottom is below the Fermi level}}$$

$$\boxed{\left(N - \tfrac{1}{2}\right)\hbar\omega_{c0} < \varepsilon_F}$$

In a <u>wide sample</u>, $\hbar\omega_{co} \approx \hbar\omega_c = \frac{\hbar eB}{m^*}$

QHE

$$\boxed{\begin{aligned} R_{xy} &= \frac{h}{2e^2}\cdot\frac{1}{n} \\ R_{xx} &= 0 \end{aligned}}$$

Shub. de Haas minima

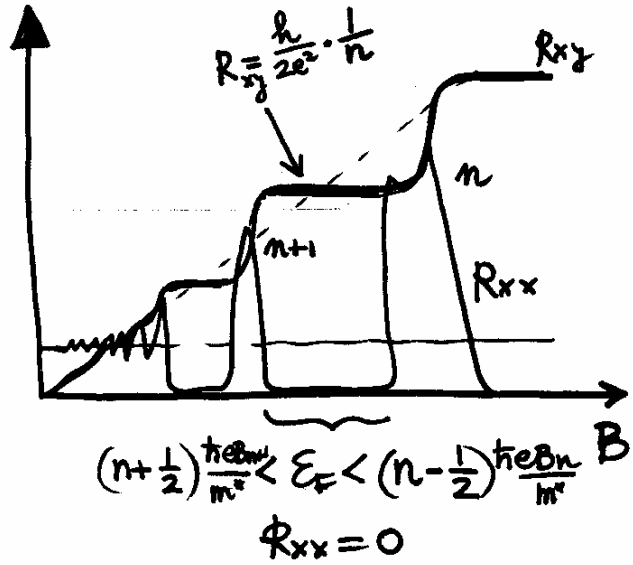

$$\boxed{G = \frac{2e^2}{h}\cdot N}$$ is a special case of the so-called <u>Landauer formula</u>

$$\boxed{G = \frac{2e^2}{h} N T(\varepsilon_F)}$$

T – transmission coefficient per mode may be < 1 due to disorder, barriers etc.

For the case of current carried by ballistic 1D edge ~~channels~~ states, a simple approach can help us determine what the longitudinal & Hall resistance are:

How is the measurement performed:
6 point probe

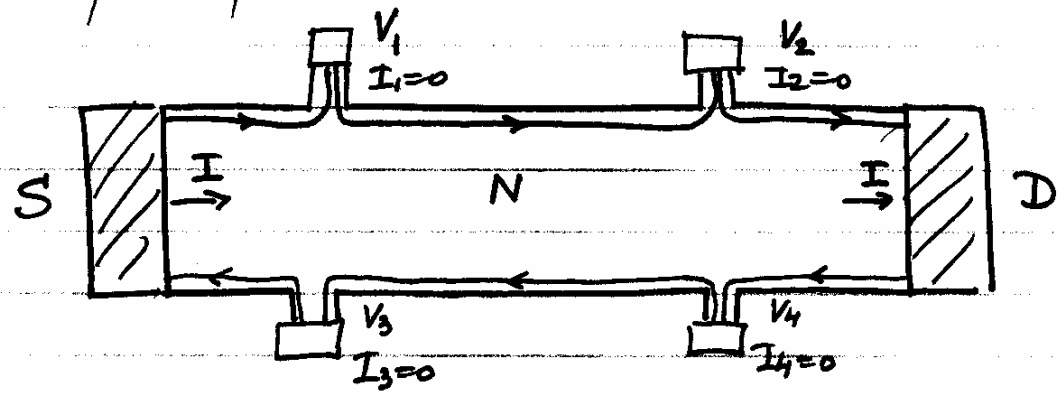

Probes S (source) and D (drain) are <u>current probes</u>, meaning there is a current source attached to them, giving current I. Probes 1 – 4 are voltage probes, meaning there will be a high – resistance voltmeter attached to them. <u>We measure V_1 to V_4.</u>

$$S: \quad I = \frac{2e^2}{h}(NV_S - NV_3)$$ Outgoing current positive

$$\text{Probe } 1: \quad 0 = \frac{2e^2}{h}(NV_1 - NV_S) \Rightarrow \boxed{V_1 = V_S}$$

$$\text{—"— } 2: \quad 0 = \frac{2e^2}{h}(NV_2 - NV_1) \Rightarrow \boxed{V_2 = V_1 = V_S}$$

$$D: \quad -I = \frac{2e^2}{h}(NV_D - NV_2) \overset{V_D=0}{\Longrightarrow} I = \frac{2e^2}{h}NV_2$$

↑ we are allowed to set one of the voltages to zero as a reference voltage. Usually $V_D = 0$.

$$\left.\begin{aligned} 3&: \; 0 = \frac{2e^2}{h}(NV_3 - NV_4) \\ 4&: \; 0 = \frac{2e^2}{h}(NV_4 - NV_D) \end{aligned}\right\} \quad \boxed{V_3 = V_4 = V_D = 0}$$

(Btw, there is no need to write eqns for both current probes.)

$$R_{xx} = \frac{V_1 - V_2}{I} = \frac{V_3 - V_4}{I} = 0$$

$$R_{xy} = \frac{V_1 - V_3}{I} = \frac{V_1 - V_4}{I} = \frac{V_2 - V_3}{I} = \frac{V_2 - V_4}{I}$$

$$= \frac{V_S - V_D}{\frac{2e^2}{h} N V_S} = \boxed{\frac{h}{2e^2} \cdot \frac{1}{N}}$$

This simple application of Landauer approach gives zero long. resistance & quantized Hall resistance in a snap!

Quantum Point Contact (QPC)

Quantum point contact is a very ~~short~~ narrow and very short (and therefore ballistic) quantum wire. In a split gate configuration, conductance G

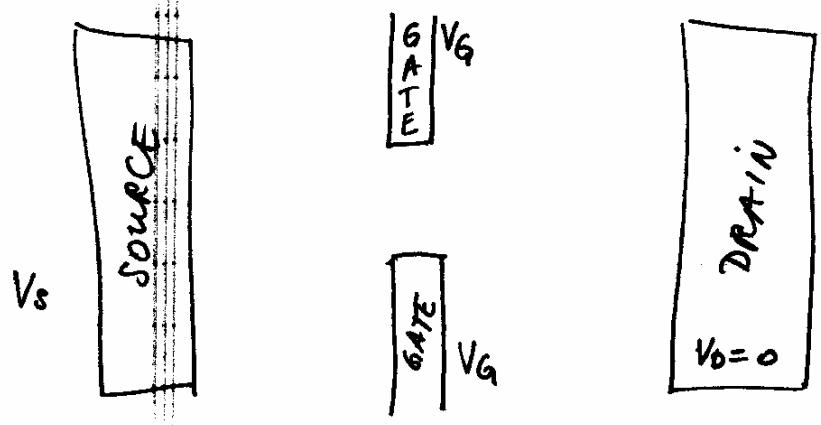

is quantized as a function of the applied gate voltage that actually forms the QPC.

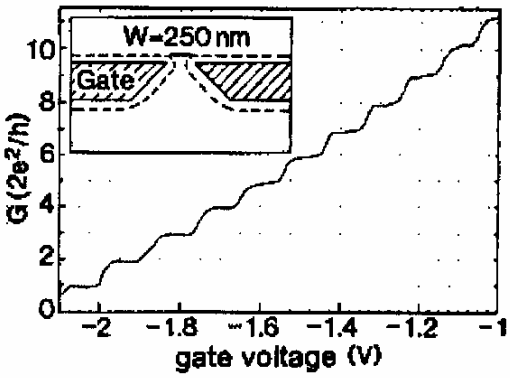

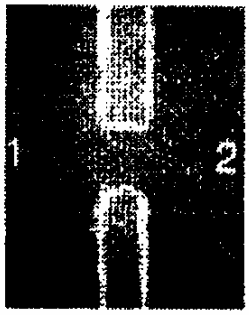

Conductance quantization as a function of gate voltage is occurring due to the fact that the number of propagating modes (channels) in the contacts is very large, and it is FINITE in the quantum point contact.

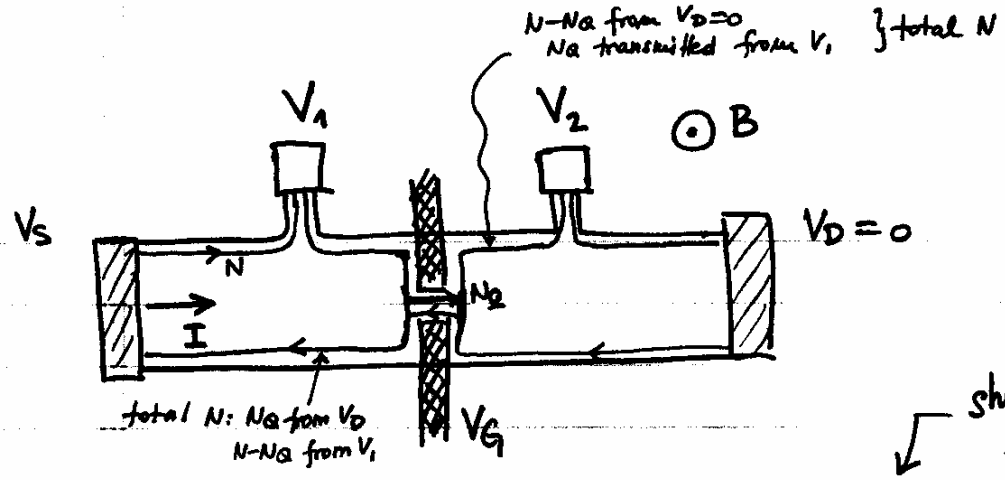

should also have $-N_a \cdot V_D$, but $V_D = 0$

Source: $I = \frac{2e^2}{h}\left(NV_s - (N-N_2)V_1\right)$

Probe 1: $0 = \frac{2e^2}{h}\left(NV_1 - NV_s\right) \Rightarrow V_1 = V_s$

should also have $-(N-N_a)V_D$ but $V_D=0$

Probe 2: $0 = \frac{2e^2}{h}\left(-V_1 N_2 + NV_2\right) \Rightarrow V_2 = V_s \frac{N_2}{N}$

$$I = \frac{2e^2}{h}\left(\cancel{NV_s} - \cancel{NV_s} + N_2 V_s\right) = \frac{2e^2}{h} N_2 V_s$$

$$R = \frac{V_1 - V_2}{I} = \frac{V_s - V_s \frac{N_2}{N}}{\frac{2e^2}{h} N_2 V_s} = \boxed{\frac{h}{2e^2}\left(\frac{1}{N_2} - \frac{1}{N}\right)}$$

- <u>Dependence of conductance on the magnetic field</u>

Low fields:

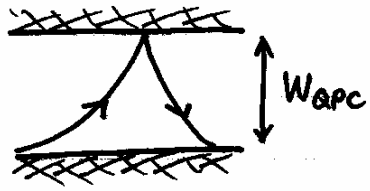

$W_{QPC} < r_c = \frac{\hbar k_F}{eB}$

The number of propagating modes is determined by the confinement potential

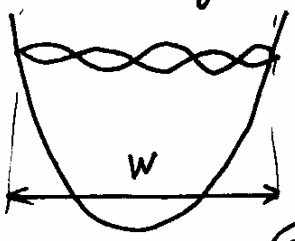

$W_{QPC} \approx N_2 \cdot \frac{\lambda_F}{2} = N_2 \frac{\pi}{k_F}$

$$\boxed{N_2 = \mathrm{Int}\left(\frac{k_F W_{QPC}}{\pi}\right)}$$

At low B, $N_2 \cong$ const., but the contacts get magneto-depopulated as

$$n_s \approx N \cdot \frac{2eB}{h}$$

$$\boxed{N \approx n_s \cdot \frac{h}{2eB}}$$

$$\boxed{R(B) = \frac{h}{2e^2}\left(\frac{1}{N_2} - \frac{2eB}{h n_s}\right)}$$

Indeed, at low fields the linear dependence is found.

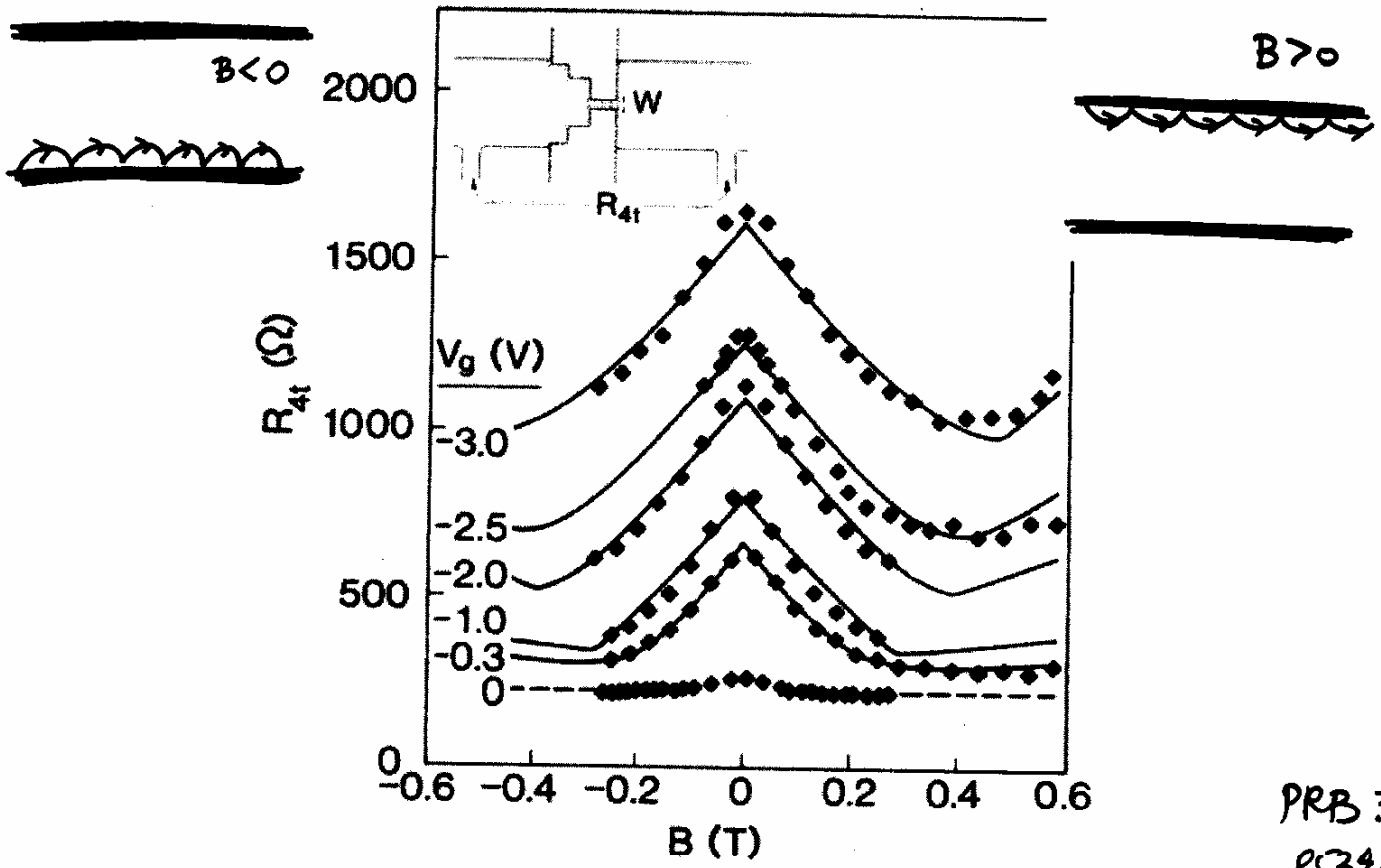

PRB 37, 8534 (1988)

FIG. 1. Four-terminal magnetoresistance for various gate voltages. Solid lines are according to Eq. (4). The sample geometry is schematically shown in the inset (dashed lines indicate the depletion boundaries). The parameter values for the curves corresponding to gate voltages from $V_g = -0.3$ to -3.0 V are, respectively, $W = 0.81$, 0.60, 0.42, 0.36, and 0.29 μm and $n_s = 3.25$, 3.08, 2.50, 2.25, and 1.90×10^{15} m^{-2}.

• <u>High fields</u> At higher fields, both the QPC and the leads are depopulated. The figure on the LHS shows

$$G_{QPC} = \frac{2e^2}{h} \cdot N_\ell ,$$

where at high fields

$$\left(N_\ell - \frac{1}{2}\right)\hbar\omega_c \leq \varepsilon_F$$

$$N_\ell = \mathrm{Int}\left(\frac{1}{2} + \frac{\varepsilon_F}{\hbar\omega_c}\right) = \mathrm{Int}\left(\frac{1}{2} + \frac{\varepsilon_F m^*}{\hbar e B}\right)$$

At low fields

$$N_\ell = \mathrm{Int}\left(\frac{1}{2} + \frac{\varepsilon_F}{\hbar\omega_0}\right)$$

↑ from the confinement potential

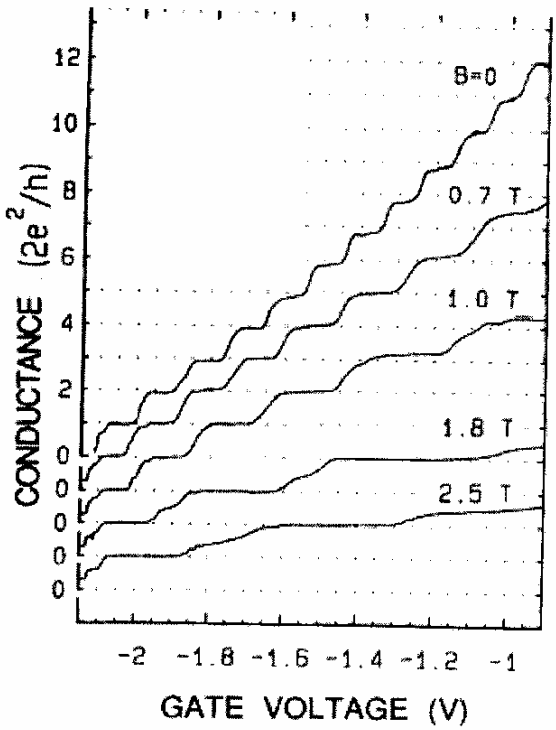

FIG. 7. Transition from quantization in zero field to quantization in high magnetic fields, obtained at several fixed values of the magnetic field at 0.6 K. The conductances were calculated from the measured resistances after subtraction of the resistances of the bulk contacts. The curves have been offset for clarity.

PRB43, 12431

• Can we have situations where $N = N_\ell$? Yes. Shubnikov-de Haas oscillations in the QPC magnetoresistance, but the resistance does not go all the way to zero, but rather has an upper non-zero limit, due to the fact that the narrowing of the lead into a QPC selects certain modes, and rejects others, so backscattering is enhanced.

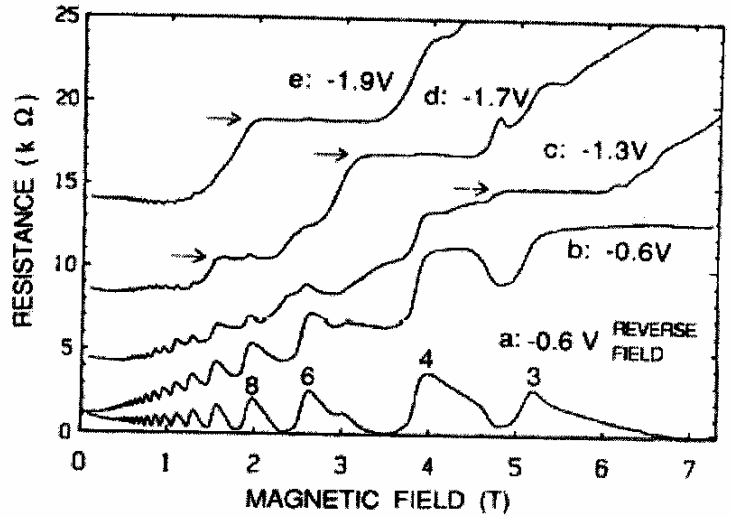

FIG. 18. Suppression of the Shubnikov–de Haas resistance oscillations due to selective population of edge channels. Curve *a* shows regular SdH oscillations, measured in a reverse field. Curves *b*–*e* show the quantized resistance of the QPC in series with the SdH oscillations of the 2DEG. Curves *c*–*e* show suppressed SdH oscillations. The arrows indicate the quantized values $h/(2e^2)$ and $h/(4e^2)$. The curves have been offset for clarity: *c*, +2 kΩ; *d*, +4 kΩ; *e*, +6 kΩ.

PRB 43, 12431.

35

Usuki Iterative Technique

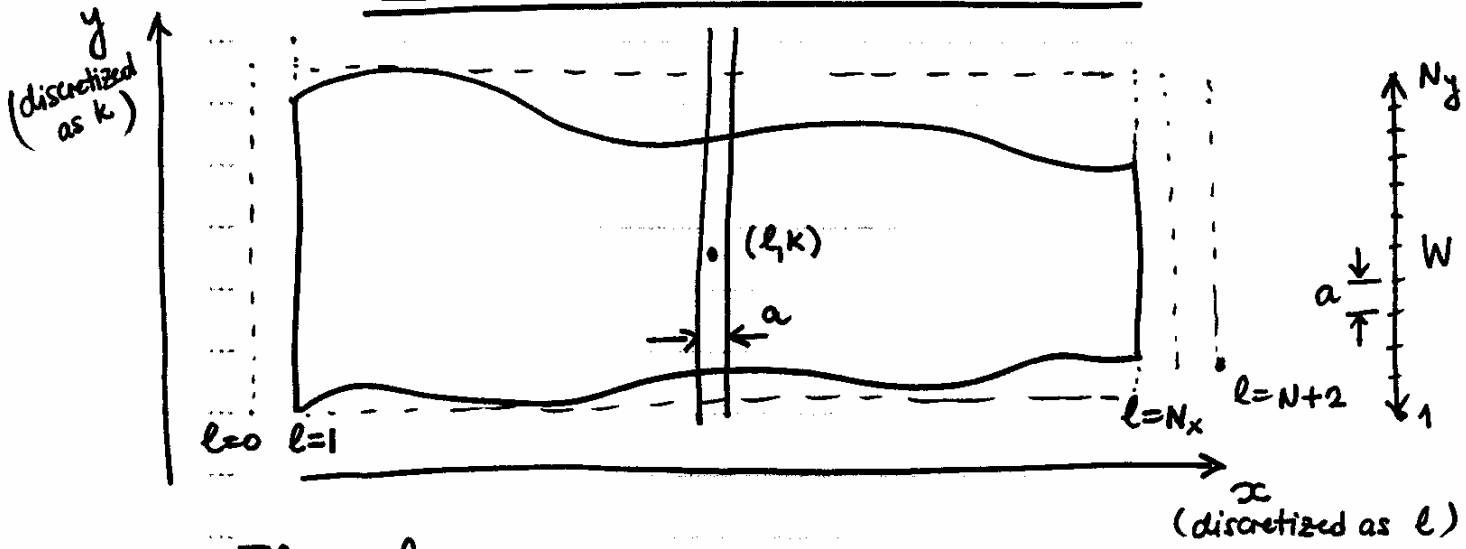

If we have an irregularly shaped sample, it is not possible to solve the Schrödinger eqn. exactly in order to get the subband structure.

Ideally, when we have a funny potential, or disorder, the conductance can be found from a generalized multi-mode Landauer formula

$$G = \frac{2e^2}{h} \sum_{m,n}' \tilde{T}_{mn} \quad ,$$

where $\tilde{T}$ is the transmission matrix (we'll introduce ~~of~~ several quantities w/ ~~the~~ a similar symbol & meaning)

The question is how much of the electronic wavefunction incident from the left is transmitted to the right?; more precisely, how much of the incident electronic current is ~~incident~~ transmitted through the structure due to potential variation and/or disorder.

Ideally, we do not really want to solve the Schrödinger equation and find the eigen~~modes~~ states, see how much current they carry etc. To be very flexible about the shape of the potential, and to potentially be able to introduce impurities if needed, it would be good if everything could be done in real space...

There are several methods to calculate conductance from the transmission matrix, and we'll cover one of them – the Usuki iterative technique [PRB 52, 8244 (1995)]. [also useful PRB 50, 7615 (1994); PRB 44, 8017 (1991).]

When given a potential $V(x,y)$, the discretized Schrödinger equation on a homogeneous mesh of meshsize a can be written as

$$-\frac{\hbar^2}{2m}\nabla^2\psi + V(x,y)\psi = \varepsilon\psi$$

$$\downarrow$$

$$-\frac{\hbar^2}{2m^*}\left[\frac{\psi_{\ell+1,k}+\psi_{\ell-1,k}+\psi_{\ell,k-1}+\psi_{\ell,k+1}-4\psi_{\ell,k}}{a^2}\right] + V_{\ell,k}\psi_{\ell,k} = \varepsilon\psi_{\ell,k}$$

Hopping energy $t \equiv \frac{\hbar^2}{2ma^2}$

Introduce column $\tilde{\psi}_\ell = [\psi_{\ell,1} \ldots \psi_{\ell,N_y}]^T$ $\quad N_y \times 1$

And matrices $\hat{H}_{\ell,\ell\mp1} = \mathrm{diag}(t, \dots, t)$

$$\hat{H}_\ell = \begin{bmatrix} 4t+V_{\ell,1} & -t & 0 & \cdots & \\ -t & 4t+V_{\ell,2} & -t & 0 & \cdots \\ 0 & & \ddots & & \\ \vdots & & & \ddots & 4t+V_{\ell,n} \end{bmatrix}$$

The above discretized Schrödinger equation can be rewritten as

$$(\hat{H}_\ell - \varepsilon\hat{I})\tilde{\Psi}_\ell = \hat{H}_{\ell,\ell-1}\tilde{\Psi}_{\ell-1} + \hat{H}_{\ell,\ell+1}\hat{\Psi}_{\ell+1}$$

$$\tilde{\Psi}_{\ell+1} = +\hat{H}_{\ell,\ell+1}^{-1}(\hat{H}_\ell - \varepsilon\hat{I})\tilde{\Psi}_\ell$$

$$- \hat{H}_{\ell,\ell+1}^{-1}\hat{H}_{\ell,\ell-1}\tilde{\Psi}_{\ell-1}$$

When we form a column of the form $[\tilde{\Psi}_\ell \; \tilde{\Psi}_{\ell+1}]^T$ we see

$$\begin{bmatrix} \tilde{\Psi}_\ell \\ \tilde{\Psi}_{\ell+1} \end{bmatrix} = \underbrace{\begin{bmatrix} 0 & \hat{I} \\ -\hat{H}_{\ell,\ell+1}^{-1}\hat{H}_{\ell,\ell-1} & \hat{H}_{\ell,\ell+1}^{-1}(\hat{H}_\ell - \varepsilon\hat{I}) \end{bmatrix}}_{\equiv \hat{T}_\ell^{(\ell)}} \begin{bmatrix} \tilde{\Psi}_{\ell-1} \\ \tilde{\Psi}_\ell \end{bmatrix}$$

(the T-matrix NOT transmission matrix

TRANSFER MATRIX of the ℓ-th slice

$(T_\ell)_{11} = 0 \quad (T_\ell)_{12} = \hat{I}$

$(T_\ell)_{21} = -\hat{H}_{\ell,\ell+1}^{-1}\hat{H}_{\ell,\ell-1}$

$(T_\ell)_{22} = \hat{H}_{\ell,\ell+1}^{-1}(\hat{H}_\ell - \varepsilon\hat{I})$

There is a different linear combination of $\tilde{\Psi}_\ell$'s that depicts how much transmission and how much reflection occurs

$$\begin{bmatrix} \tilde{\Psi}_\ell \\ \tilde{\Psi}_{\ell+1} \end{bmatrix} = \begin{bmatrix} C_1^{(\ell+1)} & C_2^{(\ell+1)} \\ 0 & \hat{I} \end{bmatrix} \begin{bmatrix} \tilde{\Phi}_\ell \\ \tilde{\Phi}_{\ell} \end{bmatrix}$$

and $C_1^{(\ell)}$ is the local transmission matrix, $C_2^{(\ell)}$ is the local reflection matrix. It also holds that

$$[\tilde{\Phi}_{\ell+1}] = \hat{P}_\ell \, [\Phi_\ell]$$

where

$$\hat{P}_\ell = \begin{array}{|c|c|} \hline \hat{I} & 0 \\ \hline P_1^{(\ell)} & P_2^{(\ell)} \\ \hline \end{array}$$

So eventually we obtain

$$\begin{bmatrix} C_1^{(\ell+1)} & C_2^{(\ell+1)} \\ 0 & \hat{I} \end{bmatrix} \begin{bmatrix} \Phi_\ell \end{bmatrix} = \hat{T}^{(\ell)} \begin{bmatrix} C_1^{(\ell)} & C_2^{(\ell)} \\ 0 & \hat{I} \end{bmatrix} \begin{bmatrix} \Phi_{\ell-1} \end{bmatrix}$$

$$(*) \quad \boxed{\begin{bmatrix} C_1^{(\ell+1)} & C_2^{(\ell+1)} \\ 0 & \hat{I} \end{bmatrix} = \hat{T}^{(\ell)} \begin{bmatrix} C_1^{(\ell)} & C_2^{(\ell)} \\ 0 & \hat{I} \end{bmatrix} \begin{bmatrix} \hat{I} & 0 \\ P_1^{(\ell)} & P_2^{(\ell)} \end{bmatrix}}$$

Eventually

$$\boxed{P_2^{(\ell)} = \left[T_{21}^{(\ell)} C_2^{(\ell)} + T_{22}^{(\ell)} \right]^{-1}}$$

$$(**) \quad \boxed{P_1^{(\ell)} = - P_2^{(\ell)} T_{21}^{(\ell)} C_1^{(\ell)}}$$

The iteration goes as follows: start with $C_1^{(0)} = \hat{I}$ and $C_2^{(0)} = 0$. We want to inject modes with unit amplitude from the ~~right~~ left. $T^{(0)}$ does that, and its form is therefore somewhat different than of other $T^{(\ell)}$, $\ell = 1, \dots N_y$. Basically, $T^{(0)}$ converts from mode representation to site representation

$$T^{(0)} \begin{bmatrix} \psi_0 \\ \psi_1 \end{bmatrix} = \lambda \begin{bmatrix} \psi_0 \\ \psi_1 \end{bmatrix} \qquad \underline{\underline{2N_y \text{ solutions}}}$$

where $\lambda^{\pm} = e^{\pm ika}$, for propagating modes in the positive/negative x direction, and $\lambda^{\pm} = e^{\mp \varkappa a}$ for evanescent modes propagating in the positive/negative x direction.

Thus, solve

this is what we'd expect for $T^{(0)}$ $\rightarrow$

$$\begin{bmatrix} 0 & \hat{I} \\ \underbrace{-\hat{H}_{0,1}\hat{H}_{0,-1}}_{\hat{I}} & \hat{H}_{0,1}^{-1}(\hat{H}_0 - \mathcal{E}\hat{I}) \end{bmatrix} \begin{bmatrix} \psi_0 \\ \psi_1 \end{bmatrix} = \lambda \begin{bmatrix} \psi_0 \\ \psi_1 \end{bmatrix}$$

There will be $2N_y$ different solutions/modes, all of them of the form

$$\begin{bmatrix} u_m(\pm) \\ \lambda_m^{\pm} u_m(\pm) \end{bmatrix}$$

because $\psi_1 = e^{\pm ika}\psi_0$ or $e^{\mp \varkappa a}\psi_0$ (one mesh cell happ.)

! Very important: ~~and~~ after ~~a~~ running the eigenvalue solver for the above $T^{(0)}$, <u>SORT the eigenvalues and eigenvectors</u>, so that the first N_y are in the positive x direction and the next N_y are in the negative x direction.

After sorting, rearrange them and that is how you obtain the matrix $T^{(0)}$ TO USE IN CALCULATION

$$\hat{T}^{(0)} = \begin{bmatrix} U^{(+)} & U^{(-)} \\ U^{(+)}\lambda^{(+)} & U^{(-)}\lambda^{(-)} \end{bmatrix}$$

N_y columns corresponding to eigenvectors of the forward propagating modes

backward propag. modes

Basically, we want this

$$\begin{bmatrix} t \\ 0 \end{bmatrix} = \hat{T}^{(N_x+1)} \hat{T}^{(N_x)} \cdots \hat{T}^{(1)} T^{(0)} \begin{bmatrix} 1 \\ r \end{bmatrix}$$

site to mode

mode to site

t and r are transmission coefficients, like for waves.

$$\hat{T}^{(N_x+1)} = \begin{bmatrix} 0 & [U^{(+)}\lambda^{(+)}]^{-1} \\ \hat{I} & -\hat{U}^{(+)}[\hat{U}^{(+)}\lambda^{(+)}]^{-1} \end{bmatrix}$$

Recipe: Initialize, for a given energy $\mathcal{E}$ (will be our Fermi energy), $C_1^{(0)} = \hat{I}$, $C_2^{(0)} = 0$, and then all $\hat{T}^{(\ell)}$, $\ell = 0, \ldots, N_y+1$.

Then iterate: get $P_2^{(0)}, P_1^{(0)}$ from (**) p. 39, with these go back to * and get $C_1^{(1)}, C_2^{(1)}$, then $P_2^{(1)}, P_1^{(1)}$, etc.

Eventually, you want to get $C_1^{(N_x+2)}$, and from $C_1^{(N_x+2)}$ you obtain the conductance as

$$\boxed{G = \frac{2e^2}{h} \sum_{m,n} \tilde{T}_{mn}}$$

, where m, n go over all forward propagating modes

$C_1^{(N_x+2)}$ is the transmission matrix $\hat{t}$.

$$T_{mn} = \frac{v_m^{(out)}}{v_n^{(in)}} |t_{mn}|^2 = \frac{v_m^{(out)}}{v_n^{(in)}} \left| C_{1,mn}^{(N_x+2)} \right|^2$$

these are for forward propagating modes only

not evanescent if you happen to have any

these you get from $\lambda_m = e^{+ik_m a}$, $v_m = \hbar k_m / m^*$

To calculate the density, use

$$n_{mode}(i, j) = \left| \hat{\Phi}^{(N_x+2,\, j)}(i, mode) \right|^2$$

row (transverse) slice (long)

(For total density, sum over all modes.) Here

$$\hat{\Phi}^{(N_x+2,\, N_x+1)} = \hat{P}_1^{(N_x+1)}$$

Substitute backwards (must store all P_1's and P_2's!!)

$$\hat{\Phi}_1^{(N_x+2,\, j-1)} = \hat{P}_1^{(j-1)} + \hat{P}_2^{(j-1)} \hat{\Phi}_1^{(N_x+2,\, j)}$$

! go $1 \ldots N_x+2$ to generate all C's and P's and find the transmission. C's you don't have to store, but P's you do. Once you've got to N_x+1 for P's, go back to find the density.

Single-Electron Transistor (incomplete)

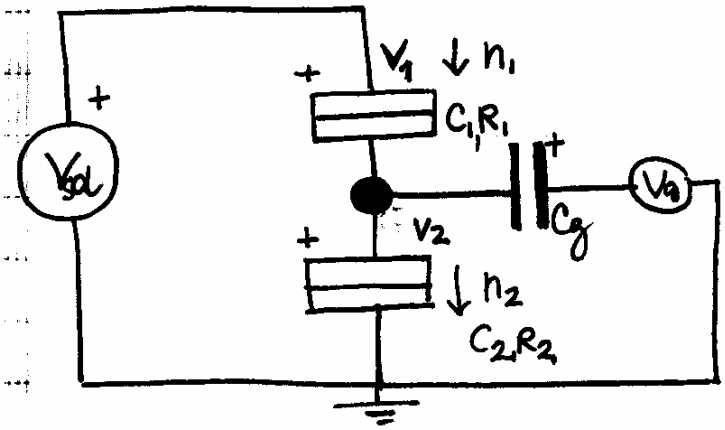

$$Q_g = C_g(V_g - V_2)$$

$$Q = Q_2 - Q_1 - Q_g$$

$$V_1 = Q_1 / C_1$$

$$V_2 = Q_2 / C_2$$

$$V_{sd} = V_1 + V_2 = \frac{Q_1}{C_1} + \frac{Q_2}{C_2} =$$

$$= V_2 + \frac{Q_2 - Q_1 - Q - Q_g}{C_1}$$

$$= V_2 + \frac{C_2}{C_1} V_2 - \frac{Q}{C_1} - \frac{C_g}{C_1}(V_g - V_2)$$

$$= V_2\left(1 + \frac{C_2}{C_1} + \frac{C_g}{C_1}\right) - \frac{Q}{C_1} - \frac{C_g}{C_1} V_g$$

$$C_{eq} = C_1 + C_2 + C_g \qquad V_{sd} = V_2 \frac{C_{eq}}{C_1} - \frac{Q}{C_1} - \frac{C_g V_g}{C_1}$$

$$V_2 = \frac{V_{sd} C_1 + Q + C_g V_g}{C_{eq}}$$

$$V_1 = V_{sd} - V_2 = \frac{1}{C_{eq}}\left[V_{sd}(C_2 + C_g) - Q - C_g V_g\right]$$

Energy stored on the capacitors

$$E_S = \frac{C_1 V_1^2}{2} + \frac{C_2 V_2^2}{2} + \frac{C_g (V_g - V_2)^2}{2}$$

Work needed to pass n_1 electrons into & n_2 electrons out of the dot

$$W_{S1} = -n_1 \left[\frac{C_2}{C_{eg}} e V_{sd} + \frac{C_g}{C_{eg}} e (V_{sd} - V_g) \right]$$

$$W_{S2} = -n_2 \left[\frac{C_1}{C_{eg}} e V_{sd} + \frac{C_g}{C_{eg}} e V_g \right]$$

Stable configurations for a given n

$$-\frac{e}{2} \mp \left(en + (C_g + C_2) V_{sd} - C_g V_g' \right) < 0 \qquad (1)$$

$n = n_1 - n_2$

$$-\frac{e}{2} \pm \left(en - C_1 V_{sd} - C_g V_g' \right) < 0 \qquad (2)$$

$$\begin{cases} V_{sd} > \left[e\left(-n - \frac{1}{2}\right) + C_g V_g' \right] \cdot \frac{1}{C_g + C_2} & (1a) \\ V_{sd} < \frac{C_g V_g'}{C_g + C_2} + \frac{e}{C_g + C_2} \left(\frac{1}{2} - n \right) & (1b) \end{cases}$$

$$V_{sd} > \frac{e}{C_1} (n - 1/2) - \frac{C_g V_g'}{C_1} \qquad (2a)$$

$$V_{sd} < \frac{e}{C_1} (n + 1/2) - \frac{C_g V_g'}{C_1} \qquad (2b)$$

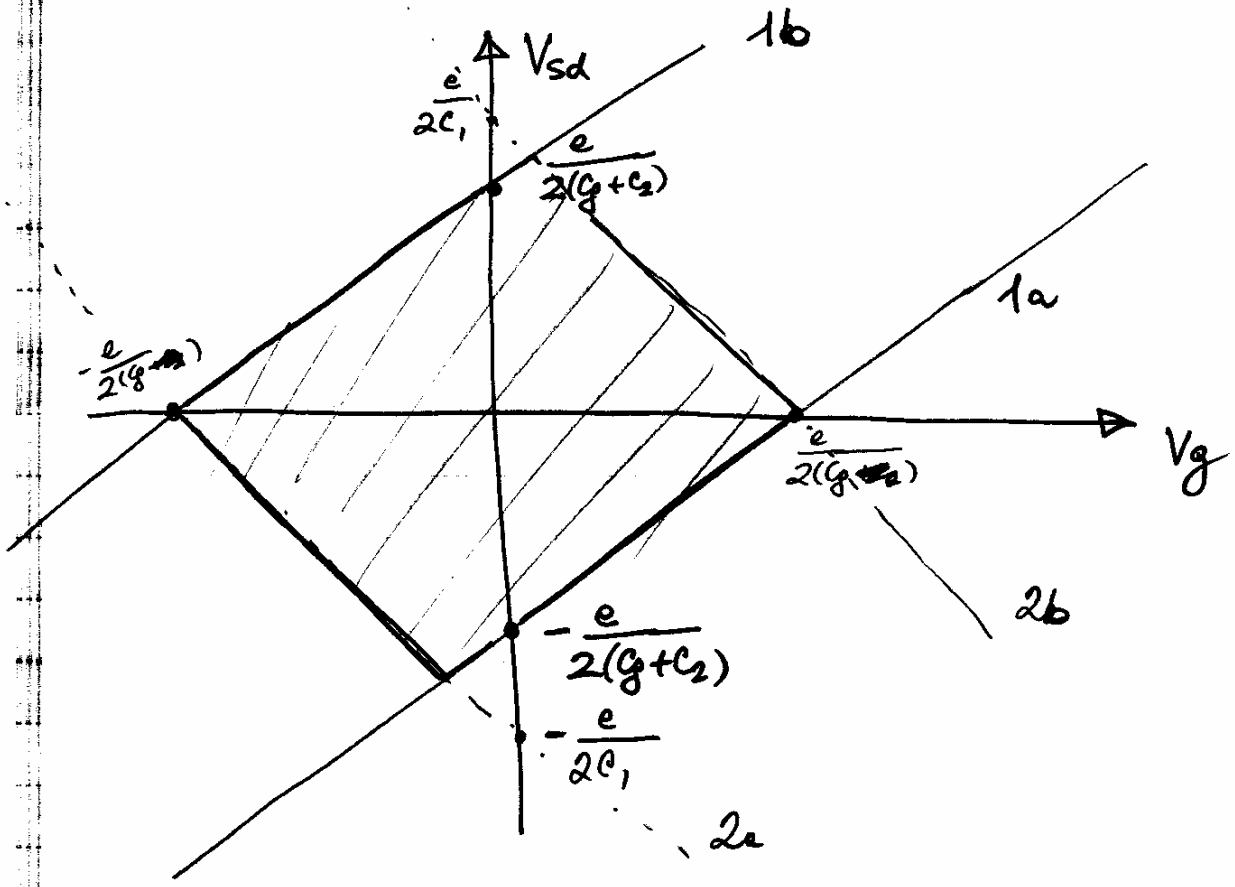

If you keep Vsd low, from ΔV_g you can determine C_g, and if you know C_g, from ΔV_{sd} you can determine $C_{1,2}$.

Aharonov – Bohm Effect

One of the most important properties of electronic transport in mesoscopic structures is whether it is <u>coherent</u> or not. Coherent transport implies that the electronic wavefunction phase is preserved throughout all (or most) of the device. If this is the case, then <u>interference</u> effects, observable only if transport is mostly coherent, become visible.

A typical quantum-mechanical phenomenon observable in nanostructures is the Aharonov-Bohm effect (thought experiment described in Phys Rev 115, 485 (1959).)

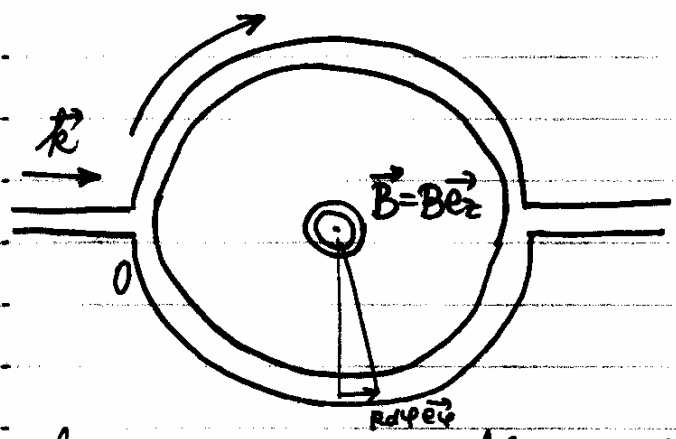

Electrons move in the ring that encloses an "infinite" solenoid, so classically they feel $B=0$. However, quantum-mechanically, the ~~vector potential~~ flux enclosed will cause a difference

$$\Delta\varphi_{up} = +\int_{\pi}^{2\pi} \left(\vec{k} + \frac{e}{\hbar}\vec{A}\right) R\, d\varphi\, (-\vec{e}_\varphi)$$

$$\Delta\varphi_{down} = \int_{0}^{\pi} \left(\vec{k} + \frac{e}{\hbar}\vec{A}\right) R\, d\varphi\, (\vec{e}_\varphi)$$

$$\Delta\varphi = -\Delta\varphi_{up} + \Delta\varphi_{down} = \int_0^{2\pi} \cancel{\vec{k}\cdot\vec{e}_\varphi R\, d\varphi}^{\,0} +$$

$$+ \int_0^{2\pi} \frac{e}{\hbar} \underbrace{\vec{A}\cdot\vec{e}_\varphi}\, R\, d\varphi = \frac{e}{\hbar} \oint_C \vec{A}\cdot d\vec{\ell}$$

$$= \frac{e}{\hbar} \int \underbrace{(\vec{\nabla}\times\vec{A})}_{\vec{B}}\cdot d\vec{S} = \frac{e}{\hbar}\cdot\Phi \leftarrow \text{flux through the ring}$$

$$= 2\pi \frac{\Phi}{\Phi_0} \qquad \Phi_0 = \frac{h}{e}$$

Quantum unit of flux

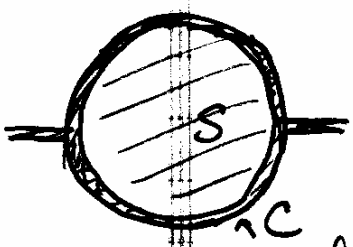

When $\Delta\varphi = 2\pi \times$ integer, there is constructive interference, and a peak in conductance, when $\Delta\varphi = 2\pi\cdot(\text{odd}/2)$, minimum.

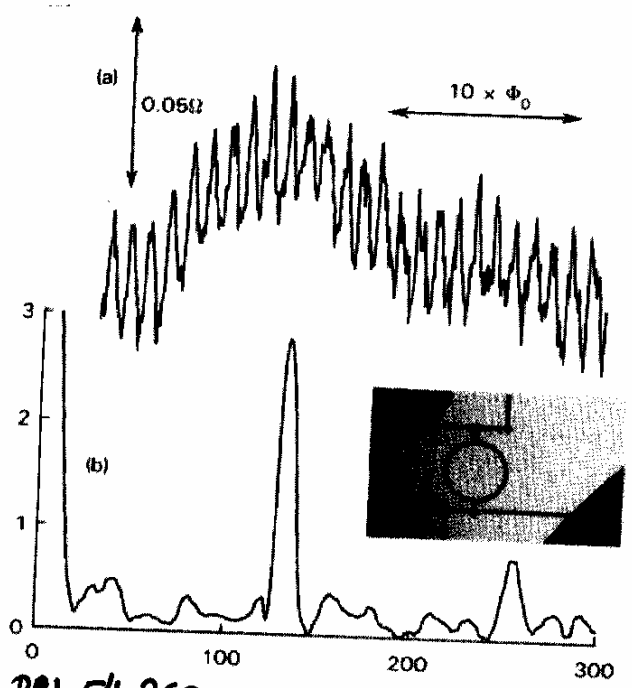

PRL 54, 2696

FIG. 1. (a) Magnetoresistance of the ring measured at $T = 0.01$ K. (b) Fourier power spectrum in arbitrary units containing peaks at h/e and $h/2e$. The inset is a photograph of the larger ring. The inside diameter of the loop is 784 nm, and the width of the wires is 41 nm.

You can get the area of the ring from the period of these high-frequency oscillations

$$\Delta B_{peak} \cdot \underset{\substack{\uparrow \\ \text{area}}}{A_{ring}} = \Phi_0$$

$$\boxed{A_{ring} = \frac{h}{e\Delta B}}$$

polycrystalline, so lots of phase preserved!!!

An important point is that the golden rings were polycrystalline, with lots of scattering events that are elastic

⇓

elastic scattering preserves coherence.

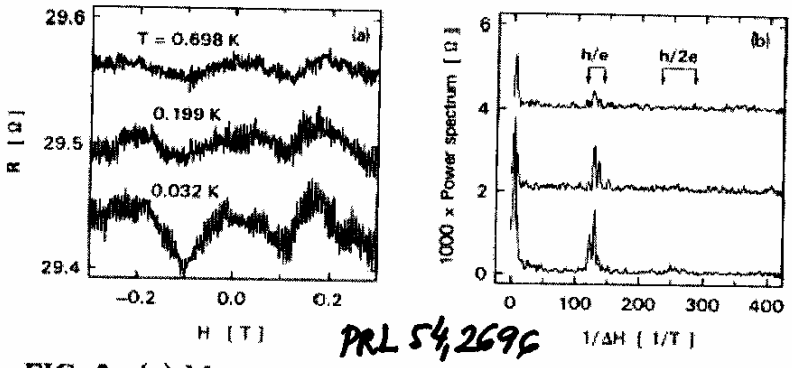

PRL 54, 2696

FIG. 2. (a) Magnetoresistance data from the ring in Fig. 1 at several temperatures. (b) The Fourier transform of the data in (a). The data at 0.199 and 0.698 K have been offset for clarity of display. The markers at the top of the figure indicate the bounds for the flux periods h/e and $h/2e$ based on the measured inside and outside diameters of the loop.

Also, as seen on the left, oscillations vanish with increasing temperature, with increased dephasing.

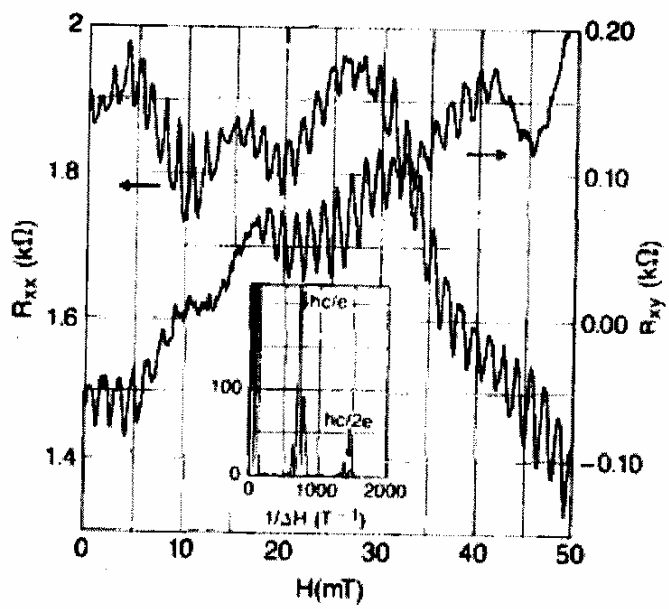

FIG. 4. Magnetoresistance and Hall resistance at 300 mK of the ring shown in Fig. 2. The inset is the Fourier transform of the magnetoresistance showing the oscillations at flux periods of hc/e and $hc/2e$. These correspond to interference from a single or double transit of an electron around the ring.

Results obtained later for semiconductor rings

Later for many different systems.

← GaAs / AlGaAs with top gate.

Mankiewich et al. J. Vac. Sci. Technol. B6, 131 (1988) 49

First studies of the Aharonov–Bohm effect were unsuccessful, and showed an aperiodic structure. They were performed on SMALL RINGS, so ~~the~~ same-arm interference was appreciable (didn't average out to zero over all different paths).

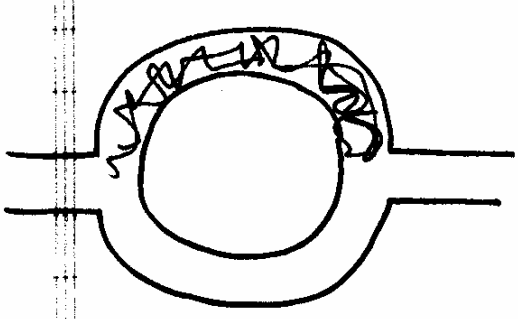

~~There~~ Interference pattern from the same-arm paths fluctuates randomly with applied B-field, giving the aperiodic feature of approximate periodicity

$$\Delta B_{\substack{\text{same}\\\text{arm}}} = \frac{h}{e A_{arm}}$$

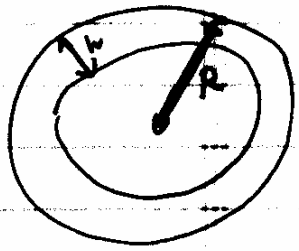

$$\frac{\Delta B_{\substack{\text{diff}\\\text{arms}}}}{\Delta B_{\substack{\text{same}\\\text{arm}}}} = \frac{A_{arm}}{A_{\substack{\text{enclosed}\\\text{by ring}}}} \approx \frac{W \pi R}{\pi R^2} = \frac{W}{R}$$

When $\frac{W}{R} \ll 1$, we clearly see interference from the two different arms, which is <u>periodic</u>.

Larger rings $\rightarrow$ periodic

Small rings $\left(\frac{W}{R} \sim 1\right) \rightarrow$ aperiodic

Weak Localization

The resistance of disordered thin films and wires shows a small increase when the temperature is lowered. The effect is more pronounced in smaller samples.

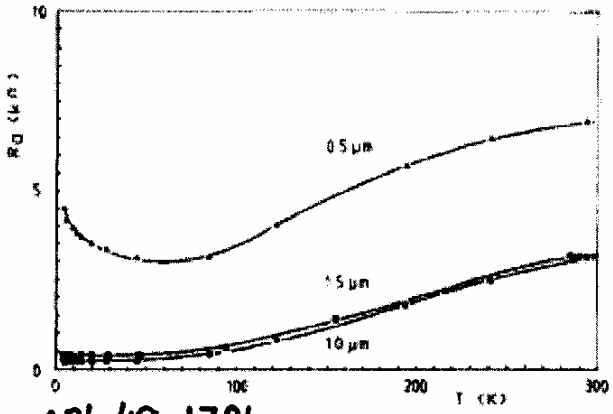

APL 49, 1781

FIG. 3. Temperature dependence of the resistivity per square for three channel widths (taken equal to the etched mesa width). Solid lines are to guide the eye.

The underlying reason is quantum-mechanical enhancement of backscattering due to the presence of disorder. ⟷ ⟷ weak localization.

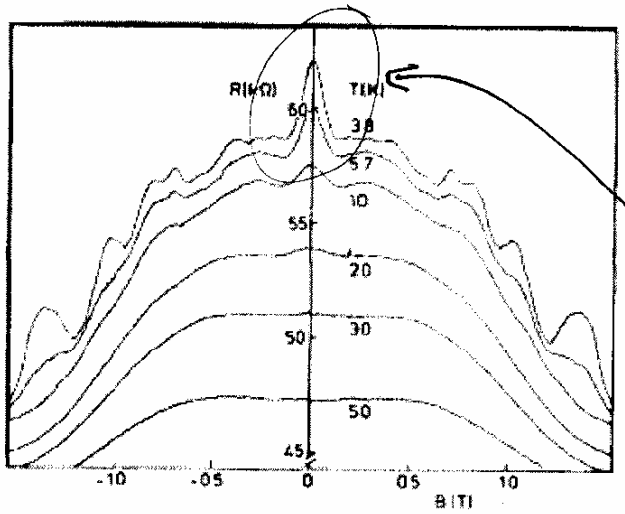

FIG. 4. Negative magnetoresistance for a nominally 500-nm-wide sample at several temperatures showing reproducible aperiodic fluctuations.

APL 49, 1781

Weak localization is usually identified from magneto-resistance measurements: it is the zero-field peak in resistance.

(i.e., magnetic field destroys the weak localiz. effect.)

Origin of the weak localization is quantum-mechanical interference, helped by <u>disorder</u>. Namely, impurity scattering is elastic, so it changes momentum, but not energy (and consequently, not the wavefunction phase either).

(Often people use the expression COHERENT BACKSCATTERING to describe the origin of weak localization. Disorder, however, is what makes coherent backscattering possible.)

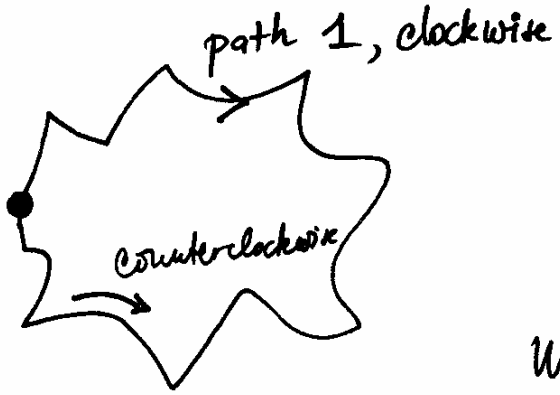

Constructive interference of wavefunctions corresponding to the two ~~paths~~ directions along the same path

With interference (constructive)

prob. density $= |A^+ + A^-|^2 = 4|A|^2$

without interference

prob. density $= 2|A|^2$

A^+, A^- — amplitudes of waves in the ~~positive~~ negative (clockwise) and positive (counterclockwise) directions

The dimensionality of the weak localization effect is determined by the ratio of dimensions and the phase coherence length

2D $l_\varphi \ll L, W$; 1D $l_\varphi \gtrsim W$

$l_\varphi \ll L$ Ω

Probability to find a particle at time t away from a source at $r=0$ satisfies the diffusion equation with a source term

$$\left(\frac{\partial}{\partial t} - D\nabla^2\right) W(\vec{r},t) = \cancel{\delta(\vec{r},t)}\,\delta(\vec{r})\delta(t)$$

d-dimensionality $\quad W(\vec{r},t) = \frac{1}{(4\pi D t)^{d/2}} e^{-r^2/4Dt}$

When there's the account of a finite lifetime of a phase

$$\frac{\partial}{\partial t} \to \frac{\partial}{\partial t} + \frac{1}{\tau_\varphi}$$

$$W(0,t) = \frac{1}{(4\pi D t)^{d/2}} e^{-t/\tau_\varphi}$$

Another trick: if transport is ballistic, this doesn't occur; so for total scattering time τ, $\tau < \tau_\varphi$, we should not be able to see much for times shorter than τ

$$W(0,t) = \frac{1}{(4\pi D t)^{d/2}} e^{-t/\tau_\varphi} \left(1 - e^{-t/\tau}\right)$$

fudge
quantum mechanics

$$\Delta\sigma/\sigma \sim \int_0^\infty W(0,t)\,dt$$

$$\Delta\sigma = -\frac{e^2}{\pi\hbar}\begin{cases} \frac{1}{2\pi l_\varphi}\left(\sqrt{1+\frac{\tau_\varphi}{\tau}}-1\right), & d=3 \\ \frac{1}{2\pi}\ln\left(1+\frac{\tau_\varphi}{\tau}\right), & d=2 \\ l_\varphi\left(1-\sqrt{\frac{\tau}{\tau+\tau_\varphi}}\right), & d=1 \end{cases}$$

Here, $l_\varphi^2 = D\tau_\varphi$.

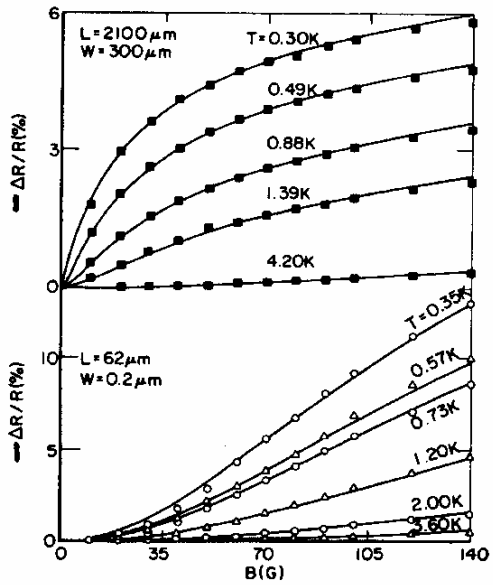

FIG. 1. The magnitude of the negative magnetoresistance for a wide channel (upper curves) and a narrow channel (lower curves) at different temperatures. The solid curves are the theoretical fittings based on Eq. (3) and Eq. (5), respectively. The fitting parameter, $1/\tau_\phi$, is plotted in Fig. 2.

In the presence of magnetic field, the phase difference accumulated between the two differently oriented trajectories is

$$\frac{\Delta\varphi}{2\pi} = \underset{\substack{\uparrow \\ \text{full} \\ \text{circle}}}{2} \cdot \frac{\Phi}{\Phi_0} = 2\,\frac{eBA_{loop}}{h}$$

PRB 36, 7751 (GaAs/AlGaAs) Mostly $\frac{\Phi}{\Phi_0} \sim 1$ is responsible for AB effect, and for weak localization. So if

$$\frac{\Phi}{\Phi_0} \gtrsim 1 \Rightarrow A_{loop} \gtrsim \frac{h}{eB}$$ ← no more appreciable contribution from constructive interference

As $B\uparrow$, the number of loops capable of exhibiting constructive interference decreases

$B\uparrow$, $R\downarrow$ (with respect to the $B=0$ peak)

Acoustic Phonons

The Hamiltonian

$$\hat{H}' = \Xi_1 \cdot [\vec{\nabla} \cdot \vec{u}(\vec{r},t)]$$

where Ξ_1 is the DEFORMATION POTENTIAL, and $\vec{u}(\vec{r},t)$ is the DISPLACEMENT OPERATOR (obtained by quantization of classical displacement). The displacement operator is related to creation & destruction of phonons with different $\vec{Q}$'s:

$$\boxed{\vec{u}(\vec{r},t) = \left(\frac{\hbar}{2\rho V}\right)^{1/2} \sum_{\vec{Q}} \left[\frac{1}{\omega_{\vec{Q}}}\right]^{1/2} \left\{ \hat{a}_{\vec{Q}}\, e^{i\vec{Q}\vec{r} - i\omega_{\vec{Q}} t} + \hat{a}^{+}_{\vec{Q}}\, e^{-i\vec{Q}\vec{r} + i\omega_{\vec{Q}} t} \right\} \vec{e}_{\vec{Q}}}$$

$$\hat{H}' = \Xi_1 \cdot \sum_{\vec{Q}} \left(\frac{\hbar}{2\rho V \omega_{\vec{Q}}}\right)^{1/2} (i\vec{Q} \cdot \vec{e}_{\vec{Q}}) \left\{ \hat{a}_{\vec{Q}}\, e^{i\vec{Q}\vec{r} - i\omega_{\vec{Q}} t} - \hat{a}^{+}_{\vec{Q}}\, e^{-i\vec{Q}\vec{r} + i\omega_{\vec{Q}} t} \right\}$$

Acoustic Phonons

Transition rate

$$\boxed{S(\vec{k},\vec{k}')_{\substack{ab\\em}} = \frac{2\pi}{\hbar} \left(\frac{\hbar \Xi_1^2}{2\rho V \omega_{\vec{k}'-\vec{k}}}\right) (\vec{k}'-\vec{k})^2 \begin{cases} N_{\vec{k}'-\vec{k}}, & abs \\ N_{\vec{k}'-\vec{k}}+1, & emis \end{cases}} \quad (31)$$

Total scattering rate (a.k.a. total relaxation rate)

$$\frac{1}{\tau(\vec{k})} = \Gamma_{tot}(\vec{k}) = \overset{0}{\Gamma}_{ab} + \overset{1}{\Gamma}_{em} = 2\Gamma_{ab}$$

$$= \frac{2\pi}{\hbar} \cdot \frac{\Xi_1^2 k_B T}{\rho \cdot v_s^2 V} \cdot \frac{V}{2} \cdot \frac{1}{2\pi^2} \left(\frac{2m^*}{\hbar^2}\right)^{3/2} \mathcal{E}(\vec{k})^{1/2}$$

$$= \boxed{\frac{\Xi_1^2 k_B T}{(2\pi)\hbar \rho v_s^2} \cdot \left(\frac{2m^*}{\hbar^2}\right)^{3/2} \mathcal{E}(\vec{k})^{1/2}}$$

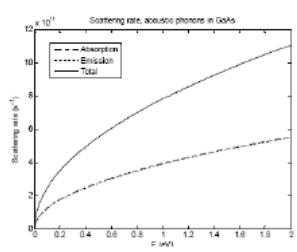

Intravalley Optical Phonon Scattering

The Hamiltonian $\hat{H}' = D_0 [\hat{u}(\vec{r})_{\parallel}]$

Total scattering rate (a.k.a. total relaxation rate)

$$\Gamma(\vec{k}) = \frac{\pi D_0^2}{2\rho\omega_0}\left\{N_0 g_{3D}[\mathcal{E}(\vec{k})+\hbar\omega_0] + (N_0+1) g_{3D}[\mathcal{E}(\vec{k})-\hbar\omega_0]\right\}$$

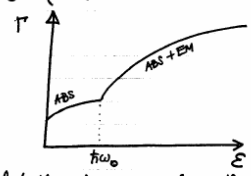

Emission forbidden for energies lower than $\hbar\omega_0$! Since $|M(\vec{k},\vec{q})|^2$ does not depend on $\vec{q}$, the total scattering rate & the momentum relaxation rate are the same!

Forbidden in Si (as minima along <100>) and GaAs (min at Γ point)

Intervalley Scattering

The Hamiltonian

Bottom line: intervalley scattering is modeled similarly to (non-polar) optical phonons

$$\hat{H}_{int} = D_{if}\, u_{\parallel}(\vec{r},t)$$

initial final

How? Via long wavelength phonons, either acoustic or optical
For Si, equivalent scattering; difference between f and g processes
For GaAs, non-equivalent scattering Γ→L and Γ→X important if carriers have enough energy

$$\frac{1}{\tau(\vec{k})} = \Gamma_{\substack{ab\\em}}(\vec{k}) = \frac{\pi D_{if}^2 Z_f}{2\rho\omega_{if}}\left(N_{if}+\frac{1}{2}\mp\frac{1}{2}\right) \times g_{3D}(\mathcal{E}(\vec{k})\pm\hbar\omega_{if}-\Delta E_{if})$$

Z_f – # of final valleys

$\Delta E_{if} = 0$ for equivalent valley scattering in Si

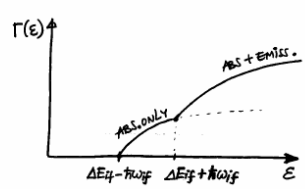

Intervalley Scattering – Cont'd

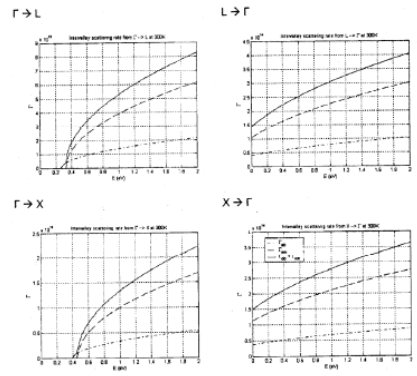

Polar-optical-phonon (POP) scattering

The Hamiltonian $\hat{H}_{int} = -e\varphi$

$$\boxed{\Gamma(\mathcal{E})_{tot} = \frac{e^2\omega_0}{8\pi}\cdot\left(\frac{2m^*}{\hbar^2}\right)^{1/2}\cdot\left[\frac{1}{\varepsilon(\infty)}-\frac{1}{\varepsilon(0)}\right]\cdot \frac{1}{\sqrt{\mathcal{E}}}\cdot\left\{N_0 \ln\left|\frac{1+\sqrt{1+\frac{\hbar\omega_0}{\mathcal{E}}}}{-1+\sqrt{1+\frac{\hbar\omega_0}{\mathcal{E}}}}\right| + (N_0+1)\ln\left|\frac{1+\sqrt{1-\frac{\hbar\omega_0}{\mathcal{E}}}}{1-\sqrt{1-\frac{\hbar\omega_0}{\mathcal{E}}}}\right|\right\}}$$

this term present only for $\mathcal{E} > \hbar\omega_0$.

How? In polar semiconductors, lattice vibrations lead to microscopic dipole moments, from which electrons scatter

This scattering mechanism is strongly inelastic (high energy optical phonons) and strongly anisotropic (due to Coulomb nature of the scattering)

$\mathcal{E}(k) > \hbar\omega_0$

$$\Gamma_m^{em}(\vec{k}) = -\frac{C_e}{2k^3}\left\{-K_{ph}^2 \ln\frac{k+\sqrt{k^2-K_{ph}^2}}{k-\sqrt{k^2-K_{ph}^2}} - \frac{1}{\cancel{2}}\cdot \cancel{2}k\cdot 2\sqrt{k^2-K_{ph}^2}\right\}$$

$$= \frac{C_e}{2k^3}\left\{K_{ph}^2 \ln\frac{k+\sqrt{k^2-K_{ph}^2}}{k-\sqrt{k^2-K_{ph}^2}} + 2k\sqrt{k^2-K_{ph}^2}\right\}$$

Absorption

$$\Gamma_m^{ab}(\vec{k}) = -\frac{C_a}{2k^3}\left\{K_{ph}^2 \ln\left|\frac{k+\sqrt{k^2+K_{ph}^2}}{-k+\sqrt{k^2+K_{ph}^2}}\right| - \frac{1}{\cancel{2}}\cdot \cancel{2}k\cdot 2\sqrt{k^2+K_{ph}^2}\right\}$$

$$= \frac{C_a}{2k^3}\left\{-K_{ph}^2 \ln\left|\frac{k+\sqrt{k^2+K_{ph}^2}}{-k+\sqrt{k^2+K_{ph}^2}}\right| + 2k\sqrt{k^2+K_{ph}^2}\right\}$$

POP scattering – cont'd

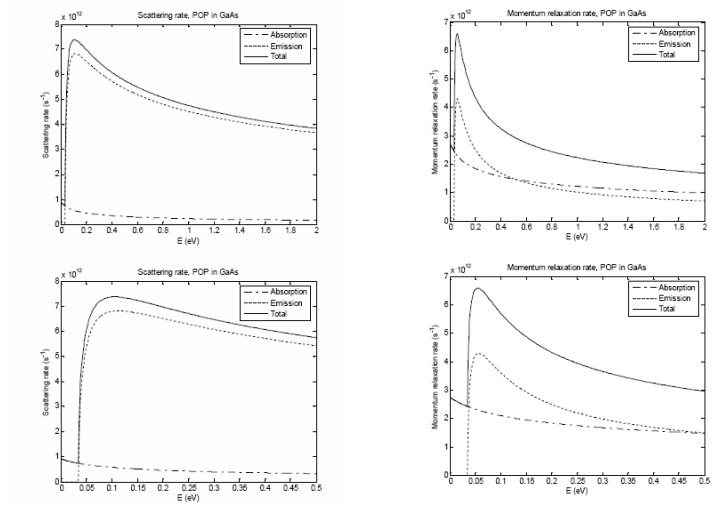

Anisotropy: $\Gamma_m < \Gamma$

Ionized impurity scattering

The Hamiltonian

$$\hat{H}_{int}^{scr.} = \frac{\mp Ze^2}{4\pi\varepsilon_0\varepsilon_s} \cdot \frac{e^{-r/L_D}}{r}$$

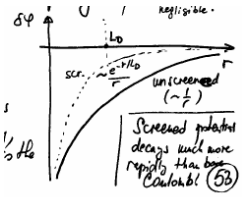

Scattering is elastic (no particles emitted or absorbed) but strongly anisotropic (due to Coulomb nature)

Transition rate

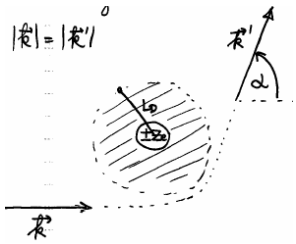

$$S(\vec{k},\vec{k}') = \frac{2\pi}{\hbar} \cdot N_I \cdot \Lambda \cdot \frac{Z^2 e^4}{V^2 \varepsilon_0^2 \varepsilon_s^2} \cdot \frac{\delta(\varepsilon(\vec{k}') - \varepsilon(\vec{k}))}{\left[4k^2 \sin^2\left(\frac{\alpha}{2}\right) + \frac{1}{L_D^2}\right]^2}$$

$$\Gamma_m(\vec{k}) = \frac{N_I Z^2 e^4}{\hbar (2\pi)^2 \varepsilon_0^2 \varepsilon_s^2} \cdot \frac{\pi m^*}{2\hbar^2 k^3} \cdot \left[\ln(1+4k^2L_D^2) - \frac{4k^2L_D^2}{1+4k^2L_D^2}\right]$$

$$= \frac{N_I Z^2 e^4 m^*}{8\pi\hbar^3 \varepsilon_0^2 \varepsilon_s^2 k^3} \left[\ln(1+4k^2L_D^2) - \frac{4k^2L_D^2}{1+4k^2L_D^2}\right] \quad (5)$$

Ionized impurity scattering – cont'd

Total scattering rate

$$\Gamma(k) = \frac{N_I Z^2 e^4 L_D^4}{\hbar (2\pi)^2 \varepsilon_0^2 \varepsilon_s^2} \cdot \frac{4\pi m^*}{\hbar^2} \cdot \frac{k}{(4k^2 L_D^2 + 1)}$$

$$= \frac{N_I Z^2 e^4 m^* L_D^4}{\hbar^3 \pi \varepsilon_0^2 \varepsilon_s^2} \left(\frac{k}{4k^2 L_D^2 + 1} \right)$$

Momentum relaxation rate

$$\Gamma_m(k) = \frac{N_I Z^2 e^4}{\hbar (2\pi)^2 \varepsilon_0^2 \varepsilon_s^2} \cdot \frac{\pi m^*}{2\hbar^2 k^3} \cdot \left[\ln(1 + 4k^2 L_D^2) - \frac{4k^2 L_D^2}{1 + 4k^2 L_D^2} \right]$$

$$= \frac{N_I Z^2 e^4 m^*}{8\pi \hbar^3 \varepsilon_0^2 \varepsilon_s^2 k^3} \left[\ln(1 + 4k^2 L_D^2) - \frac{4k^2 L_D^2}{1 + 4k^2 L_D^2} \right]$$

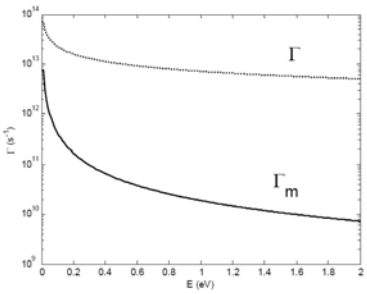

Anisotropy viewed through $\Gamma_m < \Gamma$

Low-field transport phenomena

Externally controlled: current and temperature gradients

Output: electric fields (voltage drops) and heat currents

$$\mathcal{E}_j = \rho_{jk} J_k + \alpha_{jk} \partial_k T_L \qquad (4.70a)$$

and

$$J_{Qi} = \pi_{jk} J_k - \kappa_{jk} \partial_k T_L \qquad (4.70b)$$

That these equations find more use than their counterparts is apparent from the fact that each of the coefficients in eq. (4.70) has a name:

ρ = resistivity

α = thermoelectric power

π = Peltier coefficient

κ = thermal conductivity.

Thermoelectric: electric fields and thermal gradients

Thermomagnetic: magnetic fields and thermal gradients

Galvanomagnetic: magnetic and electric fields

Low-field transport phenomena

Where is the magnetic field? As a parameter in the transport coefficients!

$$\mathcal{E}_i = \rho_{ij} J_j + \rho_{ijk} B_k J_j + \rho_{ijkl} B_k B_l J_j + \ldots \qquad (4.80)$$

resistivity Hall effect magnetoresistance

General classification of phenomena:

Thermoelectric: electric fields and thermal gradients

Thermomagnetic: magnetic fields and thermal gradients

Galvanomagnetic: magnetic and electric fields

Thermoelectric phenomena

Seebeck effect: thermal gradient into electric field

Thermal gradient across an open circuit semiconductor → voltage appears

Hot point probe – method to determine the type of carriers from the sign of the voltage

Peltier effect: absorption of heat caused by the electric current flow

Metal contacts and semiconductors have different Peltier coefficients, so one end of the device becomes cold, the other one hot → basis for Peltier coolers

Thermomagnetic and galvanomagnetic phenomena

Nernst: appearance of an electric field perpendicular to both a temperature gradient and B field

Magneto-Seebeck: second order in the B-field, corresponds to the lateral electric field emergence due to the B field and thermal grad

Hall effect: the most famous galvanomagnetic effect

Table 4.1. *Coupled current effects in the presence of transverse magnetic field*

Effect	Experimental conditions	Result
Transverse magneto-resistance (isothermal)	$\mathbf{J} = J_x\hat{x}$, $\mathbf{B} = B_z\hat{z}$ T_L = constant	$\mathcal{E}_x = (\rho_0 + \rho_{xxzz}B_z^2)J_x$
Transverse magneto-resistance (adiabatic)	$\mathbf{J} = J_x\hat{x}$, $\mathbf{B} = B_z\hat{z}$ $J_{Qy} = 0$, $\partial T_L/\partial x = 0$	$\mathcal{E}_x = \left(\rho_0 + \left(\rho_{xxzz} - \frac{T_L\alpha_1^2}{\kappa_0}\right)B_z^2\right)J_x$
Magneto-Seebeck (isothermal)	$\mathbf{J} = \mathbf{0}$, $\mathbf{B} = B_z\hat{z}$ $\partial T_L/\partial y = 0$	$\mathcal{E}_x = (\alpha_0 + \alpha_{xxzz}B_z^2)\frac{\partial T_L}{\partial x}$
Magneto-Seebeck (adiabatic)	$\mathbf{J} = 0$, $\mathbf{B} = B_z\hat{z}$ $J_{Qy} = 0$	$\mathcal{E}_x = \left[\alpha_0 + \left(\alpha_{xxzz} - \frac{\alpha_1\kappa_1}{\kappa_0}\right)B_z^2\right]\frac{T_L}{\partial x}$
Nernst (isothermal)	$\mathbf{J} = \mathbf{0}$, $\mathbf{B}_z = B_z\hat{z}$ $\partial T_L/\partial y = 0$	$\mathcal{E}_y = -\alpha_1 B_z\frac{\partial T_L}{\partial x}$
Nernst (adiabatic)	$\mathbf{J} = 0$, $\mathbf{B}_z = B_z\hat{z}$ $J_{Qy} = 0$	$\mathcal{E}_y = -(\alpha_1 - \alpha_0\frac{\kappa_1}{\kappa_0})B_z\frac{T_L}{\partial x}$
Hall (isothermal)	$\mathbf{J} = J_x\hat{x}$, $\mathbf{B} = B_z$ T_L = constant	$\mathcal{E}_y = \rho_1 B_z J_x$
Hall (adiabatic)	$\mathbf{J} = J_x\hat{x}$, $\mathbf{B} = B_z\hat{z}$ $J_{Qy} = 0$	$\mathcal{E}_y = \left[\rho_1 - \frac{T_L\alpha_0\alpha_1}{\kappa_0}\right]B_z J_x$
Ettingshausen	$\mathbf{J} = J_x\hat{x}$, $\mathbf{B} = B_z\hat{z}$ $J_{Qy} = 0$ $\partial T_L/\partial x = 0$	$\frac{\partial T_L}{\partial y} = -\frac{\pi_1}{\kappa_0}J_x B_z$
Righi–Leduc	$\mathbf{J} = 0$, $\mathbf{B} = B_z\hat{z}$ $J_{Qy} = 0$	$\frac{\partial T_L}{\partial y} = \frac{\kappa_1}{\kappa_0}B_z\frac{\partial T_L}{\partial x}$

High-field transport in Si

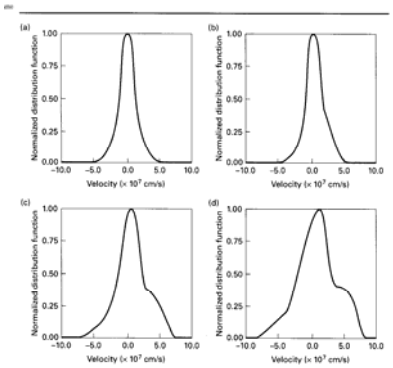

Fig. 7.5 Computed distribution functions for electrons in pure Si at room temperature for applied electric fields of: (a) 1, (b) 10, (c) 50, and (d) 100 kV/cm. The magnitude of the distribution function has been normalized to unity in each case. (Monte Carlo calculations courtesy of M. A. Stettler and A. Das.)

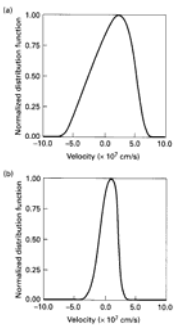

Fig. 7.6 Normalized distribution function for (a) electrons residing in the four valleys for which the major axes of the constant energy ellipsoids are oriented perpendicular to the applied field; (b) electrons residing in the two valleys for which the major axes of the constant energy ellipsoids are oriented parallel to the applied field. Pure silicon and an applied field of 50 kV/cm are assumed. The field is oriented along a (100) direction. (Monte Carlo calculations courtesy of M. A. Stettler and A. Das.)

Low field transport isotropic, but high field transport anisotropic!

High-field transport in Si - 2

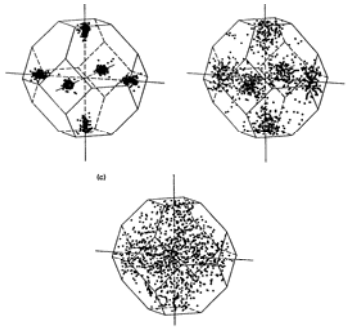

Fig. 7.12 Electron distributions in momentum space for bulk silicon at (a) 10 kV/cm, (b) 100 kV/cm, and (c) 1 MV/cm. (From Kunikiyo, T. et al., *Journal of Applied Physics*, **75**, 297–312, 1994.) (Reproduced with permission of American Institute of Physics.)

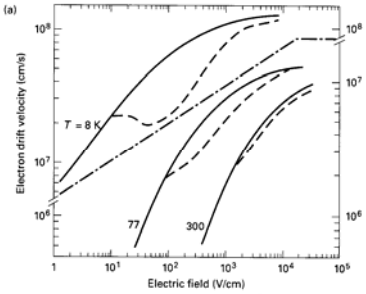

At low fields, valleys equa.lly populated.
At high fields along <100>, the valleys with light mass heat up faster and lose carriers, so most carriers in the valleys with heavy mass so v_d lower!
Field along <111> yields higher v_d than along <100>!!!

High-field transport in GaAs

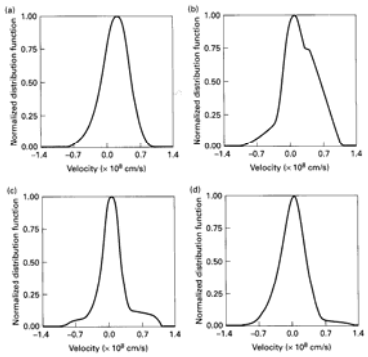

Fig. 7.8 Computed distribution functions for electrons in pure GaAs at room temperature for applied electric fields of: (a) 2, (b) 4, (c) 15, and (d) 50 kV/cm. The magnitude of the distribution function has been normalized to unity in each case. (Monte Carlo calculations courtesy of M. A. Stettler and A. Das.)

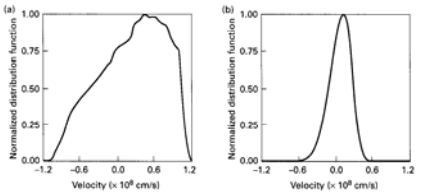

Fig. 7.9 Normalized distribution function for electrons residing in (a) the Γ-valley and (b) the L-valleys of pure GaAs. An applied field of 15 kV/cm is assumed. (Monte Carlo calculations courtesy of M. A. Stettler and A. Das.)

Transport of confined carriers

Carrier confinement leads to:
- changes in the scattering rates due to known mechanisms
- emergence or (almost) disappearance of certain mechanisms

We will focus on
1) carrier transport in the inversion layer of a MOSFET
2) carrier transport in the 2DEG in a MODFET

Reading:
Lundstrom, pp. 93-105 (phonon scattering of confined carriers)
Lundstrom, pp. 195-202 (low field transport of confined carriers)
Lundstrom, pp. 308-310 (high field transport of confined carriers)

Excellent reference:
T. Ando, A. B. Fowler, and F. Stern,
"*Electronic properties of two-dimensional systems*,"
Rev. Mod. Phys. **54**, 437 (1982).

Transport in the inversion layer of a MOSFET

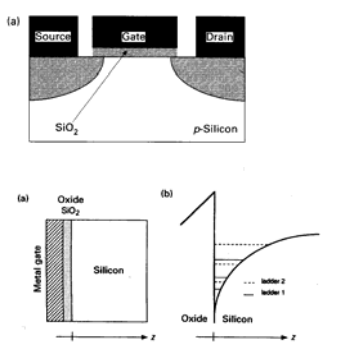

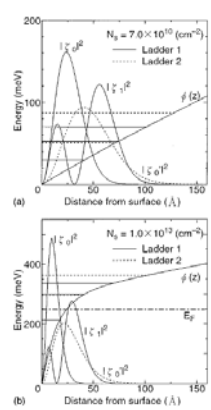

FIG. 1. Results of self consistent calculation for n-MOSFET at 300 K. (a) $N_s = 7.0 \times 10^{10}$ (cm^{-2}). (b) $N_s = 1.0 \times 10^{12}$ (cm^{-2}). $N_A = 5.0\times10^{16}$(cm^{-3}).

At low carrier densities, triangular approximation of the potential OK, solutions are Airy functions
Higher densties: must solve Poisson's equation!
Two ladders: one associated with each effective mass

Scattering mechanisms in the inversion layer of a MOSFET-1

Phonon scattering: changed rates as wavefunctions changed (still plane waves in the unconfined plane!)

$$\Gamma_{fi}(E) = \frac{\pi \Xi_A^2 k_B T_L}{\hbar v_s W_{fi}} g_{2Df}(E)$$

$$\frac{1}{W_{fi}} = \int_0^\infty dz \left|F_f(z)\right|^2 \left|F_i(z)\right|^2$$

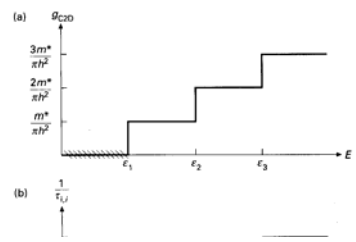

Intervalley scattering: dependence also on the density of states in the final valley

$$\Gamma_{fi}(E) \propto g_{2Df}\left(E \pm \hbar\omega_{if} - \Delta E_{fi}\right)$$

Scattering mechanisms in the inversion layer of a MOSFET-2

Suraface roughness scattering

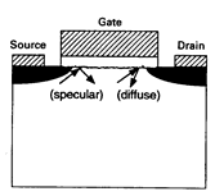

Transition rate proportional to the square of the **effective field** felt by the carriers, which can be related to the inversion sheet density by roughly the expression

$$E_{eff} = \left(\frac{e}{K_S \varepsilon_0}\right)\left(N_{depl} + \eta N_{inv}\right), \quad \eta \approx 1/2$$

Low-field transport in the inversion layer of a MOSFET

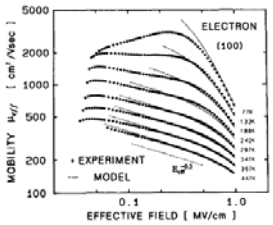

Fig. 4. E_{eff} dependences of electron mobility in the inversion layer on (100) surface in the range of 77 K to 447 K. Substrate acceptor concentration was 3.9×10^{15} cm^{-3}. Here, E_{eff} is defined with η of 1/2. Open circles show the experimental data. The solid curves were calculated using (6)–(8).

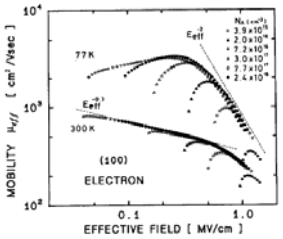

Fig. 1. Electron mobility in inversion layer at 300 K and 77 K versus effective field E_{eff}, as a parameter of substrate acceptor concentration, N_A. Here, E_{eff} is defined by $E_{eff} = q \cdot (N_{dep} + \eta \cdot N_{inv})/\varepsilon_{Si}$ with η of 1/2.

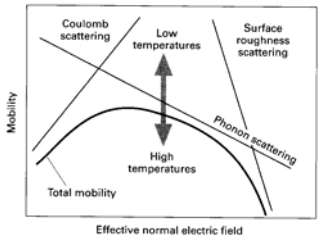

High effective field (low N_{inv}): surface roughness dominates

Low effective field (low N_{inv}): interplay of Coulomb scattering (from doping plus oxide charges) and phonons, depending on temperature

Transport in the 2DEG in a MODFET

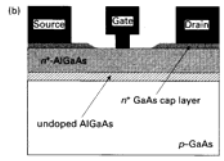

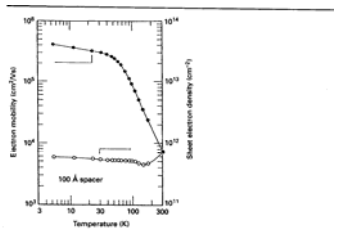

Fig. 4.17 The measured temperature dependence of the 2DEG mobility and density in an n-AlGaAs–GaAs heterostructure. (From Mori, Y., Nakamura, F. and Wanatabe, N. *Journal of Applied Physics*, **60**, 334–337, 1986.) (Reproduced with permission of American Institute of Physics.)

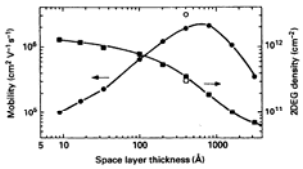

Fig. 4.18 The measured variation of the 2DEG mobility and density in an n-AlGaAs/GaAs heterostructure versus the thickness of the space layer. (From Harris, Foxon, Barnham, Lacklison, Hewett, and White. *Journal of Applied Physics*, **61**, 1219–1221, 1987.) (Reproduced with permission of American Institute of Physics.)

Major differences w/respect to MOSFET:

1) epitaxial growth as opposed to thermal oxide→
   surface roughness insignificant!!!

2) dopants separated from 2DEG
   → Coulomb scattering minimized!!!

- Mobilities in MODFET high: close to those in undoped bulk!
- At low temperatures, mobilities very high – no impurities to limit it!

High field transport in MOSFET

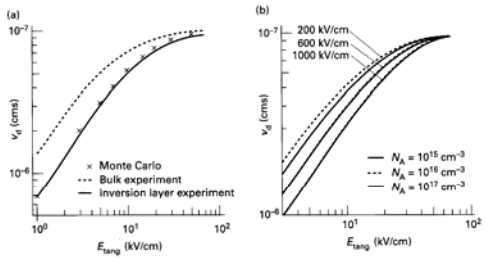

Fig. 7.17 Drift velocity vs. electric field parallel to the Si/SiO_2 interface for electron transport. (a) Monte Carlo simulations compared with experimental results for inversion layer and bulk electron transport. (b) Results for three different normal electric fields and three different doping densities. (From Jungemann et al. [7.17].) (Reproduced with permission of Pergamon Press.)

Low-field transport clearly affected by confinement,
but the saturation part not very, as it influenced predominantly by phonon emission

Transport in devices

Worry about local fields and the response of carriers to them
Small structures – the velocity not just a function of the field at a given point (nonlocality of transport)

Big differences in simulation of bipolar devices and unipolar devices

Monte Carlo: not good for bipolar devices, as G-R times comparable to scattering times

Today we will see:

Overview of MC simulation of unipolar devices:
-simulation of focused-ion-beam MOSFET (FIBMOS)
- transport in nanowires
- transport in quantum cascade lasers

Bipolar devices:
pn diode simulation using drift-diffusion model

Description of the Simulated FIBMOS Device

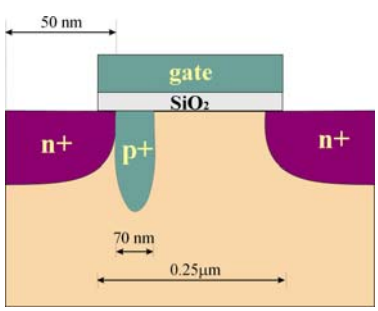

Source and drain length	50 nm
Source and drain junction depth	36 nm
Gate length	250 nm
Device width	1.4 μm
Bulk depth	400 nm
Oxide thickness	5 nm
Source and drain doping	$10^{19}cm^{-3}$
Substrate doping	$10^{16}cm^{-3}$
Implant doping	$1.6\times10^{18}cm^{-3}$
Substrate doping	$10^{16}cm^{-3}$
Implant length	70 nm

Effective Potential Approach

In principle, the effective role of the potential can be rewritten in terms of the non-local density as:

$$\bar{V} = \int d\mathbf{r} V(\mathbf{r}) \sum_i n_i(\mathbf{r})$$

$$\sim \int d\mathbf{r} V(\mathbf{r}) \sum_i \int d\mathbf{r}' \, exp\left(-\frac{|\mathbf{r}-\mathbf{r}'|^2}{\alpha^2}\right) \delta(\mathbf{r}'-\mathbf{r}_i)$$

$$\sim \sum_i \int d\mathbf{r} \delta(\mathbf{r}-\mathbf{r}_i) \int d\mathbf{r}' \, V(\mathbf{r}') \, exp\left(-\frac{|\mathbf{r}-\mathbf{r}'|^2}{\alpha^2}\right)$$

$$\sim \sum_i \int d\mathbf{r} \delta(\mathbf{r}-\mathbf{r}_i) V_{eff}(\mathbf{r})$$

Smoothed, effective potential

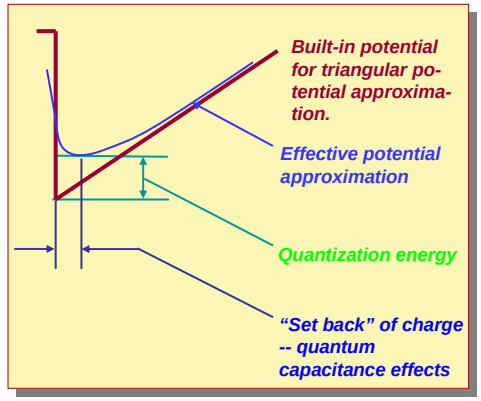

- D. K. Ferry, *Superlatt. Microstruc.* **27**, 59 (2000); *VLSI Design*, in press.

Results: Conduction Band Edge and Sheet Density

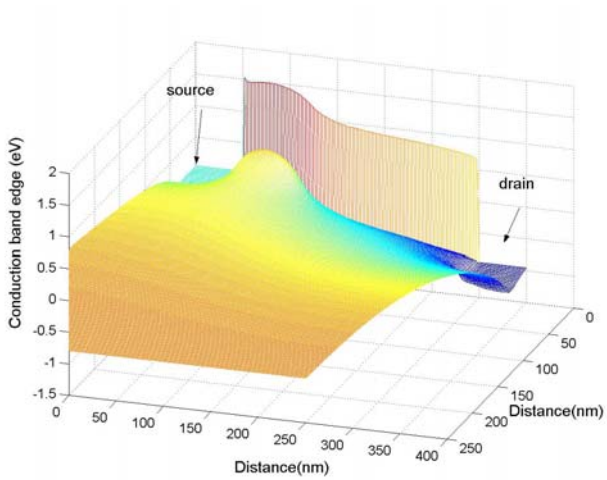

- **Near the source end, due to high p+ implant doping, majority of electrons occupy the lowest energy level in the triangular well:**

displacement of electrons from the interface → transconductance degradation

- **Bottom of the conduction band near the silicon/oxide interface elevated**

reduced inversion layer sheet density

- **Onset of inversion dictated by the p+ implant doping:**

threshold voltage higher and more stable with respect to scaling?

Results: Sheet Density

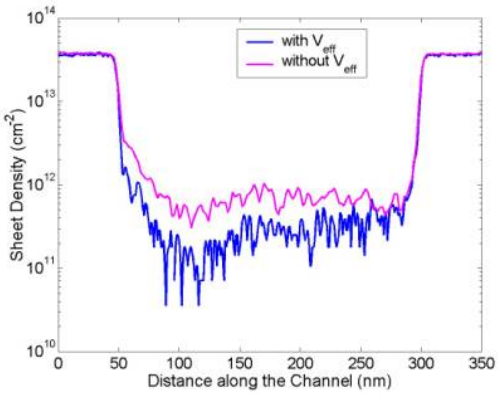

- Reduced sheet density when Veff is incorporated → an increase in the threshold voltage, with respect to the results obtain without Veff.
- Sheet density particularly low near the p+ implant → the implant has a major role in determining the onset of inversion in FIBMOS.

Results: Concentration of Electrons in the Channel

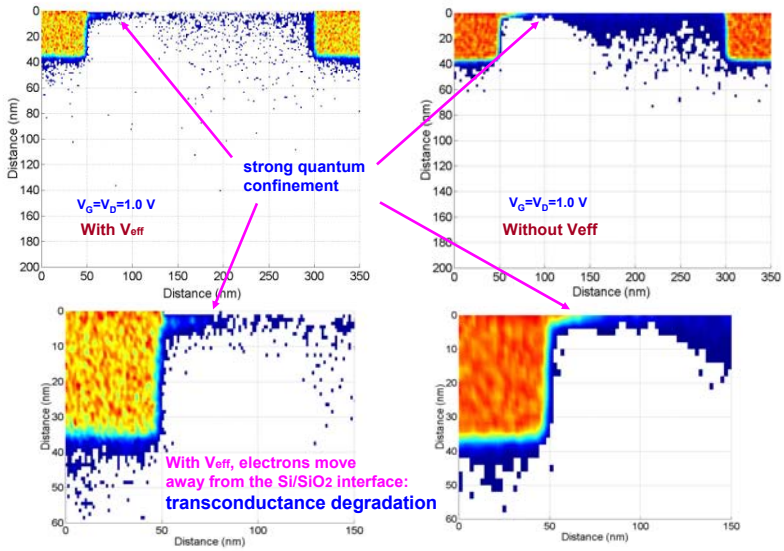

Results: Electric Field Profile and Velocity Overshoot

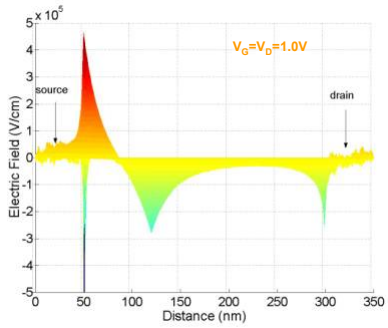

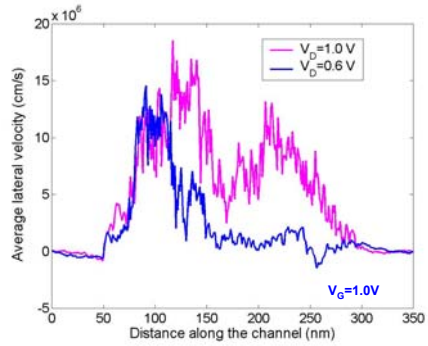

Due to large negative electric field at the source end carriers experience velocity overshoot !

Results: Electric Field Profile and Hot Electrons

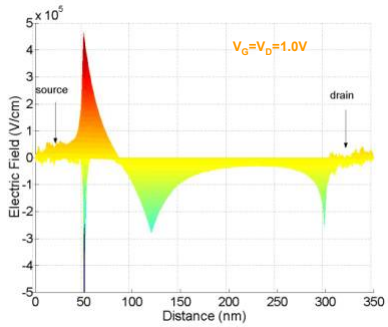

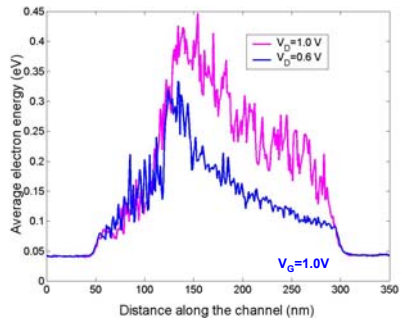

Acceleration at the source end, rather than the drain, due to large negative field; the energy peak is shifted away from the drain, implying improved hot-electron reliability with respect to electron-hole pair generation near the drain, and doping optimization may further flatten the energy profile throughout the channel.

Results: FIBMOS Current – Voltage Characteristic

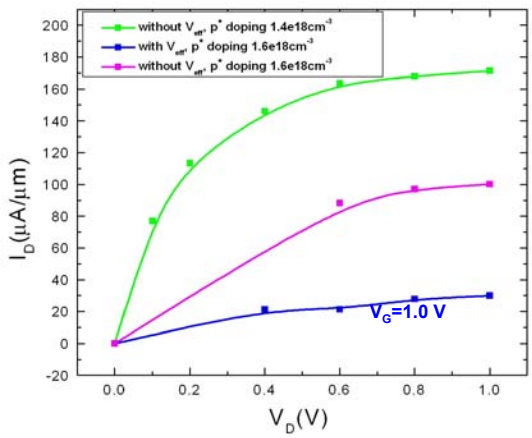

- Notable sensitivity of the drive current to the p+ implant doping.
- Inclusion of V_{eff} yields an increased threshold voltage, as seen by smaller slope of the curves in the linear region.

Monte Carlo Simulation of AlGaAs/GaAs QCLs Including Both Γ and X Valley Transport

Xujiao (Suzey) Gao, Dan Botez and Irena Knezevic

September 20, 2006

NANOELECTRONICS THEORY GROUP

THE UNIVERSITY of WISCONSIN MADISON

Apply the model to simulate two AlGaAs/GaAs QCLs: the 33% Al QCL [2] , and the 45% Al QCL [3] .

The 33% Al QCL

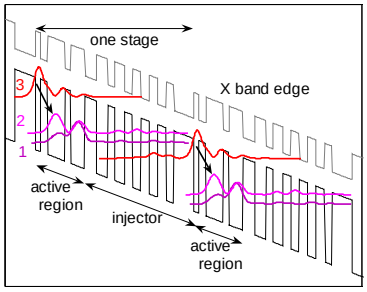

$\lambda \sim 9\ \mu m$
$Z_{32} = 1.6$ nm
$\tau_3 = 1.5$ ps
$F_{threshold} = 48$ kV/cm

The 45% Al QCL

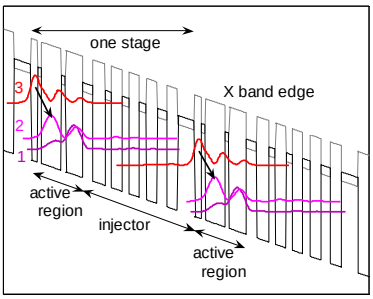

$\lambda \sim 9\ \mu m$
$Z_{32} = 1.7$ nm
$\tau_3 = 1.4$ ps
$F_{threshold} = 48$ kV/cm

[2] C. Sirtori *et al*., Appl. Phys. Lett. 73, 3486 (1998).
[3] H. Page *et al*., Appl. Phys. Lett.78, 3529 (2001).

Field vs current density

The 33% Al QCL

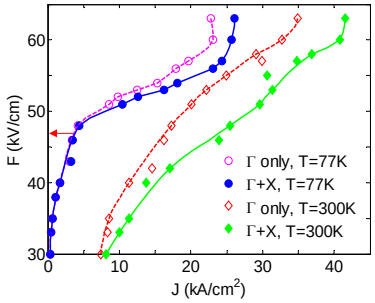

The 45% Al QCL

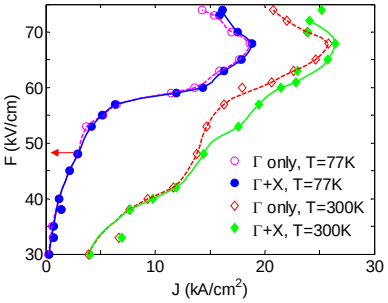

	J_{th} (kA/cm^2), T = 77 K			J_{th} (kA/cm^2), T = 300 K		
	w/o X	w/ X	Exper.	w/o X	w/ X	Exper.
33%	4.1	4.4	5 [4]	17.2	25.5	N/A
45%	2.9	2.9	4 [3]	13.7	14.4	16.7 [3]

[3] H. Page *et al*., APL 78, 3529 (2001).
[4] C. Sirtori et al, APL 75, 3911 (1999).

Γ-valley wave function moduli squared
(above-threshold field F = 53 kV/cm, T = 77 K)

The 33% Al QCL

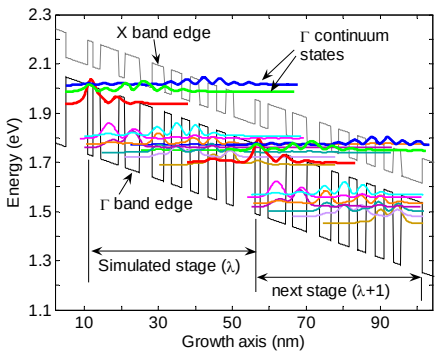

The 45% Al QCL

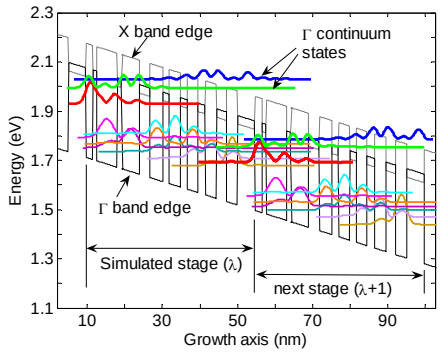

Field vs current density

The 33% Al QCL

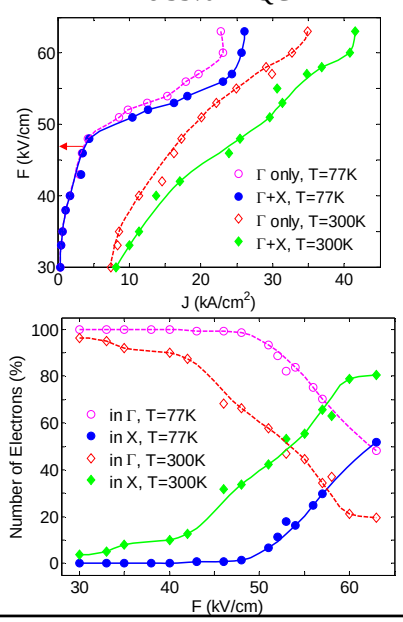

The 45% Al QCL

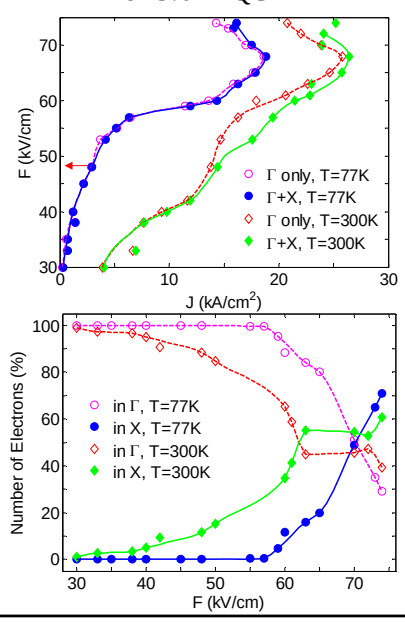

Electronic Transport in Si Nanowires

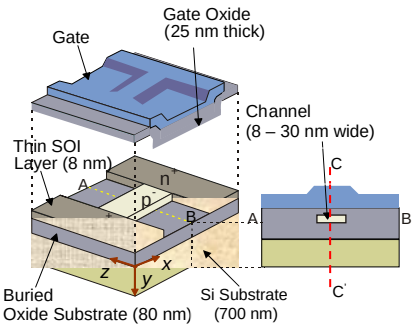

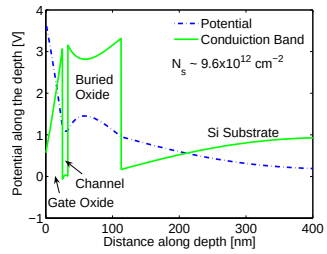

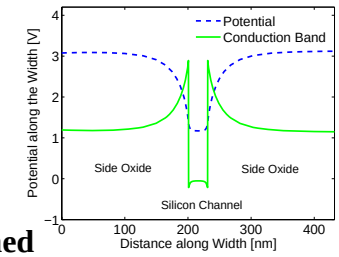

- **Four Si/SiO$_2$ interfaces**
- **Both electrons and phonons are confined**

H. Majima et al., *IEEE Electron Device Letters*, 21, 396 (2000)
E.B.Ramayya, et al., IEEE Trans. on Nanotech., 6, 113 (2007).

Effect of Decreasing Wire Width on Mobility

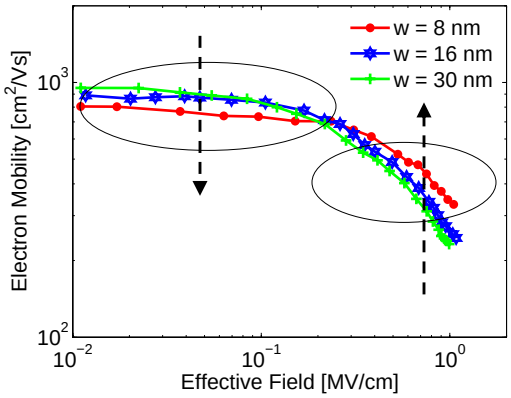

E.B. Ramayya, et al.,
IEEE Trans. on Nanotech., 2007.

- **High fields –Mobility increases**
- **Low and moderate fields – Mobility decreases**

Volume Inversion and Subband Modulation

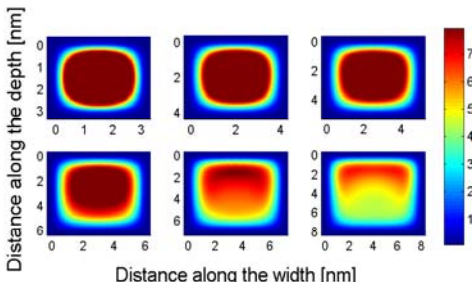

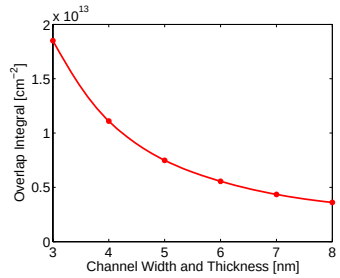

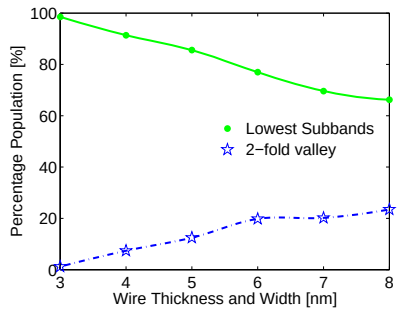

- **Onset of volume inversion 8-3 nm ($N_s \sim 1 \times 10^{13}$ /cm^2)**
- **Depopulation of higher subbands – lower intersubband scattering.**
- **Depopulation of valley pair with m_l– lower intervalley scattering higher mobility (m_t valley occ).**
- **Increase in e-p overlap higher intrasubband scattering**

Drift-diffusion equations for bipolar devices

Definitions of current components

$$\mathbf{J}_n = -nq\mu_p \nabla V + qD_n \nabla n,$$
$$\mathbf{J}_p = -pq\mu_p \nabla V - qD_n \nabla p,$$

Drift-diffusion model

Continuity equations + Poisson's equation

$$\frac{\partial n}{\partial t} = \frac{1}{q}\nabla \cdot \mathbf{J}_n - R_n$$
$$\frac{\partial p}{\partial t} = -\frac{1}{q}\nabla \cdot \mathbf{J}_p - R_p,$$

$$\frac{d^2V}{dx^2} = \frac{q}{K_S \varepsilon_0}\left(N_D - N_A + n - p\right)$$

Drift-diffusion equations for a pn junction diode: Equilibrium

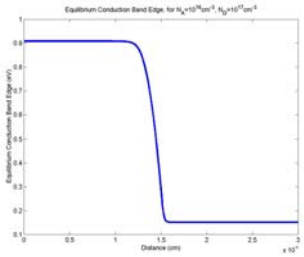

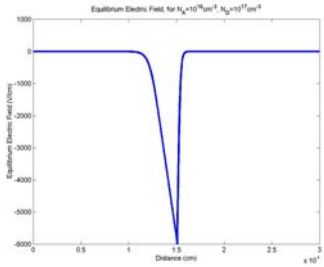

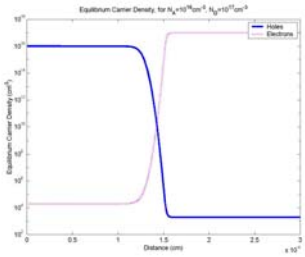

Drift-diffusion equations for a pn junction diode: Under bias

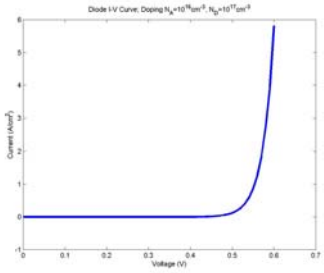

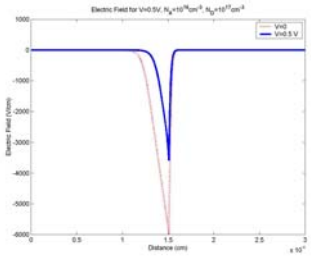

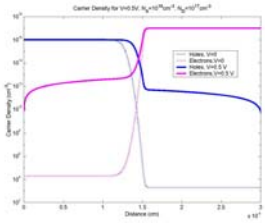

The Resonant Tunneling Diode (RTD)

The RTD is a two-barrier tunneling structure. Electronic transport occurs across the heterostructure (so-called vertical transport) as opposed to what we have seen so far (lateral transport in the plane perpendicular to the direction of growth).

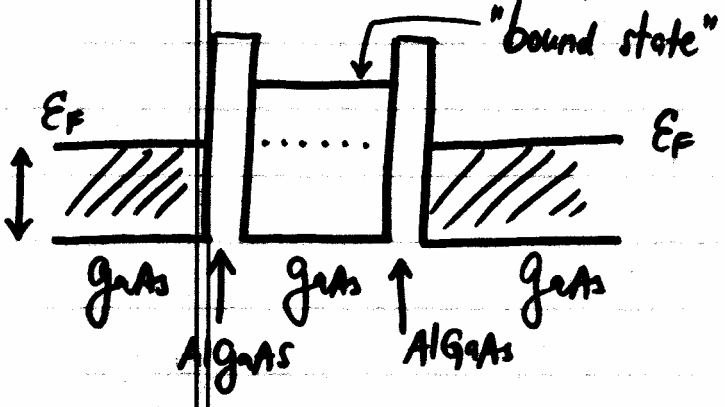

Both the barriers and the well are typically 2-5 nm thick. The height of the barriers depends on the actual heterostructure used; in GaAs/AlGaAs systems, it depends on the Al content. The height is of order ~ 0.1 eV. The barrier height, and the barrier & well thickness are chosen such that there is typically 1 "bound" state in the well, and that it is above the Fermi level in the doped bulk-like left & right contact. The existence of the quasi-bound state is directly linked to the prominent negative differential resistance feature (NDR) in the RTD's I-V curve, which makes the RTD a device that is used as a high-frequency ($\lesssim$ THz) oscillator, when biased near the valley.

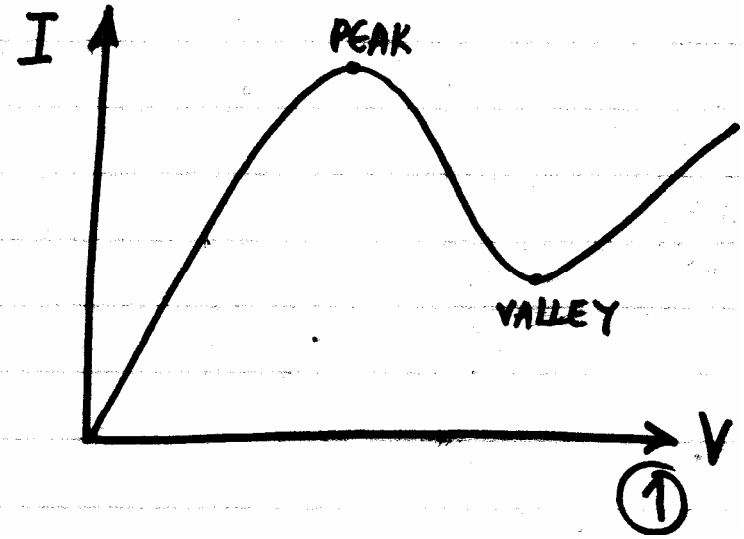

The quasi-bound state in the RTD occurs as a result of constructive superposition: Namely, the RTD is an open quantum system, and has continuous spectrum. Assume no bias has been applied. To each energy above the conduction band bottom correspond 2 solutions: one where a plane wave is incident from the left; and one where a plane wave is incident from the right.

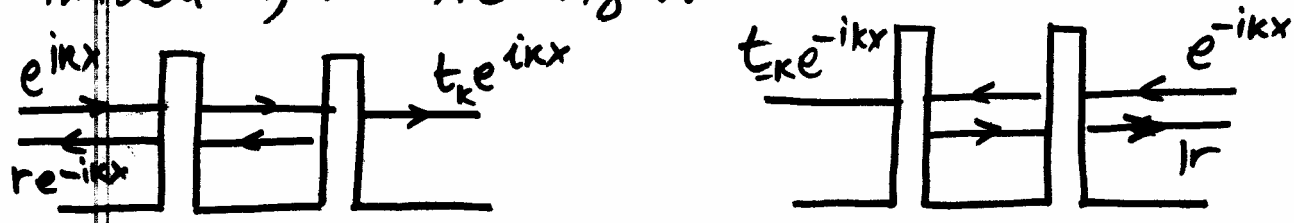

At a certain energy below the barrier energy, the wavefunction looks very much like a standing wave inside the well:

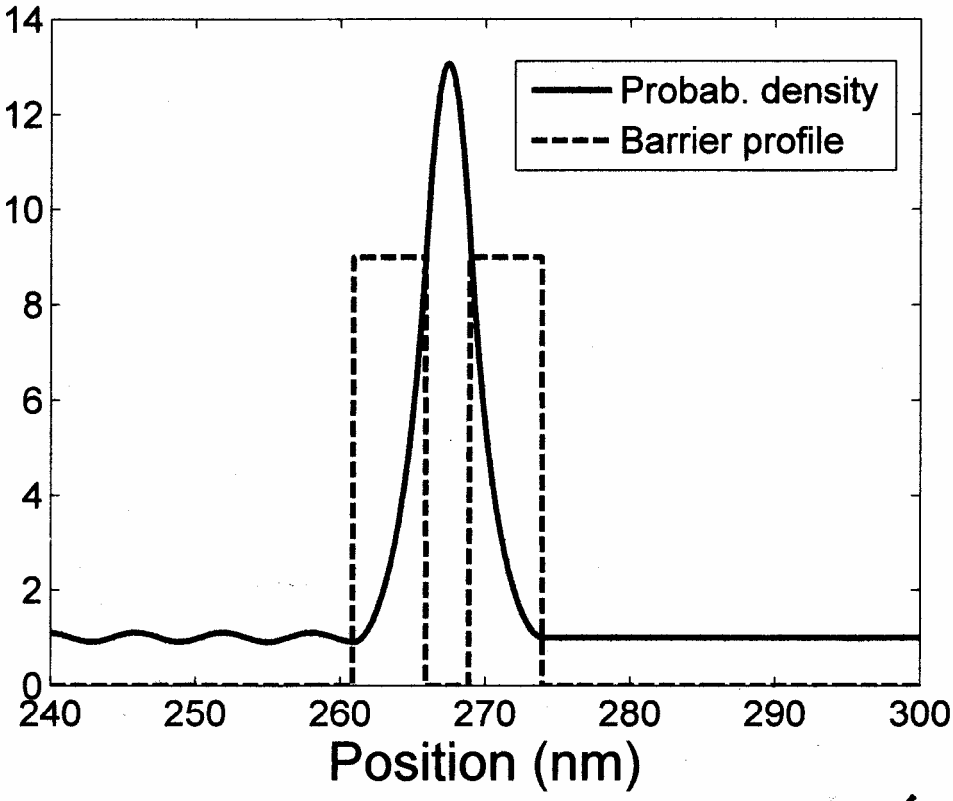

$V=0$

$\mathcal{E} \approx 0.152\ \text{eV}$
(near resonance)

($\leftarrow$ r is small but not 0)
The wiggles on the left are because
$|\psi| = \sqrt{1+|r_{-k}|^2+2\,\mathrm{Re}(re^{-2ikx})}$

On the right
$|\psi| = |t_k|$

When you really hit the resonance $|t|=1$, $|r|=0$
(The picture is pretty close.)

Linear

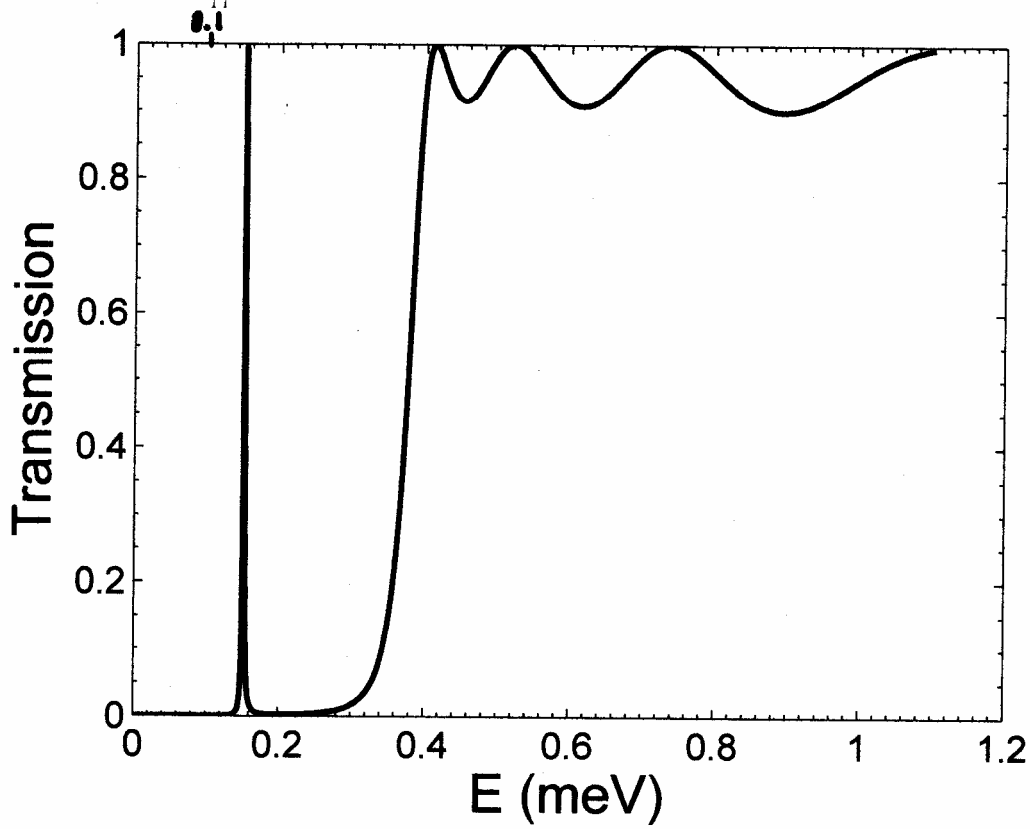

Semilog

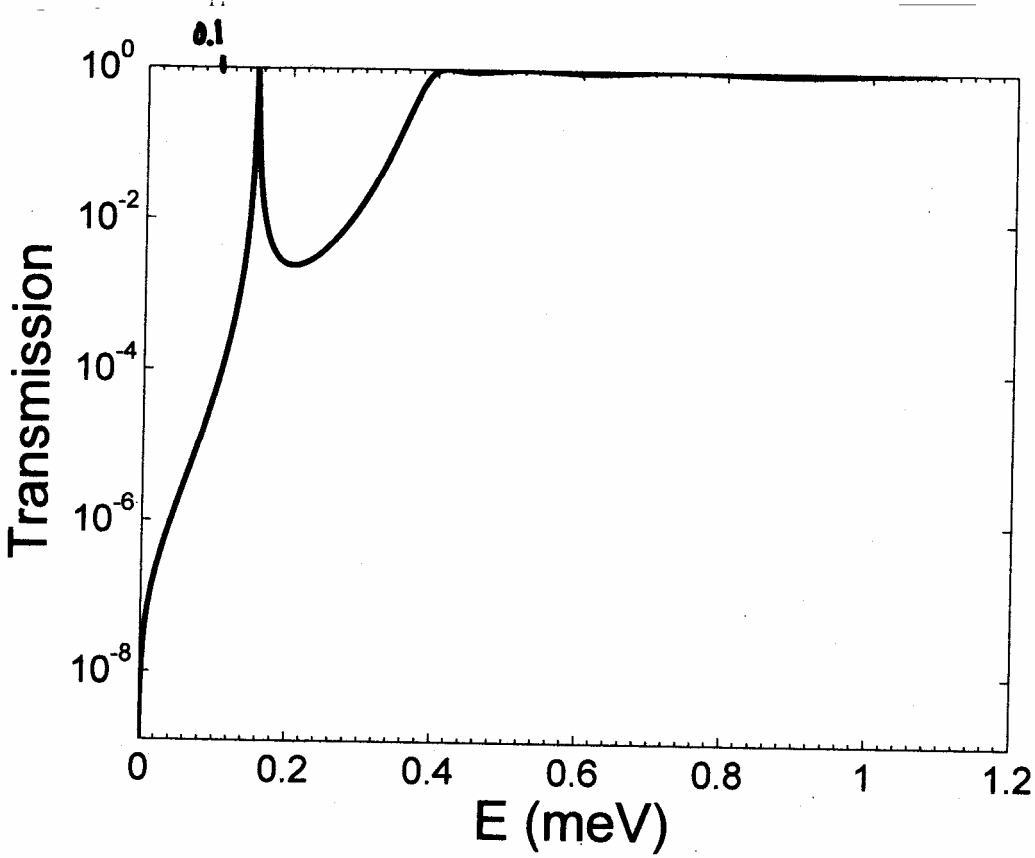

These are the plots of the transmission coeff. for the unbiased diode.
When the diode is unbiased

$$\mathcal{T}(\varepsilon) = |t_k|^2 = |t_{-k}|^2$$

See that there is a transmission peak at about 0.15 eV (barrier height is 0.3 eV, barriers are identical and 5 nm thick, while the well is 3 nm wide).

This resonance peak corresponds to $|t|^2 = \tau = 1$ (see prev. page) $\tau = 1$ for <u>symmetric barriers</u>.

Now, when bias $-V$ is applied to the left-side contact, the current starts to flow.

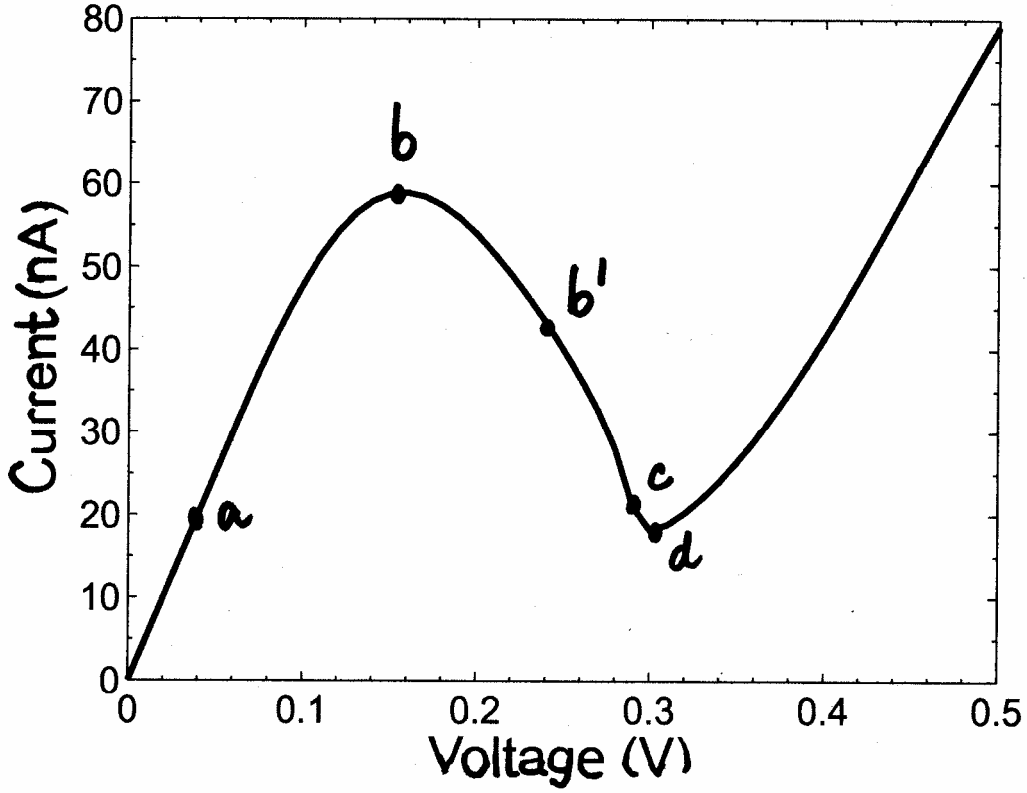

I-V curve for the 5-3-5 nm RTD at room temp $\mathcal{E}_F = 0.1$ eV. Bound state at $V=0$ is at 0.15 eV. Barrier height: 0.3 e

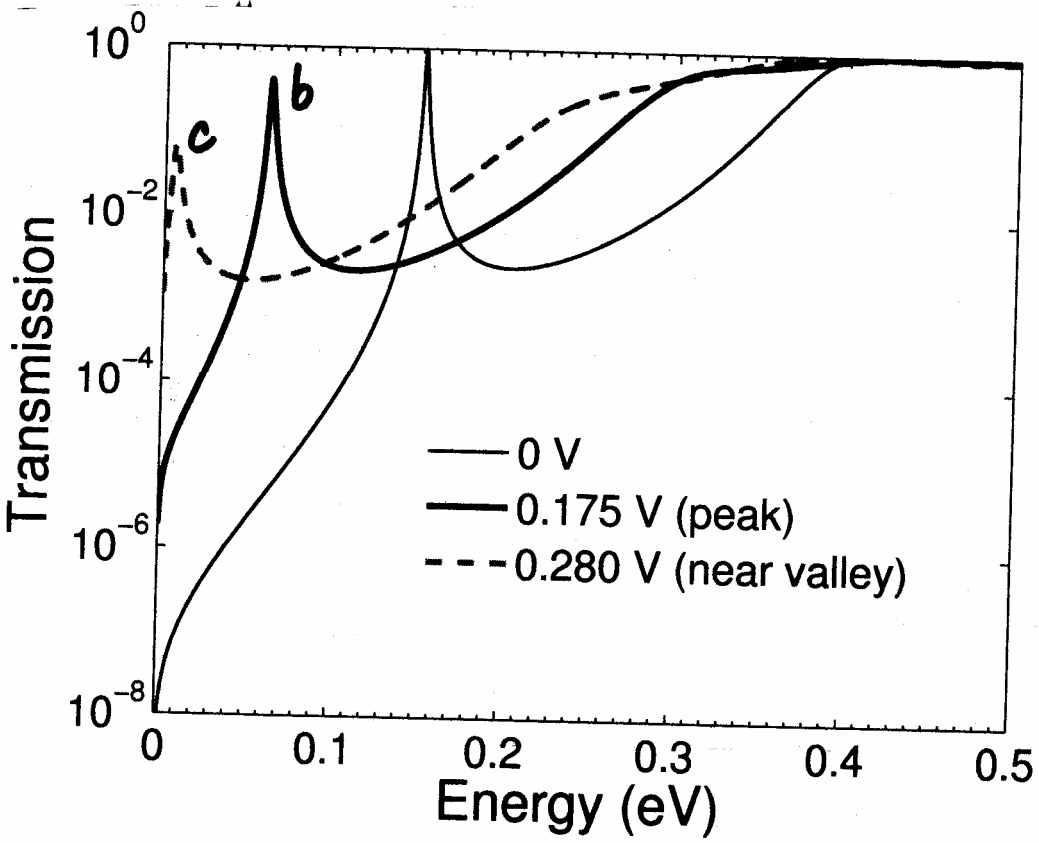

Transmission as a function of energy measured from the bottom of the higher (left) contact.
Note how the peak shifts with increasing bias and disappears near the valley bias.

How do we describe the I-V curve? Landauer formula gives

$$I = \frac{2e}{h}\int_{0}^{\infty} d\varepsilon\, T(\varepsilon)\left(f_L(\varepsilon) - f_R(\varepsilon)\right)$$

↑ bottom of higher (left) contact

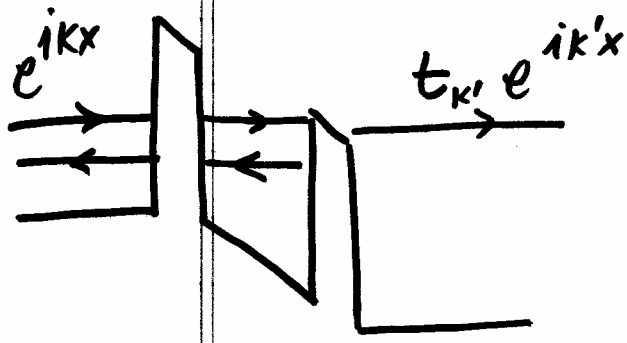

$$T(\varepsilon) = |t_{k'}|^2 \frac{k'}{k} \quad \text{from the left}$$

$$= |t_{-k}|^2 \frac{k}{k'} \quad \text{from the right}$$

where k' and k correspond to the wavevectors in the right & left contact, respectively

$$\varepsilon = \frac{\hbar^2 k^2}{2m^*} = \frac{\hbar^2 k'^2}{2m^*} - eV$$

↖ bias applied

Basically, the total current is the ~~difference~~ sum of the current from left to right $I_L = \frac{-2e}{h}\int_0^{\infty} d\varepsilon\, T(\varepsilon) f_L(\varepsilon)$

and from right to left $I_R = -\frac{(-2e)}{h}\int d\varepsilon\, T(\varepsilon) f_R(\varepsilon)$

↑ going to the left

(Total current flows R→L!)

So the question is how much of the resonance is captured between the Fermi levels in the left & right contacts!!!

Peak: almost all of the resonance captured between ε_F(left) and ε_F(right)

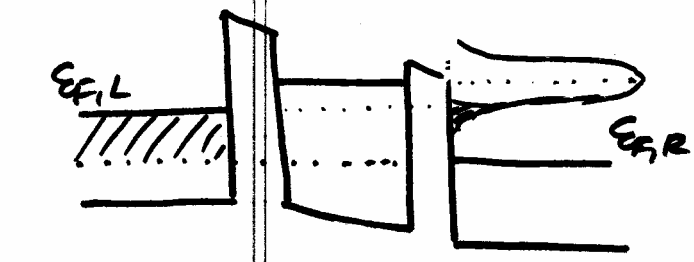

(a) Bound state above $\varepsilon_{F,L}$, only a tiny tail of the resonance is captured

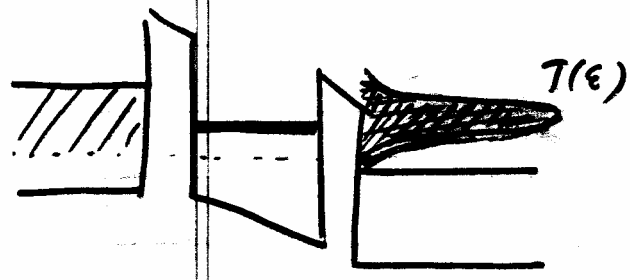

(b) Peak: almost all of the Lorentzian-shaped resonance is caught in the transport window (between $\varepsilon_{F,L}$ & $\varepsilon_{F,R}$)

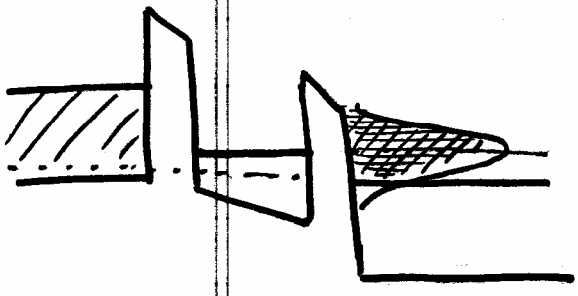

(b') The resonance moves lower & drops in magnitude, lowering the total $\int_{\varepsilon_{F,L}}^{\varepsilon_{F,R}} T(\varepsilon)\, d\varepsilon$ captured

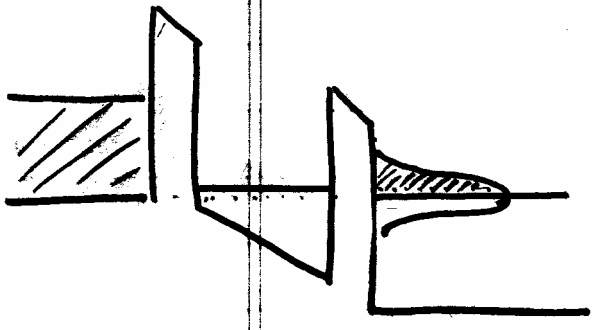

(c) The resonance almost vanishes it is close to the cond. band bottom of the left contact

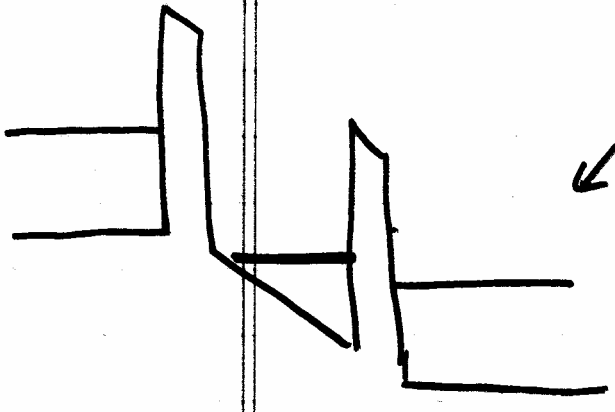

(d) The resonance has "vanished". It is now below the cond. band bottom in the left contact

For higher biases, current increases due to the increase in $J(\varepsilon)$ for the transport over the lower barrier & through the 1st (higher) barrier.

Single-Electron Tunneling. Quantum Dots

Coulomb island – small island of charge coupled to charge reservoirs by means of tunneling barriers

Coulomb island formed in split gate quantum dots;

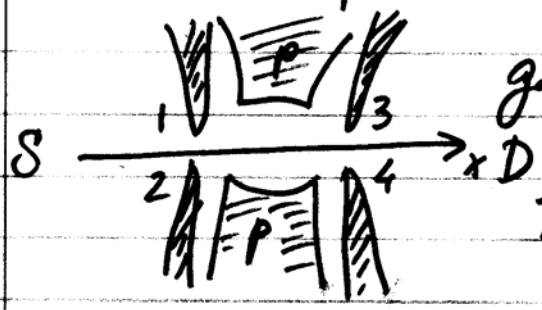

gates 1 & 2 control the resistance
3 & 4 of the quantum point contacts

Typically, you want the two QPCs to be in the TUNNELING regime

Plunger gates P provide an extra degree of control to possibly not just restrict carriers from being located underneath, but with negative enough voltage to lift the cond. band bottom in the dot (this degree of control important for single electron transistors)

When going along x,

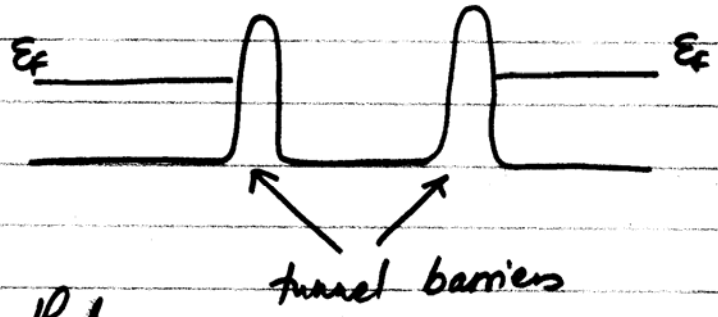

So the number of propagating modes is 0, but that does not mean that absolutely no current flows. How much current flows depends on the properties of the barriers, but also the size of the dot (more generally, the Coulomb island) and the temperature.

Quantum dots are not the only Coulomb islands there are. Actually, much work on metallic droplets with weak tunneling barriers to reservoirs has preceded work on quantum dots, and it is on these (the metallic droplets) that the phenomenon of Coulomb blockade was first observed.

In general, for a small island of charge, such as the quantum dot or metallic droplet, there are 4 characteristic energy scales

* e^2/C — the energy required to add / remove an electron to/from the island (C is the island capacitance)

* $\frac{\hbar^2}{2m^* L^2}$ — characteristic energy spacing due to confinement to a droplet/dot of size L

* $k_B T$ — thermal smearing energy; no discrete levels closer than $k_B T$ can be observed in experiment

* $\frac{\hbar}{R_t C_t}$ — energy uncertainty associated with the tunneling barrier tunneling time

$$\tau_t = R_t C_t$$

where tunneling barriers are modeled as leaky capacitors, with resistance R_t & capacitance C_t

In relatively large dots, at low temperatures, Coulomb blockade is observed:

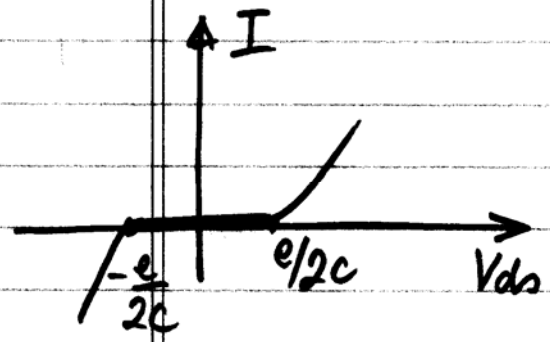

No current flows at low biases
Reason: it costs energy to add/remove an electron from the Coulomb island.

Conditions to observe Coulomb blockade:

$$\circledast \quad \boxed{e^2/C \gg k_BT,\ \hbar^2/2m^*L^2}$$

(In general, the largest energy scale of these 3 dictates the physics. If k_BT the largest, everything discrete about the levels is lost, so you basically have a resistor-like behavior

$$\circledast \quad \tau_t \gg \hbar/(e^2/C)$$

time to leak

time associated with uncertainty in energy e^2/C

You want the electrons to stay in the island long enough to block the others

$$\boxed{R_t \gg \frac{\hbar}{e^2} \sim 25\,k\Omega}$$

this basically means that you indeed have tunneling

(the resistance quantum h/e^2)

So the tunneling barrier has to have appreciable resistance, temps. have to be low & dots (or metallic droplets) should not be too small!!!

(In contrast, for example, the RTD is a structure in which $\hbar^2/2m^*L^2$ is the largest energy (so size quantization trumps Coulomb charging energy), and you want <u>resonant</u> – not sequential (one barrier at a time) tunneling, so very thin barriers with very short tunnel times $\tau_t < m^*L^2/\hbar$).

Simple circuit model of a Coulomb island

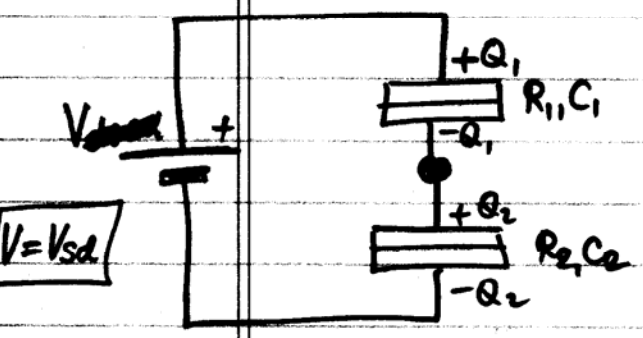

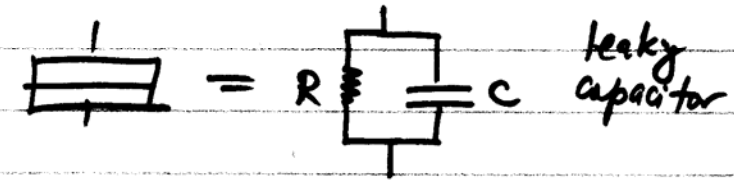

Charge on the Coulomb island:

$$Q = Q_2 - Q_1$$

$$V_1 = V_{ds} - V_2 = V_{ds} - \frac{Q+Q_1}{C_2} = V_{ds} - \frac{Q}{C_2} - \frac{C_1}{C_2}V_1$$

$$V_1\left(1+\frac{C_1}{C_2}\right) = V_{ds} - \frac{Q}{C_2} \qquad \boxed{V_1 = \frac{V_{ds}C_2}{C_1+C_2} - \frac{Q}{C_1+C_2}}$$

$$V_2 = V_{ds} - \frac{Q_1}{C_1} = V_{ds} - \frac{Q_2-Q}{C_1} \ldots \Rightarrow \boxed{V_2 = \frac{V_{ds}C_1}{C_1+C_2} + \frac{Q}{C_1+C_2}}$$

Clearly, if $Q=0$ (no island), the simple circuit reduces to the well known behavior completely determined by the capacitances. $\boxed{C_1+C_2 \text{ – effective island capacitance}}$

However, charge on the island (Q) is an extra variable that influences the exact voltage drops! Think of Q as an extra control parameter!

Let's assume that the charge $Q = -ne$ is due to n_1 electrons having tunneled onto the island, ~~and n_2~~ through the 1st barrier and n_2 having tunneled out of the 2nd barrier. $Q = -ne$, $n = n_1 - n_2$

If n_1 electrons tunnel onto the island, $\Delta Q = -n_1 e$, and the voltage drop on the 2nd barrier must then change by $\Delta V_2 = \Delta Q / C_1 + C_2 = -n_1 e / C_1 + C_2$, i.e. the charge that must have flown through the battery is $\Delta Q_2 = C_2 \Delta V_2 = -n_1 e C_2 / C_1 + C_2$, and the work done by the battery to do so is $W(n_1) = V_{sd} \Delta Q_2 = -n_1 e C_2 V / C_1 + C_2$. In a similar fashion, to get n_2 electrons out of the island through barrier 2, $\Delta Q_1 = -n_2 e C_1 / C_1 + C_2$ flows through the battery, and has it do the work $W(n_2) = \frac{-n_2 e C_1 V}{C_1 + C_2}$.

So the <u>total energy of the entire circuit</u>, when there is $n = n_1 - n_2$ electrons on the Coulomb island, is given by

$$E(n_1, n_2) = \frac{C_1 V_1^2}{2} + \frac{C_2 V_2^2}{2} \underbrace{- W(n_1) - W(n_2)}_{\text{this is the energy of the battery, equal to the negative work performed by it}}$$

$$E(n_1, n_2) = \frac{C_1}{2} \frac{(VC_2 - Q)^2}{C_{eq}^2} + \frac{C_2}{2} \frac{(VC_1 + Q)^2}{C_{eq}^2} + \frac{(n_1 C_2 + n_2 C_1) eV}{C_{eq}}$$

$$= \frac{V^2 C_1 C_2}{2 C_{eq}} + \frac{Q^2}{2 C_{eq}} + \frac{(n_1 C_2 + n_2 C_1) eV}{C_{eq}}$$

($C_{eq} = C_1 + C_2$, the Coulomb island equiv. capacitance)

*** See next page (5') on a bit more detail as to how to obtain E

• Q' tunnels through 1 onto island

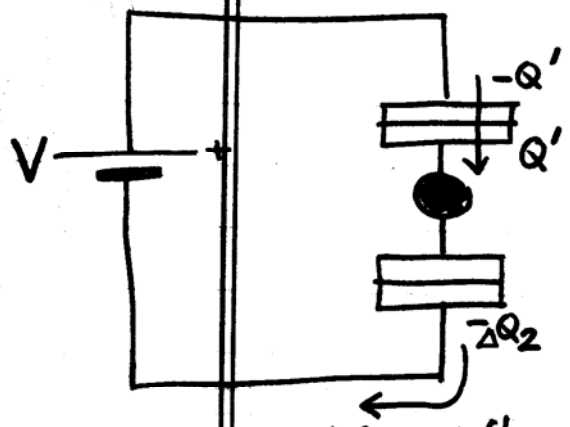

$+\Delta Q_2$ must flow through battery

• Q'' tunnels through 2 onto island

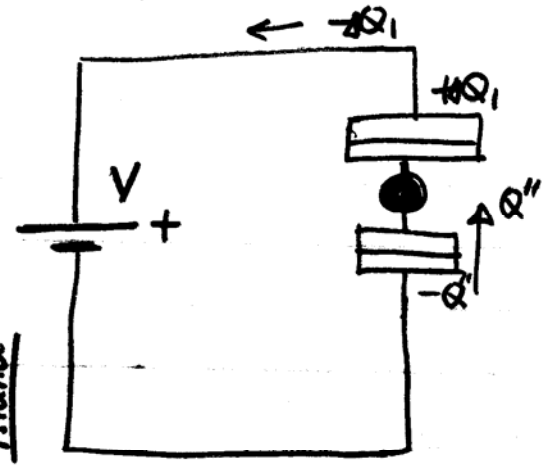

$-\Delta Q_1$ must flow through the battery

work done: $W' = \Delta Q_2' V$

$$\Delta Q_2' = C_2 \frac{Q'}{C_1 + C_2}$$

$$W' = \frac{C_2 Q' V}{C_1 + C_2}$$

$$W'' = -\Delta Q_1 \cdot (-V)$$

see the sign! going + to − through battery

$$\Delta Q_1'' = -\frac{C_1 Q''}{C_1 + C_2}$$

$$W'' = -\frac{C_1 Q'' V}{C_1 + C_2}$$

total $Q = Q' + Q''$
$= -(n_1 - n_2) e$

What if $Q' = -n_1 e$ (through the 1st barrier)

and $-Q'' = n_2 e$ (through the 2nd barrier)

$$W' = -\frac{C_2 n_1 e V}{C_1 + C_2} \qquad W'' = -\frac{C_1 n_2 e V}{C_1 + C_2}$$

$$E(n_1, n_2) = \frac{C_1}{2C_{eq}^2}(VC_2 - Q)^2 + \frac{C_2}{2C_{eq}^2}(VC_1 + Q)^2 - W(n_1) - W(n_2)$$

$$= \frac{V^2 C_1 C_2}{2C_{eq}} + \frac{Q^2}{2C_{eq}} + \frac{eV(C_1 n_2 + C_2 n_1)}{C_{eq}}$$

(A bit more detail on how one gets this energy...)

$$E(n_1,n_2)-E(n_1,n_2\pm 1)=\frac{Q^2}{2C_{eq}}-\frac{(Q\pm e)^2}{2C_{eq}}\mp\frac{eVC_1}{C_{eq}}$$

$$=-\frac{e^2}{2C_{eq}}\mp\frac{Qe}{C_{eq}}\mp\frac{eVC_1}{C_{eq}}=\frac{e}{C_{eq}}\left[-\frac{e}{2}\pm(ne-VC_1)\right]$$

$$E(n_1,n_2)-E(n_1\pm 1,n_2)=\frac{Q^2}{2C_{eq}}-\frac{(Q\mp e)^2}{2C_{eq}}\mp\frac{eVC_2}{C_{eq}}$$

$$=-\frac{e^2}{2C_{eq}}\pm\frac{Qe}{C_{eq}}\mp\frac{eVC_2}{C_{eq}}$$

$$=\frac{e}{C_{eq}}\left(-\frac{e}{2}\mp(ne+VC_2)\right)$$

$$\begin{cases}\text{if } <0, & (n_1,n_2) \text{ conf favorable}\\ \text{if } >0, & (n_1\pm 1,n_2) \text{ conf. favorable}\\ \text{if } =0, & \text{fluctuations OK (current flows!!!)}\end{cases}$$

If the island is initially neutral ($n=0$), we see that at $V=0$ the configurations with $n_1-n_2=n=0$ is more favorable than the ones with ± 1 net electrons (both differences are positive.)

However, when the bias is changed, when it reaches $\frac{e}{2C_1}$ or $\frac{e}{2C_2}$, whichever is smaller, the number is allowed to fluctuate by 1 so the current flows.

If $C_1=C_2=C$

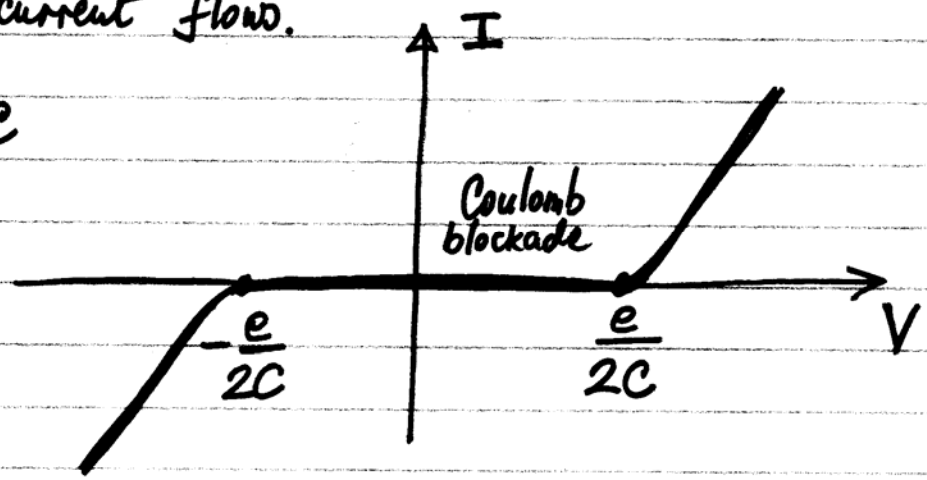

<u>Coulomb staircase</u> – feature observed in highly asymmetric setups (the RC constants of the two tunneling barriers are very different).

Say $C_1 = C_2 = C$, but $R_1 \gg R_2$. The time constant of barrier 2 is then much smaller, i.e., it leaks very quickly. So in the regime where there should be n electrons fixed on the dot, the leaky barrier leaks the electrons too fast → they must be replenished through 1. To maintain a constant number of electrons in the dot, they tunnel through 1 at the rate

$$I \approx \frac{ne}{R_1 C_1}$$

(this is the current needed to maintain the constant number of carriers on the island)

As a result, a step-like I–V curve is observed.

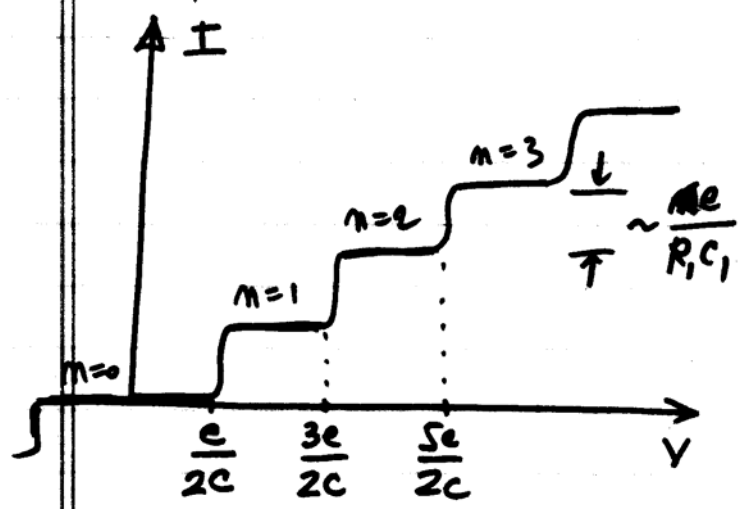

(Some people refer to the Coulomb staircase as n vs. V, where n is the number of electrons in the dot.)

[Asymmetry of the curve around 0, observed in experiment, is attributed to background polarization charge – see Wilkins et al., Phys. Rev. Lett. 63, 801 (1989)]